

## ABSTRACT

Title of Document: DESIGN OF COMPLIANCE ASSISTED  
GAITS FOR A QUADRUPEDAL  
AMPHIBIOUS ROBOT

Andrew Richard Vogel, M.S., 2013

Directed By: Professor Satyandra K. Gupta  
Department of Mechanical Engineering

The goal of this thesis was to develop an amphibious legged quadrupedal robot and associated gaits. Gaits of interest included walking, swimming, and smoothly transitioning between the two. Compliance was employed in the robot's legs to achieve swimming. Various types and configurations of compliant legs were evaluated using physical experiments and simulation. Three primary, two secondary, and two transition gaits were developed. An algorithm was developed to determine the appropriate course of action based on the current gait performance and the desired performance. The robot developed in this thesis met the goals of the design and demonstrated the technical feasibility of using compliance in amphibious legged robots.

DESIGN OF COMPLIANCE ASSISTED GAITS FOR A QUADRUPEDAL  
AMPHIBIOUS ROBOT

By

Andrew Richard Vogel

Thesis submitted to the Faculty of the Graduate School of the  
University of Maryland, College Park, in partial fulfillment  
of the requirements for the degree of  
Master of Science  
2013

Advisory Committee:  
Professor Satyandra K. Gupta, Chair  
Professor Hugh A. Bruck  
Professor Gilmer L. Blankenship

© Copyright by  
Andrew Richard Vogel  
2013

## Acknowledgements

I would first like to thank Dr. Gupta for the time, effort, and advice he has given me over these years, both regarding this thesis and with respect to my graduate studies in general. His patience given this thesis's rolling schedule is to be commended. Special thanks also go to Dr. Bruck, whose expertise served this thesis well in the experimental portion, and Dr. Blankenship, who helped foster my interest in the field of robotics.

I owe significant gratitude to Gregory Krummel, who has consistently supported the efforts of this thesis in brainstorming, manufacturing, troubleshooting, and performing experiments. His mechanical know-how and ability to turn my less orthodox ideas into something useful have gotten me out of many a fix.

Everyone else in the Advanced Manufacturing Laboratory has provided significant aid, be it moral support, previous work to consider during design, or another set of hands during a tricky experiment, especially Graeme Fukuda, Beth LeBrun, and David Billet. Everyone in the lab deserves significant thanks for making the work environment as appealing as possible.

Finally, I would like to thank my parents for putting up with my long work schedule, especially in the few weeks leading up to this thesis's completion, and for their constant support throughout.

# Table of Contents

Acknowledgements	ii
List of Tables	v
List of Figures	vi
Chapter 1: Introduction	1
1.1 Motivation	1
1.2 Research Challenges	6
1.2.1 Amphibious Quadruped Mechanical Design	6
1.2.2 Amphibious Quadruped Gait Design	6
1.2.3 Gait Transition Control	8
1.3 Thesis Goal and Scope	8
1.4 Organization of the thesis	10
Chapter 2: Related Work	11
2.1 Overview	11
2.2 Swimming Robots	11
2.2.1 Fish Inspired Robots	11
2.2.1 Snake Inspired Robots	13
2.2.3 Madeline [11]	15
2.3 Legged Terrestrial Robots	17
2.3.3 ELIRO-I [17]	21
2.3.4 AiDIN [18] and central control system	22
2.4 Legged Amphibious Robots	24
2.4.1 Shelley-RHex [20]	25
2.4.2 Rugged-RHex [20]	25
2.4.3 AQUA [22]	26
2.4.4 ASGUARD	29
2.4.5 Salamander robot [27]	31
2.5 Summary	33
Chapter 3: Design and Construction	35
3.1 Design Evolution	35
3.1.1 Enclosed chassis	35
3.1.2 Waterproof servo chassis	39
3.2 Physical specification	41
3.2.1 Components	41
3.2.2 Sensing and electronic circuit design	45
3.2.3 Physical design	48
3.3 Experimental Leg Testing	51
3.3.1 Overview	51
3.3.2 Setup	52
3.3.3 Horizontal and Vertical Comparison	58
3.3.4 Front and Back Comparison	60
3.3.5 Inside and Outside Configuration Comparison	62
3.3.6 Peak-trough distance comparison	64
3.3.7 Conclusions	66

3.4 Simulation	67
3.4.1 Overview	67
3.4.2 Fluid simulation preparation	69
3.5 Simulation Results	72
3.5.1 Vertical and Horizontal Leg Configuration Performance	73
3.5.2 Anti-spline and pro-spline leg configurations	76
3.6 Summary of Design	81
Chapter 4: Design of Gaits	83
4.1 Overview	83
4.2 Primary Gaits	83
4.2.1 Semi-aquatic environments and required modes of locomotion	83
4.2.2 Terrestrial gait	85
4.2.3 Shallow aquatic gait	88
4.2.4 Aquatic Terrain	91
4.3 Secondary Gaits	92
4.3.1 Secondary walking gaits	93
4.3.2 Transition Gaits	95
4.4 Gait Switching Algorithm	101
4.4.1 Primary loop	101
4.4.2 Desired state subroutine	102
4.4.3 Transition subroutine	104
4.5 Experimental Testing	106
4.5.1 Experimental setup	106
4.5.2 Experimental testing	108
4.6 Results and Conclusions	110
Chapter 5: Conclusions	113
5.1 Intellectual Contributions	113
5.2 Anticipated Benefits	114
5.3 Future Work	114
5.3.1 Structural improvement	115
5.3.2 Energy considerations	115
5.3.3 Introduction of sophisticated sensing and controls	116
5.3.4 Broadening of terrains and conditions for operation	116
5.3.5 Submerged swimming	117
Scholarly References	118

## List of Tables

Table 1: Solidworks simulation operating parameters.....	72
Table 2: Trotting servomotor position table .....	86
Table 3: Walking servomotor position table.....	89
Table 4: Swimming servomotor position graph.....	92
Table 5: Water to land transition servomotor position table.....	97
Table 6: Land to water transition servomotor position table .....	99

## List of Figures

Figure 1: Swimming sea turtle [38] .....	3
Figure 2: Platypus free body diagram [36] .....	3
Figure 3: A platypus with front and back feet prominently displayed [1].....	4
Figure 4: An alligator, commonly used for quadrupedal robot reference [2].....	7
Figure 5: Musculature of a crocodile [37] .....	8
Figure 6: RoboTuna II [6].....	12
Figure 7: BoxyBot [4].....	12
Figure 8: ACM-R5 snake robot [7].....	14
Figure 9: Amphibot I [8] and II [10].....	15
Figure 10: Madeline swimming robot [11].....	17
Figure 11: RHex with original legs and curved legs [12].....	18
Figure 12: Shelley-RHex, Rugged-RHex, and AQUA [12] .....	19
Figure 13: Biosbot and diagram of possible knee configurations [16].....	20
Figure 14: ELIRO-I turning with 5-degree waist bending [15].....	22
Figure 15: AiDIN with components labeled [18] .....	24
Figure 16: Rugged-RHex in a creek [21].....	26
Figure 17: AQUA robot with diver, showing symmetric flipper legs [23] .....	28
Figure 18: AQUA swimming [23] and walking [24].....	29
Figure 19: ASGUARD in water [26] .....	30
Figure 20: ASGUARD [25].....	31
Figure 21: Salamander robot with pattern generator diagram [27].....	32
Figure 22: Enclosed Chassis Robot .....	36
Figure 23: Joint Configuration and Reference Frames for Enclosed Chassis Robot Legs.....	37
Figure 24: Internal Physical Configuration of Enclosed Chassis Robot.....	38
Figure 25: Free Body Diagram for Enclosed Chassis Robot Leg.....	39
Figure 26: Joint Configuration and Reference Frames for Waterproof Servo Chassis .....	40
Figure 27: Delrin Acetal Resin Sheet [25].....	42
Figure 28: 1554UGY Plastic Enclosure [30].....	43
Figure 29: HS-646WP Analog Waterproof High Voltage Servomotor [28] .....	43
Figure 30: Arduino Mega 2560 [31].....	44
Figure 31: Tenergy 6V 2000mAh NiMH battery [32].....	45
Figure 32: Water sensor circuit modeled on Arduino Nano .....	46
Figure 33: Lower water sensor on robot.....	47
Figure 34: Full robot circuit.....	48
Figure 35: Knee Joint Construction .....	49
Figure 36: Horizontal and Vertical Leg Configurations Demonstrating Forward Stroke and Back Stroke.....	50
Figure 37: Robot in test chamber.....	53
Figure 38: LabVIEW block diagram .....	54
Figure 39: Horizontal and vertical leg and flap assemblies.....	55



Figure 40: Demonstration of outside (left) and inside (right) configurations.....	56
Figure 41: Baseline data and the resulting transfer function .....	57
Figure 42: Sample Data from 16 <sup>th</sup> /40A/Outside/Back.....	58
Figure 43: Thrust averages for vertical legs .....	59
Figure 44: Thrust averages for horizontal legs .....	60
Figure 45: Outside front and outside back configurations relative to tub wall.....	61
Figure 46: Thrust averages for front legs.....	61
Figure 47: Thrust averages for back legs .....	62
Figure 48: Thrust averages for inside legs .....	63
Figure 49: Thrust averages for outside legs.....	63
Figure 50: Peak-trough distances for vertical configurations .....	65
Figure 51: Peak-trough distances for horizontal configurations.....	65
Figure 52: Pictorial representation of input equation for simulation.....	71
Figure 53: Absolute and X-directional velocity for vertical leg configuration during thrust phase .....	74
Figure 54: Absolute and X-directional velocity for horizontal leg configuration during thrust phase .....	74
Figure 55: Absolute and X-directional velocity for vertical leg configuration during recovery phase .....	75
Figure 56: Absolute and X-directional velocity for horizontal leg configuration during recovery phase .....	75
Figure 57: Velocity profiles for anti-spline (left) and pro-spline (right) legs during thrust phase .....	77
Figure 58: X-directional velocity for anti-spline (left) and pro-spline (right) legs during thrust phase.....	77
Figure 59: Absolute and X-directional velocities for both spline configurations during recovery phase .....	78
Figure 60: Absolute and X-directional velocities for vertical configurations during thrust phase .....	79
Figure 61: Absolute and X-directional velocities for vertical configurations during recovery phase .....	80
Figure 62: Shallow aquatic terrain [34] .....	84
Figure 63: Trotting gait.....	86
Figure 64: Trotting servomotor position graphs .....	87
Figure 65: Walking Gait .....	89
Figure 66: Walking servomotor position graph .....	90
Figure 67: Swimming Gait .....	91
Figure 68: Swimming servomotor position graph .....	92
Figure 69: An example of sloped terrain in water [35].....	93
Figure 70: Robot holding at biased zero position on upward and downward slope ...	94
Figure 71: Walking gait servomotor position diagram comparing changes in sweep values .....	95
Figure 72: Water to Land Transition .....	97
Figure 73: Water to land transition servomotor position diagram .....	98
Figure 74: Land to Water Transition .....	99

Figure 75: Land to water transition servomotor position table.....	99
Figure 76: Diagram showing minor and major transitions between swimming, walking, and trotting .....	100
Figure 77: Flowchart for main loop .....	102
Figure 78: Flowchart for desired state decision subroutine .....	104
Figure 79: Flowchart for transition subroutine .....	105
Figure 80: Experimental setup for walk/trot transitions .....	107
Figure 81: Experimental setup for swim/walk transitions. ....	108

# Chapter 1: Introduction

## 1.1 Motivation

Robotics is a swiftly growing field, especially with regard to its applications. Robots are employed in many areas of society today, whether at home, in manufacturing, or in military operations. This has especially been accelerated by the growth of microcontrollers and other similar compact computing solutions. As small-scale computing and sensors continue to become smaller and more powerful, robots can be more complex and robotic solutions are more viable for previously unexplored areas. This is especially true for mobile robots, for which reductions in weight and power requirements for new controllers and sensors increase the viability of certain locomotion methods and control systems.

Mobile robots can be useful for a number of pursuits, including military and search and rescue. As technology improves, these fields expand to include other difficult or delicate situations such as fire rescue and environmental monitoring. While many mobile robots maintain locomotion methods similar to those used in traditional vehicles such as automobiles and boats, others have more varied locomotion methods adapted to their situation.

One such environment is semi-aquatic terrain. Many swamps, for instance, have enough tree cover to limit significantly the effectiveness of an aerial robot, while terrestrially focused robots typically are not designed to handle water and moisture in both locomotion and reliability. For these kinds of environments, a specialized robot is necessary.

Such a robot would require the ability to move well on varied ground, move well in water, and transition between land and water efficiently, especially on slopes. This requires a method of locomotion more seen in animals than to human-designed vehicles; indeed, many animals, such as crocodiles and turtles, are amphibious by nature. A legged platform meets these requirements, as it could potentially use its legs for both complex terrestrial locomotion and swimming if properly configured.

Legged robots have very versatile chassis for terrain locomotion. The ability to vary foot position as necessary and change the gait dynamics may be necessary, as many problems that look to mobile robotics for solutions require movement over varied environments, and many solutions have been developed to handle various environment types. Certain body patterns are also quite stable.

The assumed configuration for such a platform would be quadrupedal; however, common forms with more or fewer legs must be considered, and this choice must be justified. Bipedal configurations, especially for swimming, are relatively common in nature. The platypus is a very good example of a bipedal swimmer: only its forelegs propel the animal, while its hind legs and some limited body undulation provide stabilization [36]. Another example is the sea turtle, which employs a similar idea [38]. These can be seen below in Figure 1, Figure 2, and Figure 3.

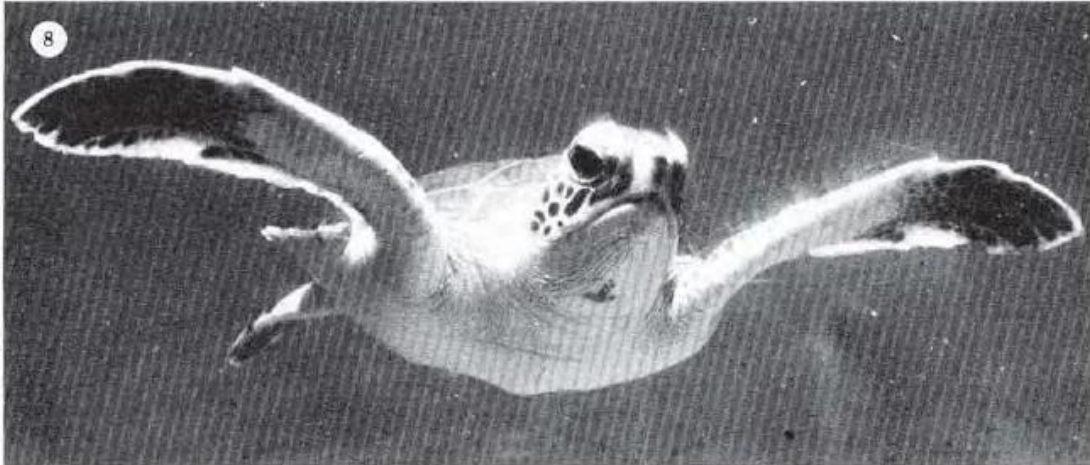


Figure 1: Swimming sea turtle [38]

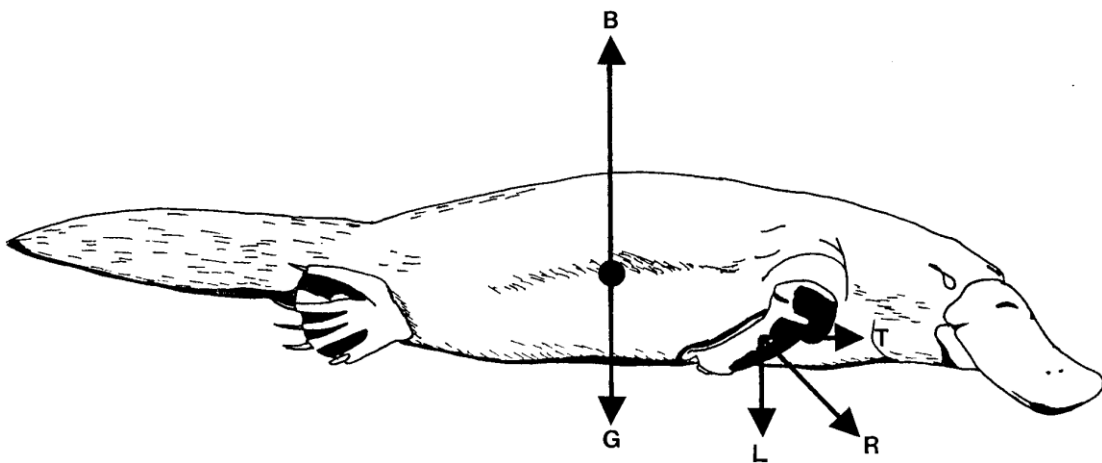


Figure 2: Platypus free body diagram [36]

In theory, a bipedal gait can be more efficient than a quadrupedal gait. However, the body undulation necessary to maintain stabilization makes low-cost manufacturing and simple control algorithms more difficult. Without that undulation, any given design will quickly become unbalanced, requiring algorithms specifically for that, which is undesirable. In addition, a bipedal configuration to swimming does not lend itself well to terrestrial locomotion, which is a major part of the design. Bipedal walking requires significant balancing considerations which can be obviated

by having at least four legs, for which there is an option for three feet to remain on the ground while one advances.



**Figure 3: A platypus with front and back feet prominently displayed [1]**

Many current legged robots employ greater than four legs. Hexapedal robots are especially common, due to a major advantage in stability granted by the ability to maintain three points of contact on the ground mid-step without slowing the gait significantly. This in turn grants significant advantages on uneven ground, as more points of contact on the ground can be used for stability if necessary. However, this design comes with some considerable disadvantages. The gait and control algorithm complexity rises with an increase in the number of legs. Additionally, more legs necessitate an increase in size, weight, or power requirements, all of which reduce potential payload capacity and increase the amount of buoyant force necessary for the robot to float to achieve surface swimming.

Legged platforms in general, however, are not without inherent disadvantages. Traditional wheeled or tracked platforms are significantly easier to control due to having far less controlled degrees of freedom, and for the same power consumption can move notably faster on favorable terrains. In most cases, a legged platform can hardly hope to reach the maximum speed that a comparable wheeled or tracked platform can. The nature of wheels or tracks being in constant contact with the ground ensures stability on flat ground assuming the platform has a low center of gravity and barring extreme circumstances. In addition, many legged platforms are incapable of standing unpowered without putting significant stress on their legs. That said, in this particular case, the number and type of advantages outweigh the disadvantages, as successful operation in this case is more of a priority than speed or stability past the ability to walk well.

This thesis is intended to explore such a concept by designing, manufacturing, and testing a robot that can both walk and swim using legs, and developing the required gaits. More than that, however, this robot needs to be able to traverse a swamp-like or semi-aquatic area. This means that two interchangeable forms of transition locomotion must also be explored: walking on unstable, slick, or unsteady flat ground and walking on a slope to and from water. The robot itself should be designed in a compact form with as little mechanical complication as possible. While there have been several amphibious robots created prior to the one described in this thesis, as will be described in Chapter 2, those particular robots tend to take a different approach to address the two necessary locomotion modes.

The field of quadrupeds offers adequate flexibility in terms of the gait design and control and manageable complexity in terms of realizing a waterproof design. Hence, this thesis will only focus on quadrupeds. The successful realization of a quadruped will provide model for realizing other more complex amphibious legged robots.

## 1.2 Research Challenges

Realizing a quadruped that can walk and swim requires addressing many different challenges.

### 1.2.1 Amphibious Quadruped Mechanical Design

While there are many quadrupedal walking robots and many swimming robots, there are exceedingly few examples of quadrupedal robots that can both walk and swim, especially not robots that employ a design based on traditionally bounded servomotors and joints rather than fully-rotating servomotors or motors. As such, a major component of this thesis is to provide such a design, using eight degrees of freedom total with two per leg to both walk and swim, with any added modules necessary to achieve this. A major component that drives the design of such a robot is the challenge of waterproofing its components, a problem that has been and will be approached in several ways. Additionally, given that applications discussed involve some degree of autonomy and separation from a base unit, the considerations given to inclusion of a self-contained controller and sensor package will be discussed.

### 1.2.2 Amphibious Quadruped Gait Design

Gaits for a quadrupedal robot are both very common and very well tested, and doubly so for lizard-like or crocodile-like leg configurations, seen below in Figure 4



and Figure 5. However, as mentioned before, quadrupedal robot performance in the water is not well studied. Because of this, a major design challenge is to develop default gaits specific to the determined solution of aquatic locomotion for swimming, walking in water too shallow to swim in, and ascending or descending slopes. These gaits will be modified in testing so as to achieve the best performance with each.



**Figure 4: An alligator, commonly used for quadrupedal robot reference [2]**

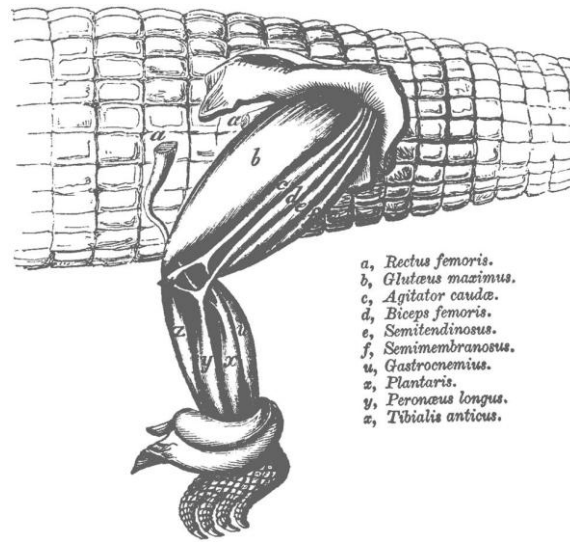


**Figure 5: Musculature of a crocodile [37]**

### 1.2.3 Gait Transition Control

In addition to the general gait design, a vital component to gait control is transition, specifically the flow of one gait to another. Fluid transition between gait patterns is a major factor in maintaining stability and similar alignment, which is vital for more autonomous operation. Such a transition is also noted as a major problem in the AQUA robot, as will be discussed in Chapter 2. Therefore, there is significant motivation to develop such a transition between swimming, walking in water, and walking on land modes.

### 1.3 Thesis Goal and Scope

The scope of this thesis, and the goals thereof, can be extracted from the challenges listed above. First, a method of achieving both walking and swimming locomotion with two degrees of freedom per leg will be developed and established. This will be compared to possible methods of waterproofing all vulnerable

electronics. The robot will employ commercially available components, including servomotors for joint movement, batteries for power sources, a microcontroller, and sensors. Combined with both commercial and custom-made structural components, these will be used to create the prototype robot. Tests with both force sensors on a prototype and fluid simulations will be constructed and performed to determine the viability of the swimming solution as presented, and depending on these tests the robot prototype will either be revised and retested or accepted.

Once the robot is constructed, a full kinematic analysis of the leg mechanism will be performed for the purpose of developing a full kinematic analysis of the entire body. Gaits will then be developed and tested for four categories: walking, swimming, walking in water, and walking up and down slopes. Transition gaits will also be developed and tested for switching between each of those. The robot will be arrayed with simple water sensors to detect the presence of water for automatic switching, and put in a representative situation to test this. The goals of the robot for the purpose of this thesis are:

- The robot will be able to walk on ground, swim, walk in water, and walk on slopes. Force sensor testing and simulation should be used to verify the efficacy of the method in question.
- Utilizing only sensors and electronics contained on the robot, the robot should be able to smoothly transition between states without significant perturbation of motion.

#### 1.4 Organization of the thesis

**Chapter 2** is the survey of literature relevant to walking robots, swimming robots, and amphibious legged robots. Various fish-like, snake-like, and flippered swimming robots, as well as several legged walking robots relevant to the thesis, are discussed. Afterwards, five of the most relevant amphibious robots are examined in detail, and show that each cannot achieve one of terrestrial motion, aquatic motion, and switching between the two adequately.

**Chapter 3** describes the design process in detail, including the evolution of previous designs prior to the final design. The shortcomings of these prior designs are explored, and the component selection to accomplish the final design is described in detail. This includes actuator selection for driving the robot's joints, battery selection for powering actuators, sensors, and controllers, controller selection, and material selection. This also includes selection and design of any special modules made especially for any of the four primary modes of locomotion. Methods of and results from empirical and simulation-based testing of the robot are included.

**Chapter 4** extends Chapter 3 by examining the process behind the development of the four gaits as described earlier. Walking gaits are relatively simple in concept and well-developed among quadrupedal robots of most configurations. This chapter presents a walking gait for the robot described in Chapter 3. This chapter also presents swimming gaits, gaits designed to walk in water, and gaits designed for slippery slopes.

Finally, **Chapter 5** summarizes the main body of work. In addition, future improvement possibilities are discussed.

## Chapter 2: Related Work

### 2.1 Overview

Prior to developing a strategy for the design of the robot, it was necessary to review literature that describes similar approaches for the purpose of investigating the current methods of locomotion in terrestrial, aquatic, and amphibious robots. First, robots that are created to swim by various means will be discussed. This establishes the baseline methods of swimming that, while not directly applicable to a quadrupedal robot, are nonetheless useful for considering basic swimming principles. Second, robots that are created specifically to walk using legs are examined. This establishes the scope and baseline performance of currently available robots, as well as provides exploitable walking principles. Third, the robots that have achieved legged amphibious locomotion are discussed. These have shown some solutions to the myriad of challenges facing amphibious locomotion.

### 2.2 Swimming Robots

#### 2.2.1 Fish Inspired Robots

Fish robots often employ a method of locomotion focused around a single, vertical caudal fin that oscillates laterally [3], [4], [5]. MIT's Robotuna is a prime example of this, citing high thrust and efficiency from tail-based propulsion as motivation. Efficiency is created due to the fact that the tail's surface and the vortices created by its movement are both conducive and compatible with forward thrust. This stands in contrast to propeller motion, which typically creates a vortex moving in the direction of the propeller rotation perpendicular to the desired direction of motion.



**Figure 6: RoboTuna II [6]**

Some fish robots, including BoxyBot from the Swiss Federal Institute of Technology, use pectoral fins as well as a caudal fin [4]. These secondary fins allow for more precise control over motion in the water, allowing for an expanded library of movement methods, such as rolling, vertical mobility, and quick turning. These pectoral flippers can also be used for underwater crawling.



**Figure 7: BoxyBot [4]**

One study from Boston University focused upon further increases in efficiency through the use of passive elastic elements [3]. Building upon and combining the foundations created by researchers of both fish locomotion and airfoil properties, a hydrodynamic model was established. This model was subsequently used to determine the difference in energy input between systems with no elasticity assumed and systems with lateral springs placed. The conclusion drawn was that lateral spring usage increases the efficiency of travel: for each oscillation, less energy was required. This operating principle could be employed to reduce the power drain of a robot for the same speed, or to increase the speed while employing the same power drain. This is a significant advantage of a lateral-actuation design, and could be very useful in consideration of passive actuation for swimming even for non-fish robots.

### 2.2.1 Snake Inspired Robots

While there are many snake robots, two in particular are especially notable with regards to swimming: The ACM-R5 snake robot by HiBot and Amphibot by the Swiss Federal Institute of Technology. Both of these robots exhibit both walking and swimming behavior, as the snake's locomotion mechanism is similar enough in both cases as to facilitate both easily with the development of one. The ACM-R5 [7] was developed especially to swim like a sea snake. It is composed of any number of links and a head, of which each link features a two degree-of-freedom joint; with this setup, the ACM-R5 can operate three-dimensionally. In addition, each link has a paddle with a wheel attached to the end, which allows a normal component of force to be applied to a tangential direction for swimming or walking. The links are all

independent, with each containing battery, CPU, and motors, but when connected the number the head detects the number of links chained together. A suitable algorithm for swimming is configured based upon the current length of the robot, which allows the robot versatility in different situations.

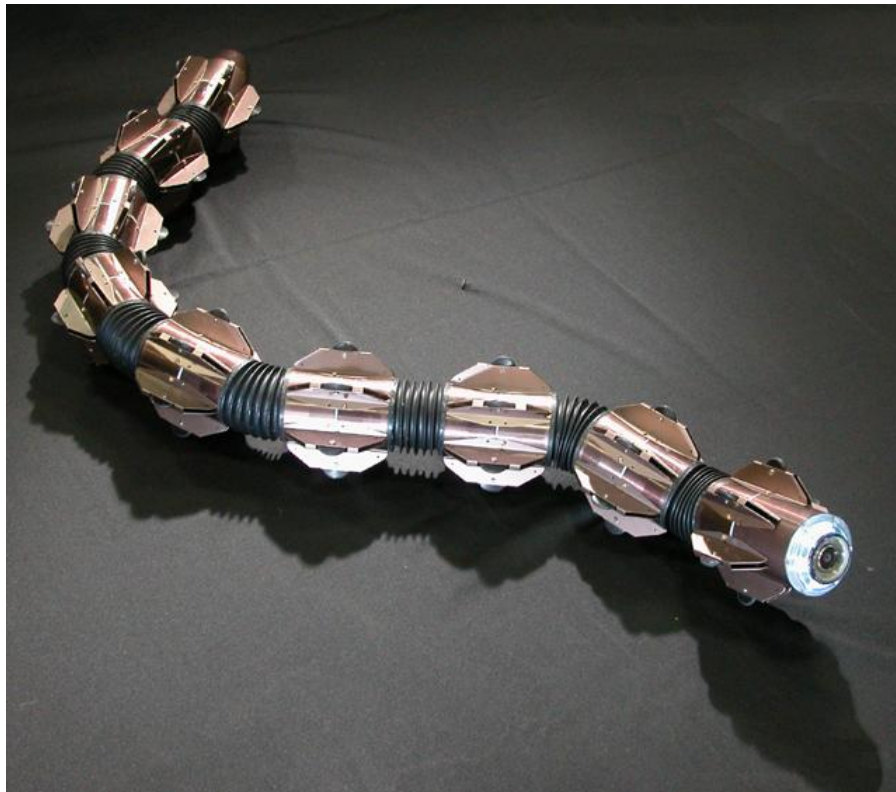


**Figure 8: ACM-R5 snake robot [7]**

In development since 2004, the Amphibot project was created to model snake-like movement on land and in water [8], [9]. The initial robot, Amphibot I, was made up of seven 7-cm segments, referred to as elements, which are required to remain independent and stable while maintaining waterproofness and vertical stability. Amphibot II increased element size and number, bringing total length from 49cm to 77cm [10]. Each element has an encased motor, kept waterproofed at its axis by an



O-ring, and with a significant motor reduction and external axis potentiometers precise positioning of each motor can be achieved. Additionally, passive wheels were affixed to the robot for terrestrial locomotion.

Both swimming and terrestrial locomotion are achieved by gaits composed from oscillation amplitude, frequency, and phase lag parameters. In Amphibot I, frequency was measured at 0.25 and 0.5 Hz due to larger amounts being unfeasible with the given motors, with the maximum swim speed of 0.0454 m/s, or 0.1 body lengths per second. Improvements in Amphibot II's motors allowed frequencies up to 1Hz, which in turn allowed a swimming speed of 0.23 m/s, or 0.32 body lengths per second, and a land speed of 0.4 m/s, or 0.55 body lengths per second. Most notably, forward speed increased with frequency.



**Figure 9: Amphibot I [8] and II [10]**

### 2.2.3 Madeline [11]

Madeline is a tetrapodal, self-contained swimming robot. The robot is comprised of four degrees of freedom; each actuator is an independent flipper that can oscillate perpendicular to the axis of movement. Madeline was inspired by

biological designs from a number of sources, but most specifically to discover the reasoning for a shift from using both pectoral and pelvic limb sets for swimming to using one or the other.

Eight gaits were tested: four with four flippers and four with two flippers. While propulsion with two flippers was carried out, the two inoperative flippers were held steady. Four gaits for each were determined by creating a matrix between in-phase and anti-phase for each of port-starboard and fore-aft leg pairs. Videos of each of these were recorded, with the data assembled and analyzed statistically. Two dimensionless parameters, cost of transport and surge scope, were defined to measure efficiency at constant speed and unsteady linear movement performance respectively.

A number of conclusions were drawn from this. Four-flippered swimming was shown to have generally higher starting and stopping acceleration, with gaits where fore-aft flippers were in phase maximized peak starting acceleration. Four-flippered gaits, however, had a universally higher cost of transport than two-flippered, with only a small gain in surge scope to show for it. Additionally, maximum cruise speeds were not statistically different between four-flippered and two-flippered. These are all important considerations for any legged or flippered swimming robot.

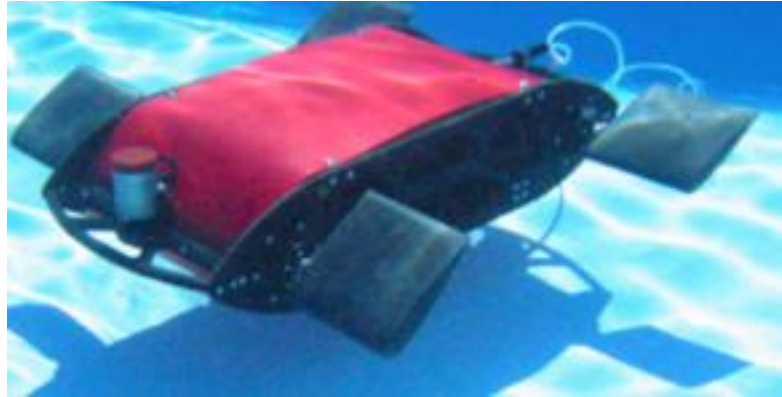


Figure 10: Madeline swimming robot [11]

### 2.3 Legged Terrestrial Robots

Many legged robots of a wide variety have been created and documented, for which the design of many have drawn from biological inspiration. Some are more so created for the investigation of climbing than walking, but nonetheless, this fact does not exclude those specific robots from consideration. The robots presented below were chosen to display a variety of approaches.

#### 2.3.1 RHex

The RHex robot design has been in publications since 2001 [12]. Since then, it has been the theoretical basis of several different types of robots, some of which will be discussed later. The initial platform consisted of six compliant spokes as legs, each attached to a rotary actuator, to create a hexapedal robot. The concept behind using a single spoke per leg was that the angle of contact could be varied more because of the increased contact angle range. This would allow more control over ground reaction forces to achieve a significant speed relative to its size. Moving

forward is accomplished by the simple alternating tripod gait common to most hexapedal robots, while turning is either accomplished by reversing the direction of opposite legs or by introducing a perturbation in the normal leg pattern.

A later incarnation of RHex would improve on the legs significantly, retrofitting the robot for complex terrain handling [13]. The legs changed from the “compass” spoke-like pattern, to a “four bar” ankle-like pattern, to the final “half circle” pattern. The final iteration ensures constant ground contact during the entire step, affording the robot advantages similar to those given by another degree of freedom per leg without the power consumption, weight, and reliability issues. This allows for effective stair traversal.



**Figure 11: RHex with original legs and curved legs [12]**

RHex has inspired many further improvements, many of which tackled the problems of amphibious operation. These altered models include Shelley-RHex, Rugged-RHex, and AQUA. Additionally, while not technically being part of the RHex development path, ASGUARD claims significant influence from the original

design. Each of these presented different modifications to RHex, of which some achieved varying levels of success in the alteration's design goal. AQUA and ASGUARD both differ significantly in the model's legs, changing the base operation significantly, while Shelley-RHex and Rugged-RHex are primarily modifications to the main body. Each of these will be presented later in this section.



**Figure 12: Shelley-RHex, Rugged-RHex, and AQUA [12]**

### 2.3.2 Biosbot [15],[16]

Biosbot, created by Tsinghua University, was born from the idea of mimicking a housecat's leg motion while studying the effects that certain alterations to the initial design would have on slippage and ground clearance in a typical gait for the leg design. The initial leg structure, comprised of five joints with 1 to 3 degrees of freedom each, was drastically reduced for the sake of simplicity: The design was refined to two active degrees of freedom and one passive degree of freedom per leg, a hip joint, a knee joint, and an ankle joint respectively. The knee starting point was varied between four models: pointing inward, pointing outward, facing forward, and facing backward.

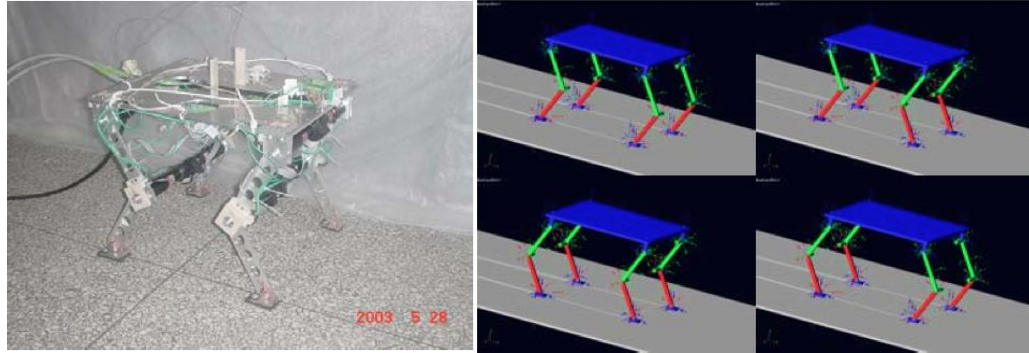


**Figure 13: Biosbot and diagram of possible knee configurations [16]**

To determine an initial gait, cat footage was analyzed, and the relationship between the hip and knee joints was noted. The resulting gait was applied to all four configurations, and the resulting data led to several conclusions. The leg model in which each leg had its knee pointed backwards performed the worst, with considerable slippage noted. This was attributed to the center of gravity being shifted towards the back of the robot, which prevented the hind legs from achieving full clearance. Knee-forward models performed better for speed while balanced models moved more stably.

Biosbot's creators also examined trot, gallop, pace, and walk gaits. Using the sinusoidal patterns that each of these created, a transition function was created as a subsection of the normal gaits. This creates a sub-gait that acts as a bridge between gaits with different leg patterns, allowing for smooth transition, which is a useful concept for all quadrupedal robots.

### 2.3.3 ELIRO-I [17]

The idea of a robot gait built to incorporate discontinuous twisting at the waist was approached by Kyungpook National University first from a theoretical perspective; later, this theory was used to create a robot based upon the principles demonstrated. Many natural walking gaits incorporate a central degree of freedom at the spine, which increases speed and stability, especially while turning. The approach taken was systematic: first, the assumption was made that the robot would be on flat terrain, parallel to the ground, with massless legs, a uniformly massed body, and a single degree of freedom along the z-axis at the center as the waist joint. From this set of assumptions, the kinematics were determined, noting especially that in a non-rigid body an optimal hip position can be created.

From these kinematic observations, some additional features were drawn: the stride increases drastically from a rigid body, maneuverability in unfavorable situations was greatly improved, and the general gait stability was improved. In gait planning, ten timesteps were used, with the center of gravity shifted at varying intervals; the bending angle for the center and the leg order were varied.

Eventually the conclusions from this were used in a quadrupedal robot with three degrees of freedom pantograph legs called ELIRO-I. This robot achieved stable turning on flat ground, and it is noted that with implementation of a three degree of freedom spine, stability on rough terrain could similarly be achieved.

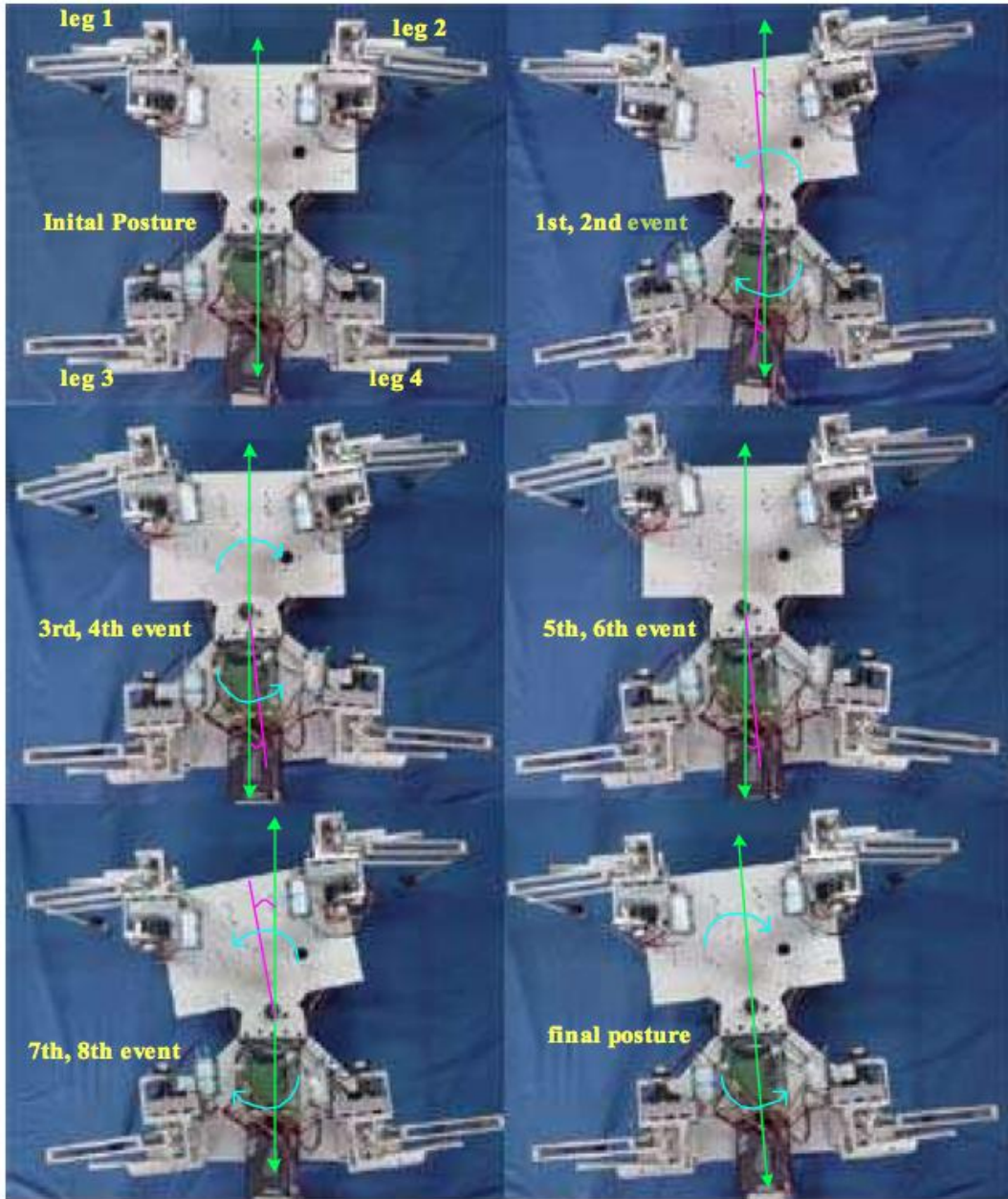


Figure 14: ELIRO-I turning with 5-degree waist bending [15]

#### 2.3.4 AiDIN [18] and central control system

AiDIN (Artificial Digitigrade for Natural Environment) is a quadrupedal robot built around the biological concept of a central pattern generator inherent to the



neural system that controls rhythmic outputs for locomotion, as applied to a vertically asymmetric quadrupedal robot with three degrees of freedom per leg. The joint controller, in particular, was based upon the gravitational load for each joint as well as the natural stimulus-reaction mechanism from nature. The response is altered depending on whether the information from force sensors, touch sensors, and gyroscopes exceed a certain threshold, and is split into exceeding and nonexceeding categories based upon this threshold. All responses engage a standard set of flexors and extensors with values based upon the stimulus level, while situations with stimulus levels exceeding thresholds also engage a secondary set of extensors.

With this concept in mind, the state is defined as recurrent neural network, with each neuron's state dependent on the inner neuron state, weighting to the next neuron in sequence, and the neuron base; this creates a repetitive motion. Each of these values adds to the central and intermittent stimuli to obtain a total response value which comprises a joint angle. This method was tested both experimentally and in dynamic simulation, and in both cases, provided a stable rhythmic gait with significant feedback to adapt.

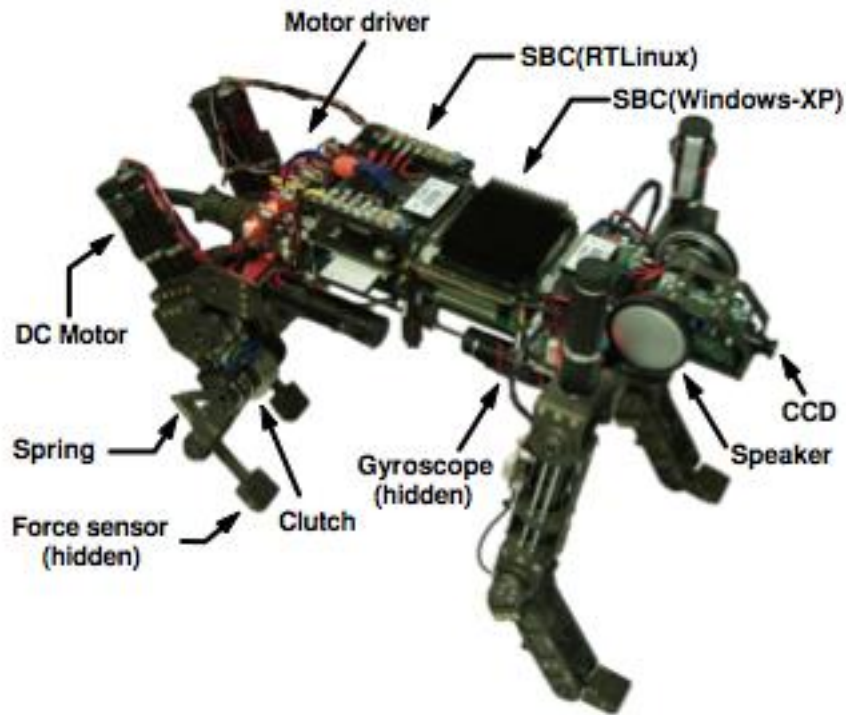


Figure 15: AiDIN with components labeled [18]

#### 2.4 Legged Amphibious Robots

There have been multiple efforts into robots capable of both walking on land and swimming in water. One possible solution is to incorporate both walking and swimming mechanisms separately on one robot; for example, an unnamed amphibious robot from the Shenyang Institute of Automation has legs and wheels with propeller-wheels which are rotated inward to swim and outward to crawl [19]. However, the primary amphibious robots that will be explored in detail are those that employ the same mechanisms to move terrestrially and to swim, and more

specifically those that employ legs to do so. Many of the most successful robots are variants of RHex, which was described earlier.

#### 2.4.1 Shelley-RHex [20]

Shelley is a branch of RHex. It is designed almost identically from a mechanical perspective, but with the added goal of amphibious movement without an increase in weight or size. To accomplish this, the frame of RHex was replaced with a closed shell. The shell was formed from carbon fiber into a curved shape for hydrodynamics and impact resistance, with Neoprene to dampen impacts and vibrations. Some waterproofing issues arose from the power switch, antenna, access panel, and motor connection; these were fixed by various solutions such as adding clamping force and waterproof material, encasing the entry port with silicone, and O-rings.

Shelley was able to achieve surface swimming. However, the nature of the shell prevented design alteration without significant expenses in both time and money, and the carbon fiber shell alone proved too brittle to remain watertight when subjected to repeated impact. The consequence of these two facts was relative unpopularity compared to the original RHex. Nevertheless, the design's construction and solutions were useful concepts to consider for both future RHex iterations and unrelated robots.

#### 2.4.2 Rugged-RHex [20]

Rugged-RHex was a design made using Shelley-RHex as a basis, with the goal of fixing the inherent problems with Shelley's design. To avoid the problem of external brittleness, the shell was formed from impact-resistant nylon, with an internal skeleton made of aluminum to distribute loads well. These materials

necessitated an increase in motor size and battery power. Sealing of electronic component compartments was achieved through the use of O-rings and collar plugs; notably, soft rubber was used for the primary body seal due to better coordination with the rough Nylon surface. These changes solved many of Shelley's durability issues, and Rugged performed very successfully in water, both while swimming on the surface and while ballasted to up to 5m in depth, and on land. However, increased size and mass caused issues with portability, component fatigue, and impact, as well as hindered its use in similar applications to the original RHex.



**Figure 16: Rugged-RHex in a creek [21]**

### 2.4.3 AQUA [22]

The AQUA robot is a later alteration to the RHex design than Shelley and Rugged. It was designed specifically for the purpose of swimming and diving in the

water: most notably, the RHex's legs are substituted for flippers, which aid it significantly in aquatic movement. In the water, the AQUA can achieve swimming speeds up to 1.0 m/s, or approximately 1.54 body lengths per second. It achieves swimming motion by creating small oscillations rather than large rotary motions, and when engaging all six legs, it has the capability to control five degrees of freedom directly: surging, heaving, pitch, roll, and yaw are all possible. Phase offsets are used to change between gaits, with amplitude offsets used for pitch and roll and a change in amplitude scale factor between the sides used for yaw [23].

Additionally, AQUA can still walk on land. The flippers work largely the same way as RHex's legs, with spring energy from bending under load contributing greatly to forward motion. However, the need for symmetry in AQUA's legs due to its method of swimming prevents the leg structure from being as efficient as the asymmetric "half circle" RHex leg pattern.

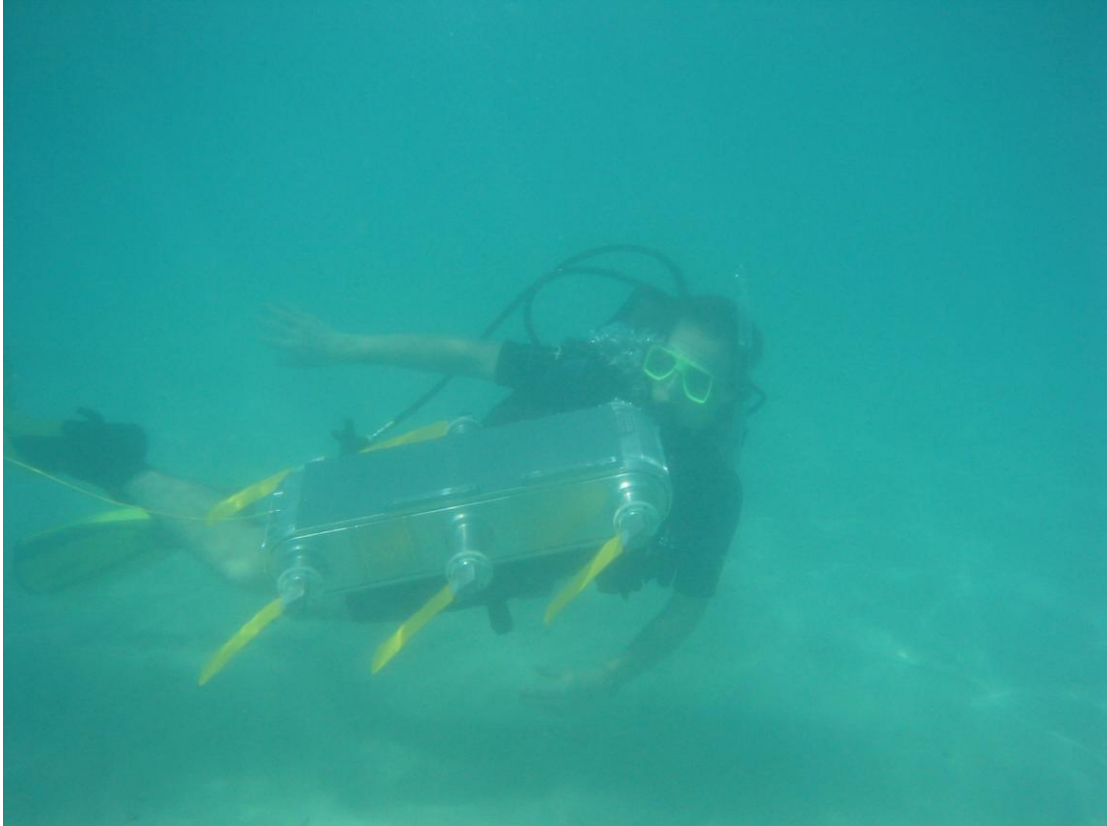


**Figure 17: AQUA robot with diver, showing symmetric flipper legs [23]**

Another important consideration is the gait transitions. The AQUA has numerous different patterns of both terrestrial and aquatic motion, but the difference between terrestrial and aquatic gaits is drastic. AQUA's swimming gait engages its legs as flippers, oscillating the flippers slightly up and down while the legs are pointed toward the back of the robot. In contrast, AQUA's walking gait resembles RHex's walking gait, in that it employs the full range of rotary motion. As neither of these gaits resembles one another, this leads to motion inefficiency, undesirable forces upon the robot, and subsequently unwanted displacement when transitioning between AQUA's walking and swimming gaits. This can have heavy impact upon

tasks such as target acquisition, as an unexpected location or pitch shift can move a target out of sight of AQUA's vision-based sensing.

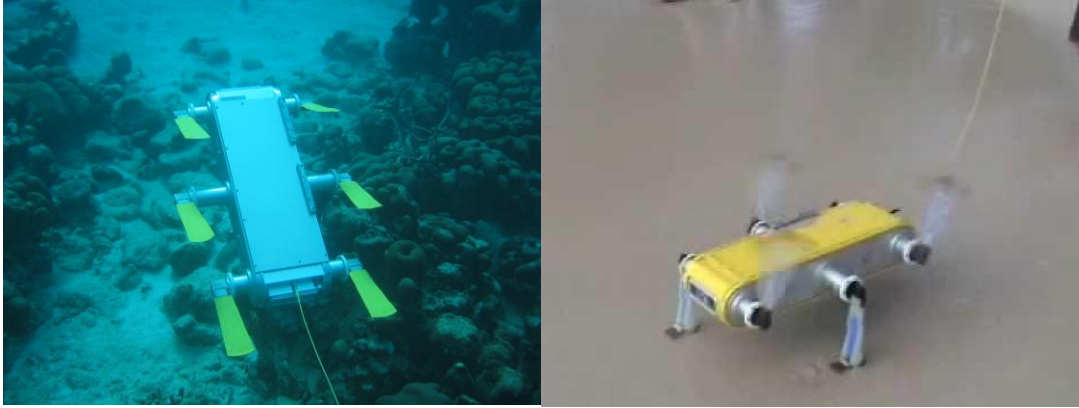


**Figure 18: AQUA swimming [23] and walking [24]**

#### 2.4.4 ASGUARD

The ASGUARD robot has been in development since 2008, and is currently on its second version [25]. It is founded upon the initial basis of compliant rotary legs determined by RHex [12], but treats this basis in a slightly different manner. Instead of RHex's design of six actuators with singular protrusions on each, each motor is attached to an assembly that resembles a five-spoked wheel with no rim (referred to as a multi-legged wheel), of which each leg is slightly compliant. This dramatically reduces the continuous out-of-phase time for each leg rotation, allowing for greater stability to the point where it operates stably with four actuators instead of six. Additionally, a passive degree of freedom was added along the spinal column to maximize ground traction in case of uneven footing. When floats are added, the platform can propel itself in the water. However, the swimming motion requires

significant disturbance of the water it is in to be achieved and can only maintain a swim speed of 0.5 body lengths per second.



**Figure 19: ASGUARD in water [26]**

ASGUARD is primarily controlled by velocity modulation, but due to the fact that it does not employ a traditional wheel design in which contact with the ground is constantly maintained, at low velocities the positioning of each leg spoke must be taken into account to maintain the desired degree of synchronization and therefore stability. This necessitated the development of a control algorithm that took error feedback between the target and the position as an input.





**Figure 20: ASGUARD [25]**

#### 2.4.5 Salamander robot [27]

The salamander's locomotion consists of both walking and swimming, of which each locomotion type uses a central spine as a primary actuator. The salamander's swimming is achieved by body undulations creating a traveling wave configuration, while walking is achieved by creating a standing wave configuration in the body, engaging small legs to help progress forward. A salamander robot was created to define the specific modifications undergone in the evolutionary process to allow this amphibious nature, explain the phenomenon of gait switching, and understand the necessary mechanisms for coordination of the limbs and spine.

Using these assumptions, a robot was created with ten actuators – four for the legs, six for the body, using a central pattern generator comprised of sixteen

oscillators as the gait basis. Relationships between each were defined by matrices of weights and phase biases, and modeled in formulae representing the phase and amplitude of any given oscillator as well as the positive signal representing the central burst action. In creating this robot, it was shown to be consistent with the actual salamander's movement in both walking and swimming. Ultimately, it is noted that the central pattern generator concepts used here would be very helpful in general robotics, given that the dimensionality of a control problem may be reduced while remaining versatile.

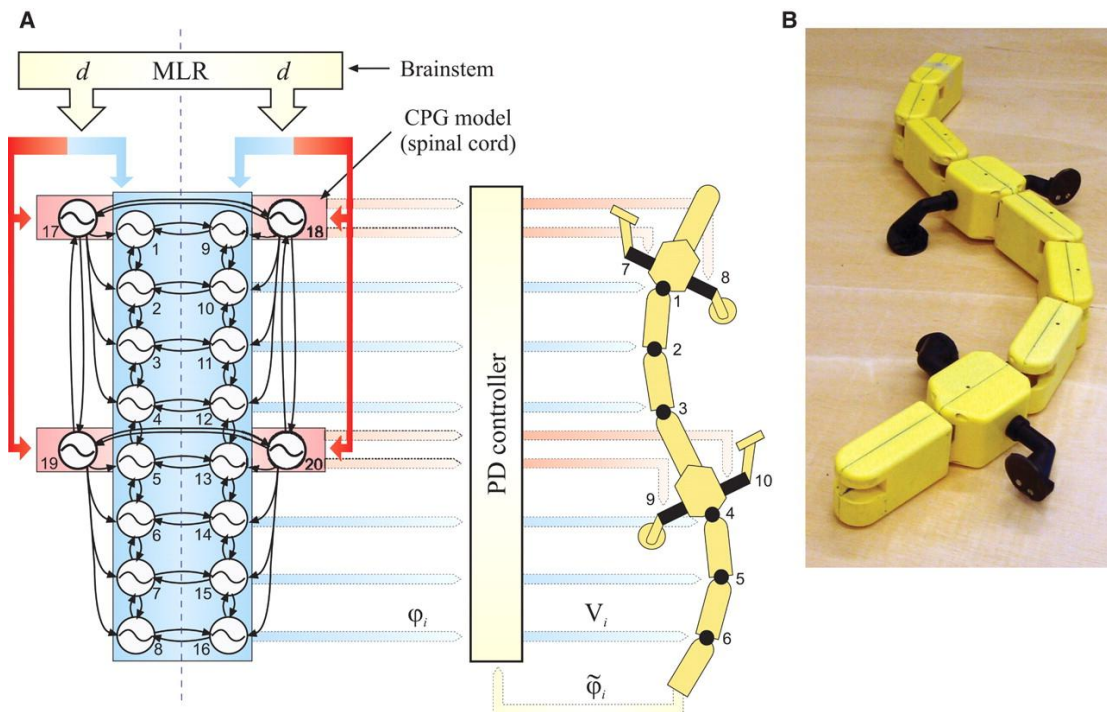


Figure 21: Salamander robot with pattern generator diagram [27]

## 2.5 Summary

Most of these selected works are specifically from robots that perform either walking or swimming. As such, those robots mostly do not conform to the initial amphibious movement goals set out in Chapter 1, though they are useful. The robots that specifically address the issue are ASGUARD and AQUA, and thus they are considered in light of the enumerated challenges.

ASGUARD absolutely addresses terrestrial movement, especially across land. Its use of four wheel-like leg mechanisms provides it ample stability and the ability to manage diverse terrains. It has no special handling for treacherous sloped environments besides speed adjustment; however, this is likely not an issue on representative slopes given the low center of gravity. Swimming, however, is a more contentious form of motion. ASGUARD's swimming motion requires high-speed rotation to maintain a reasonable speed, which is both inefficient and potentially problematic based on the environment. Obstructions such as surface vegetation can easily catch on a quickly rotating leg and jam a motor.

Conversely, AQUA is secure in its ability to swim both on the surface and underwater, and it can perform rudimentary walking on sand and similar surfaces. Its legs move between small angles, which eliminates many potential tangling issues. However, walking is not nearly as robust. AQUA's flippered feet do not move as smoothly as they could in homogenous beach-like environments, much less the irregularities of a semi-aquatic environment. Additionally, the robot has noted issues with shoreline transitions.

These considerations show that there is a niche for a robot that can perform these actions. In the following chapter, a design for such a robot will be described and tested.

## Chapter 3: Design and Construction

### 3.1 Design Evolution

The amphibious robot around which this thesis is centered has gone through several iterations between two chassis. This has refined the concept from the theoretical concept of a robot that walks and swims with legs to a functional form.

A major, if not the primary, challenge surrounding any aquatic or amphibious robotic platform is dealing with the incongruence of keeping significant electronics dry while the platform is surrounded by water. This is especially true regarding a legged platform employing servomotors. The enclosed chassis attempted to address this problem by means of encasing everything electronic in a central unit, while the waterproof servo chassis scaled down the amount of electronics inside the central unit while separately waterproofing or water-adapting external electronics.

#### 3.1.1 Enclosed chassis

The first attempt at an amphibious robot posited the concept that all electronics could be encased in one central unit. In concept, leg movement to the degree necessary for walking would be facilitated by the use of watertight membranes stretched across a cut out area in which the leg needs to move. A two-degree of freedom leg was used in the design explicitly to minimize the necessary travel area to avoid excessive membrane stretch. This leg design involved a hip servo that allowed the upper leg to swing horizontally, combined with an elbow servo that allowed the lower leg to rotate in an axis parallel the upper leg. The lower leg is fixed at a ninety-degree angle relative to the upper leg, and is flanged out to provide for surface area

for paddling in water. The leg converges to a foot at the base. This robot can be seen below in Figure 22.



**Figure 22: Enclosed Chassis Robot**

Walking is accomplished by either keeping the elbow joint in the straight-down position for the parts of the gait in which that specific leg is moving from fore to aft or actuating the rotary joint to lift the foot off the ground to recover. Swimming is accomplished by oscillating the elbow back and forth with the foot pointed toward the aft. This allowed the flanged lower leg to act as a rigid flipper and propel the robot forward in the water. The configuration for this robot can be seen in Figure 23.

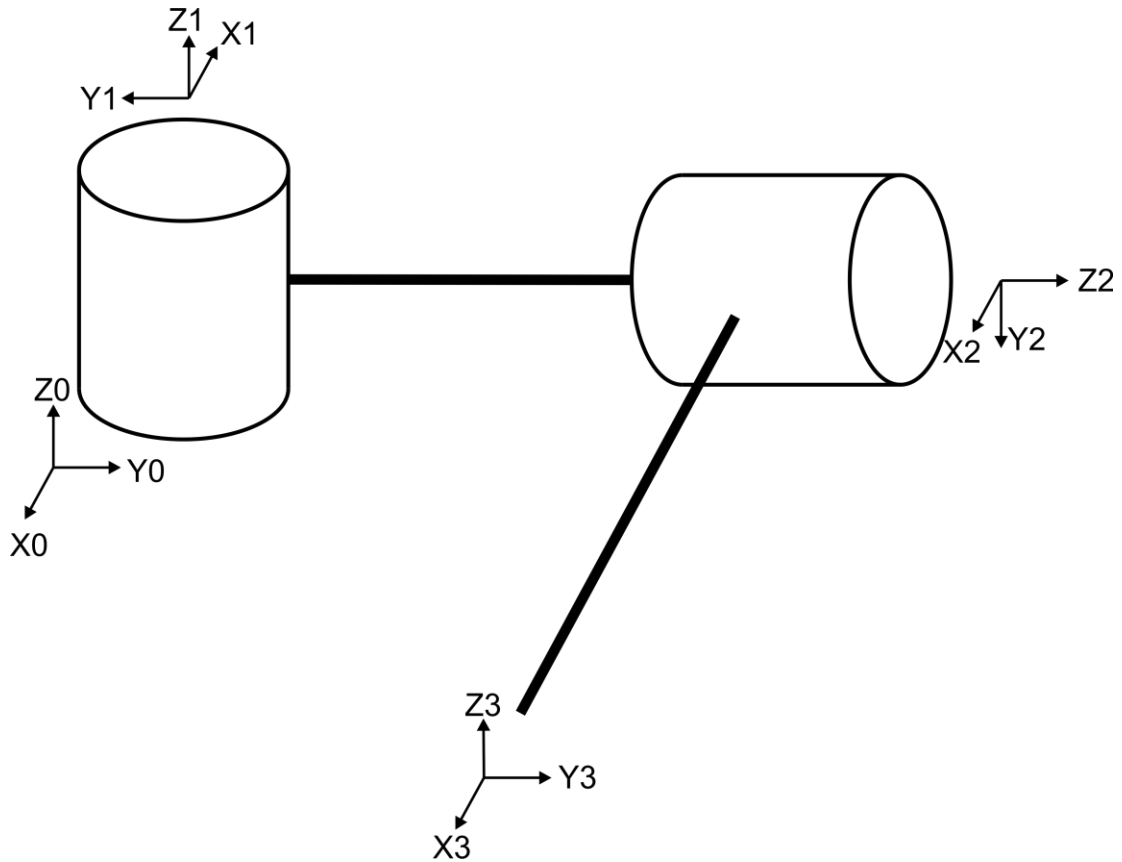


**Figure 23: Joint Configuration and Reference Frames for Enclosed Chassis Robot Legs**

In construction, the main body was converted from a plastic storage container. Pieces were cut out of the sides to make space for the legs to protrude through, and over those apertures, membranes created from rubber balloons were placed loosely to prevent water from entering while allowing for compliance. Internally, to support the servomotors, a skeleton was made from Delrin Acetal Resin. [25]

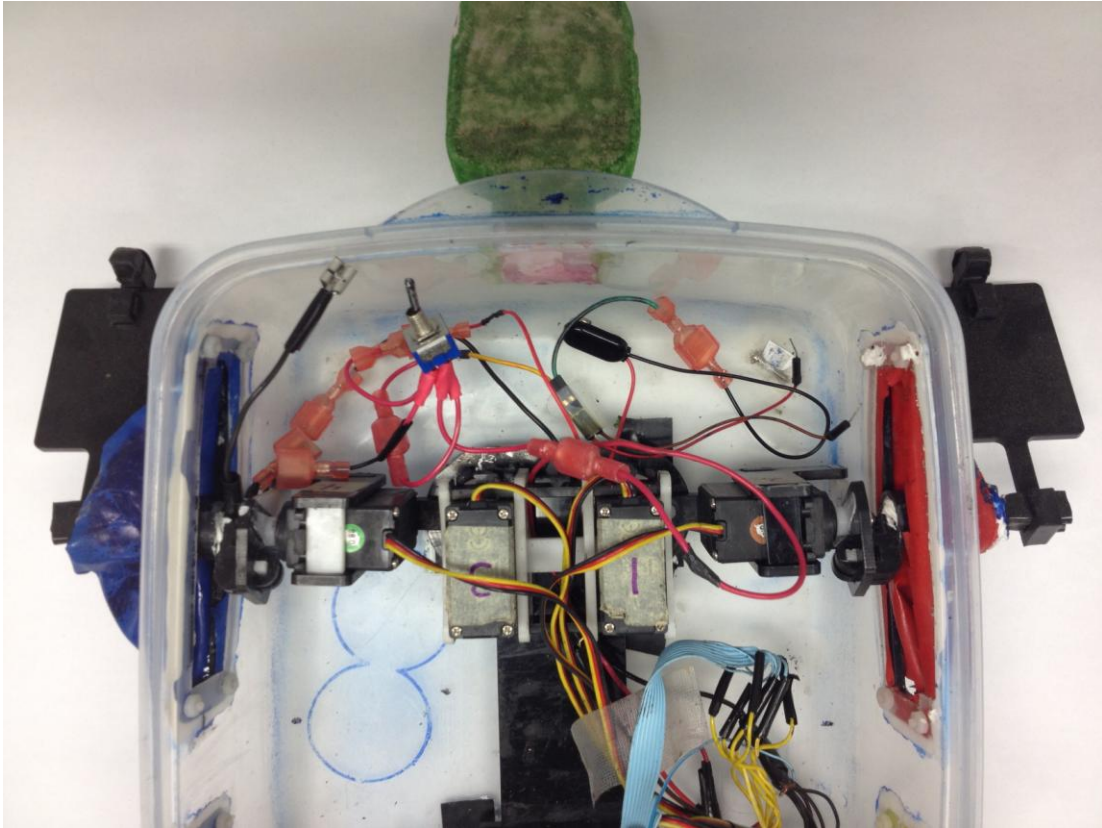


**Figure 24: Internal Physical Configuration of Enclosed Chassis Robot**

This design had several noted flaws. The primary flaw to the design was a conflict of design to maximize both walking and swimming motion. The elbow servomotor had to handle simultaneously both the moment created by vertical reaction forces due to weight and the moment created by horizontal friction from propulsion. Due to the fact that both reaction moments were based upon the distance from the hip to the contact point, longer legs put significant amounts of stress on the elbow servomotors, given that the increased horizontal distance from lifting to the same angle created a larger moment arm and greatly increased the necessary torque; any instability, some of which was unavoidable, exasperated this problem significantly and created positions in which the robot could not lift itself up, thus



severely hampering ground movement. However, due to the principles of surface area being exploited for swimming, shorter legs provided a smaller area, causing the robot not to swim as quickly or stably when implemented. This is shown below in Figure 25: the knee servomotor moment  $M$  is countered by the force from horizontal motion  $RH$  and the weight of the robot  $RL$ .

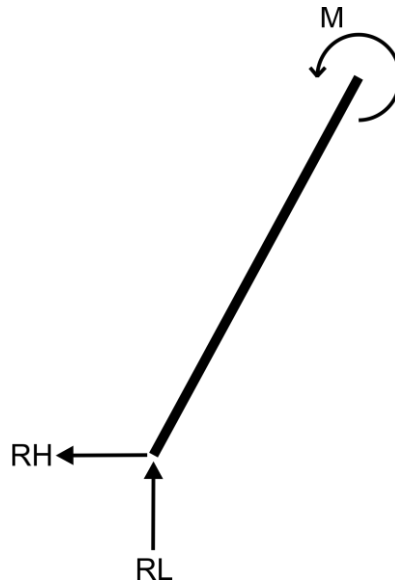


Figure 25: Free Body Diagram for Enclosed Chassis Robot Leg

To create further issues, the rubber membranes had significant, consistent issues, either with restrictive movement even with loose placement or with leakage at the leg itself or around edges. Ultimately, the combination of joint geometry creating conflicts between swimming and walking and the failure of leg membranes even in a geometrically suitable configuration necessitated a reimagining of the chassis.

### 3.1.2 Waterproof servo chassis

The second major design iteration began by considering how to tackle the issue of waterproofing and swimming with a more traditional two degree of freedom

leg design. This design was very similar to the previous, but with the elbow joint placed with its axis of rotation orthogonal to the hip joint's axis and the upper leg. This provided a method for walking that minimized the moment imposed on servomotors from weight and put the moment imposed on servomotors from friction created during propulsion at an orthogonal axis from both servomotors. This configuration can be seen below.

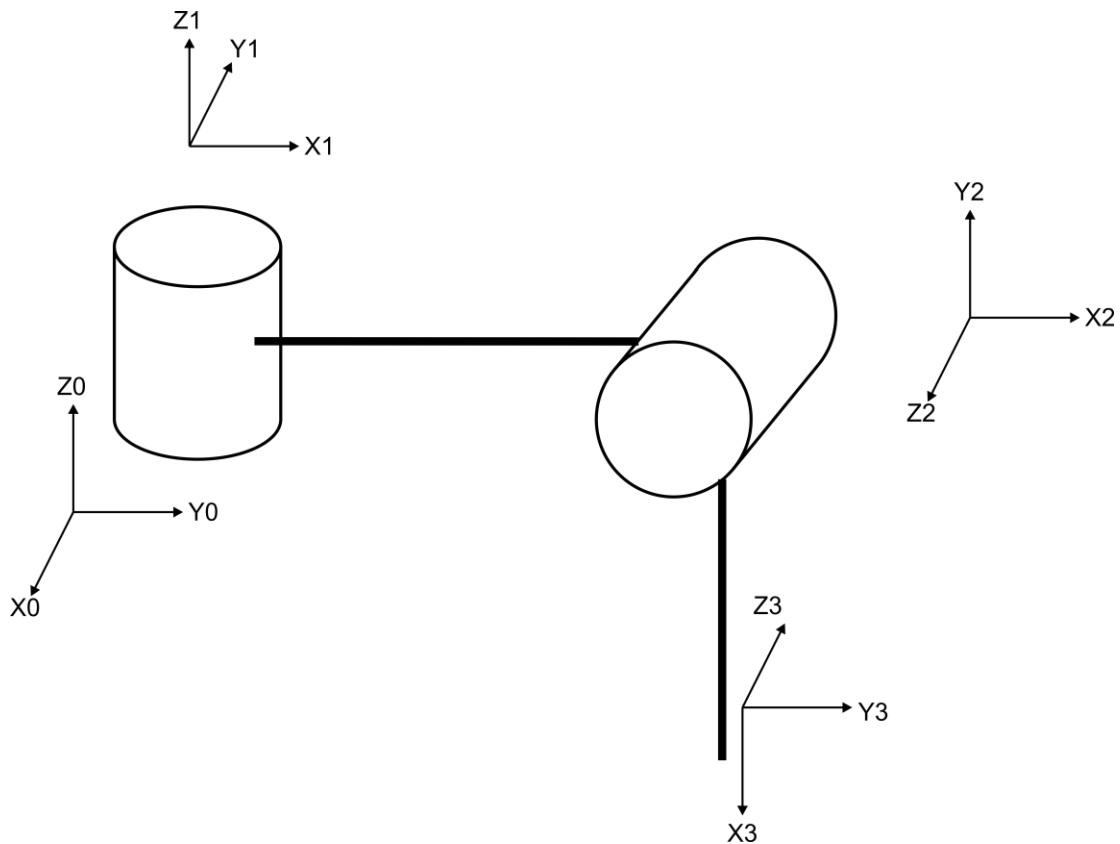


**Figure 26: Joint Configuration and Reference Frames for Waterproof Servo Chassis**

Unfortunately, this design required the elbow servomotor to be placed at a position far out from the center due to geometry. Structurally, this was simply a matter of converting the internal Delrin skeleton into an external frame with housings to hold the motors. However, a design employing fully contained electronics could

not be implemented. Instead, research into waterproof servomotors was done. As such, a simple solution was found: standard servomotors, in this case Futaba S3114 High-torque micro servomotors [26], were modified so as to be waterproof. This was accomplished in a three-step process. First, the compartments of the servomotor without moving parts would be filled with liquid silicone, so as to protect valuable electronics. Second, the exterior of the servomotor would be coated with Plasti Dip synthetic rubber [27] to preserve the moving parts inside the main compartment of the servomotor. Third, a rubber O-ring was placed on the seam where the shaft of the servomotor moves to prevent water entering via the servo shaft. While this method worked to an extent, the servomotors suffered a significant failure rate after short periods of time. The O-rings required to maintain shaft sealing placed too much resistance on the servomotor while in motion, which would eventually lead to gears within the servomotors failing.

The solution was to seek out a pre-waterproofed servomotor model, instead. The resulting move to a larger motor, the Hitec HS-646WP [28], necessitated a moderate structural change to accommodate the larger size. Specifically, the motor position was rotated so as to fit lengthwise at the hip joints, and the elbow joints were enlarged to accommodate the larger size.

### 3.2 Physical specification

#### 3.2.1 Components

As mentioned earlier, Delrin Acetal Resin [25] was chosen as the primary construction material. Delrin is a thermoplastic polymer with some significant advantages. It has high tensile and compressive strength, it resists water well, and it

has significant fracture and fatigue resistance. It is available in sheet form, of which 1/8<sup>th</sup> inch and 1/4<sup>th</sup> inch thick sheets were used for the construction of this platform. The custom frame components required were designed in Pro Engineer and manufactured using a Universal Laser Systems VLS3.60 Laser Cutter [29], which has a 60-watt laser. This laser was accurate enough to manufacture the small parts necessary.



**Figure 27: Delrin Acetal Resin Sheet [25]**

Initially, a small project box was selected arbitrarily; however, this proved of insufficient size for the components and wiring inside, and waterproofing proved insufficient. As such, a larger, more deliberately waterproof box was required. Hammond Manufacturing's 1554UGY [30] enclosure was eventually selected for this. At 7.9" x 4.7" x 3.5" it was sufficiently big for all electronics required for the robot's operation, and the lid was designed with sealing in mind.



**Figure 28: 1554UGY Plastic Enclosure [30]**

The servomotors eventually selected were the HS-646WP Analog Waterproof High Voltage Servos. These servomotors have an average weight to torque ratio and operate at a relatively low speed, but are waterproofed well. They have the capability to be driven by a 7.4V battery for extra torque and speed, if necessary, but in this case, they were considered and selected based upon their operating parameters at 6V.



**Figure 29: HS-646WP Analog Waterproof High Voltage Servomotor [28]**

To send signal to the motors and engage in gait switching, an Arduino Mega 2560 microcontroller [31] was employed. This microcontroller features numerous digital and PWM outputs, a simple programming method due to a USB plugin port, and a cross-platform client to program behavior. The Arduino uses a functional programming language based on C and C++ that is very powerful and easy to prototype. Additionally, the model used, the Mega 2560, boasts a large range of digital and PWM ports so as to enable easy switching in case of a pin failure.

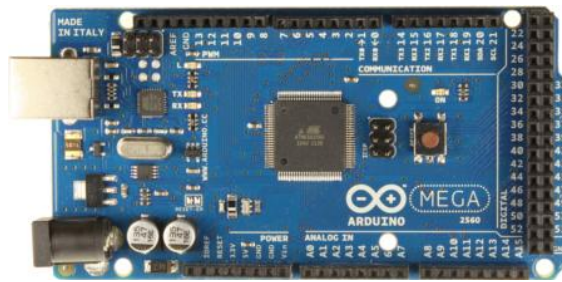


Figure 30: Arduino Mega 2560 [31]

To power the servomotors and microcontroller, two battery packs were selected. One is a Tenergy 6V 2000mAh NiMH battery [32], and the other is a standard alkaline 9-volt battery. The former battery is inexpensive, capacious, and has a very large output potential to account for the case of stalled servomotors. The C-rating, which denotes the potential discharge rate, is 10C, which signifies a maximum safe discharge of 20A. Given that the servomotors can potentially discharge 2.5A each, this value would be matched in the unlikely occurrence that each motor is stalled. The more typical loaded motor values are approximated at 1A each for a total of 8A; assuming each motor is fully loaded, this amounts to a fifteen minute runtime. This suffices for the short-term usage in development and testing;

however, a more capacious battery will be required for more long-term operation. Mechanically, weight concerns are the primary reason not to upgrade to a more capacious NiMH battery.

The robustness of NiMH batteries is a good fit for the adverse conditions that the inside of an amphibious robot could potentially be subjected to upon failure. The second battery selected is a battery solely for the sake of powering the microcontroller. The Arduino can accept input voltage from 6-20V, but it is not recommended to stray past the 7-12V limit, and specifically a 9V input is recommended for optimal performance. Any sudden increases in current also have the potential to damage the microcontroller if connected to the same power source as the servos.



Figure 31: Tenergy 6V 2000mAh NiMH battery [32]

### 3.2.2 Sensing and electronic circuit design

To allow for autonomous gait switching, an important aspect of this robot's operation, four water sensors were necessary. Two of these sensors were placed just under the floating waterline, and two were placed at the bottom of the robot. Given that there were four of them, the sensors needed a lightweight and efficient solution.

This came in the form of acknowledgement of the Arduino's capabilities in reading simple signals in combination with basic electrical conductivity properties.

The sensor created is a combination of a 10 kΩ resistor and several pieces of wire. A digital pin is connected to both a grounded terminal by way of the aforementioned resistor and a discontinuous wire connected to the Arduino's 5V output. The 5V wire's discontinuity is exposed to the outside, with wire ends close. This acts as a switch: if the area where the ends were located were to be submerged, the circuit would close and the digital pin would be shorted directly to 5V. This creates a situation where the digital pin is either 0V or 5V, which allows it to be treated with Boolean logic in the code.

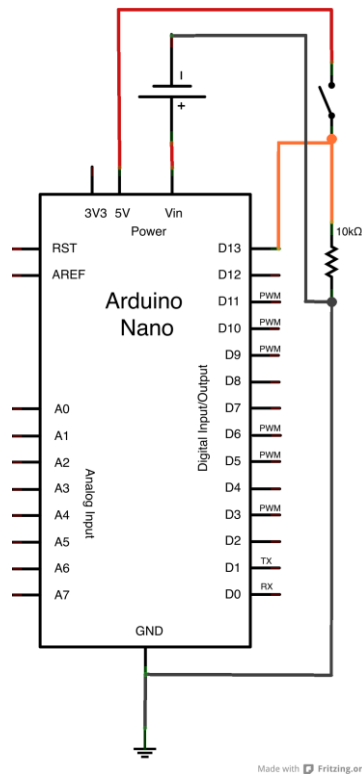
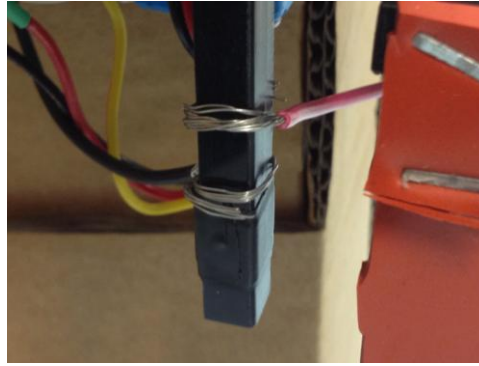


Figure 32: Water sensor circuit modeled on Arduino Nano





**Figure 33: Lower water sensor on robot**

The circuit as a whole handles four water sensors and eight servomotors. Where appropriate, pins were connected by means of jumper wire. Pin connections were spaced out where appropriate to avoid any issues with overcrowding. Regardless of precautions, due to the sheer volume of wiring inside the box, pins would often become bent or snapped off, which was a noted reliability issue.

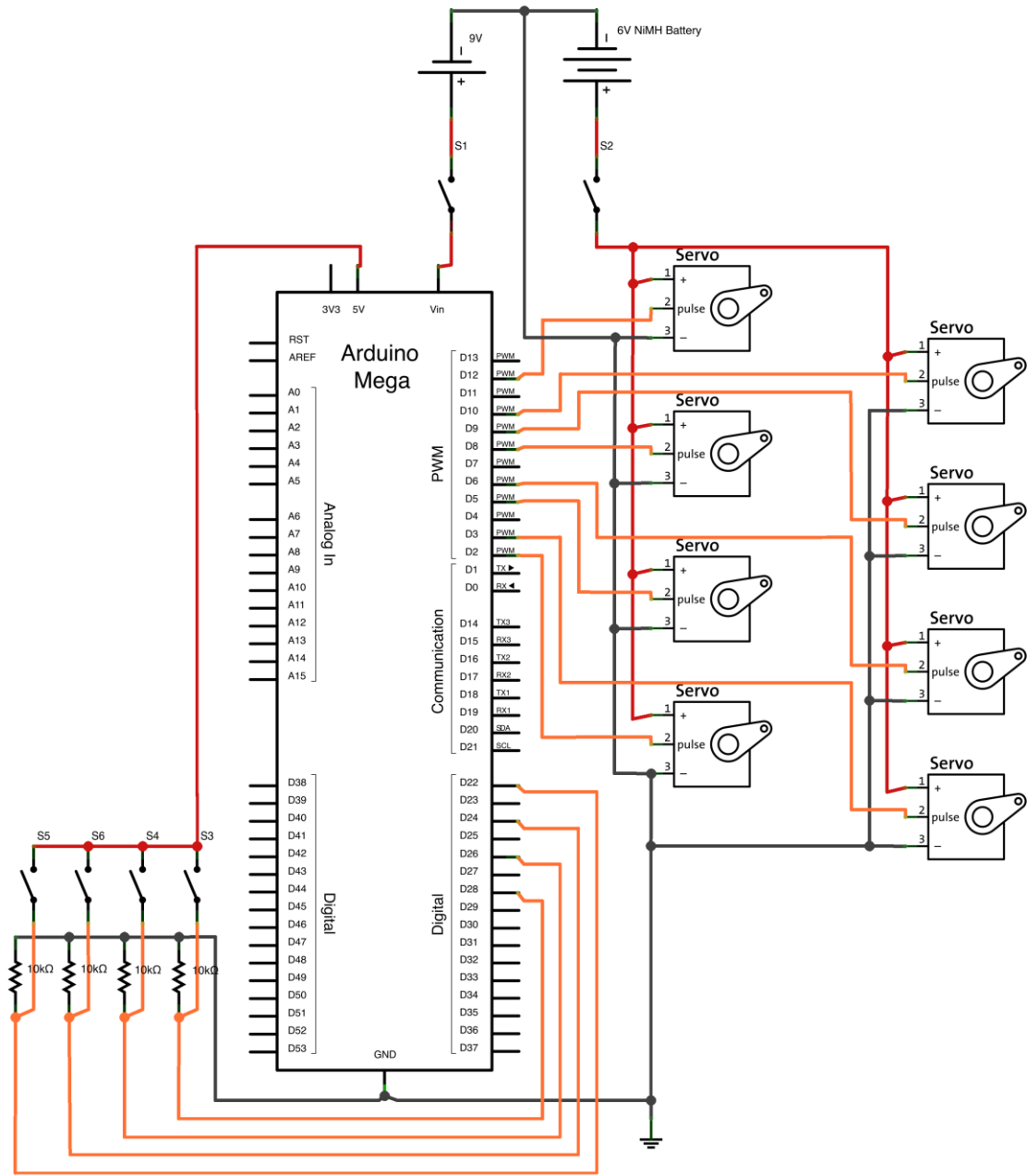


**Figure 34: Full robot circuit**

### 3.2.3 Physical design

Structurally, the robot is built around the two factors of the central enclosure and the leg configuration. Everything is designed to support the servomotors in the leg configuration while remaining as light as possible. In addition, the manufacturing

constraints imposed by the use of the laser cutter require each assembly to be comprised of flat components.

To support the servomotors properly, besides simply holding the motors in place, the hip and knee joints must avoid a situation in which the servomotor spline acts as a cantilever weighted down by the protruding leg piece. Combating this involves providing support from the end of the spline. This was relatively simple for the hip joint, but complex for the knee joint due to the need for a self-supporting structure. The configuration shown below in Figure 35 was the eventual solution. The motor is supported on top by the upper leg structure and below by a horizontal tab. Two plates that slide onto the upper leg constrain the servomotor's sides while providing support for both the lower tab and the spline support. At the spline, the motor is prevented from cantilevering by means of a brass rod press-fitted into the spline support. This rod slots into the front of the servomotor horn, which in turn is screwed into the servomotor. To prevent motor slippage, each was coated with Plasti Dip around its sides before being put into place.

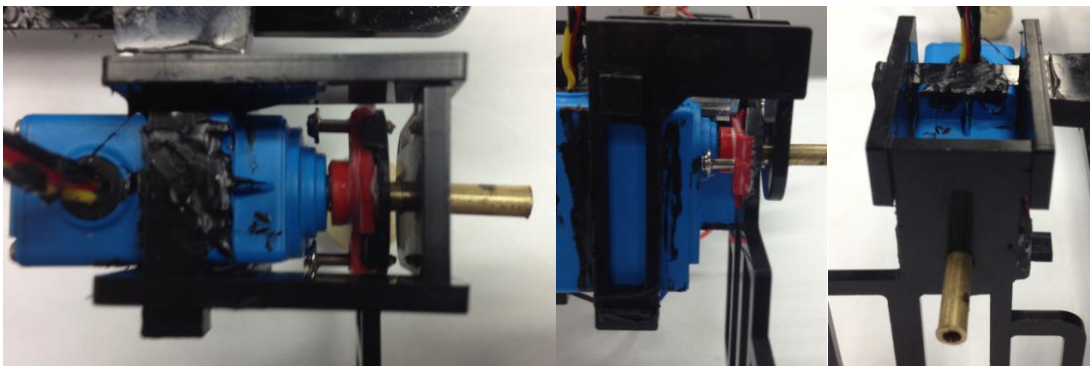


**Figure 35: Knee Joint Construction**

The leg design itself was developed from a relatively simple construct in the earliest configurations to the most novel component of the design itself as configurations progressed. The eventual leg type that was settled on employed compliant rubber to make up for the less advantageous design. Compliance, in this case, was added to allow the legs to produce a greater differential force on the forward stroke than the backstroke. The legs were created with a large central aperture, over which a compliant rubber flap was draped. During forward thrust, the rubber is pressed flat against the frame, providing resistance for the water; during the recovery stroke, it is allowed to flap back due to the oncoming water, providing less resistance. An illustration of this is shown in Figure 36.

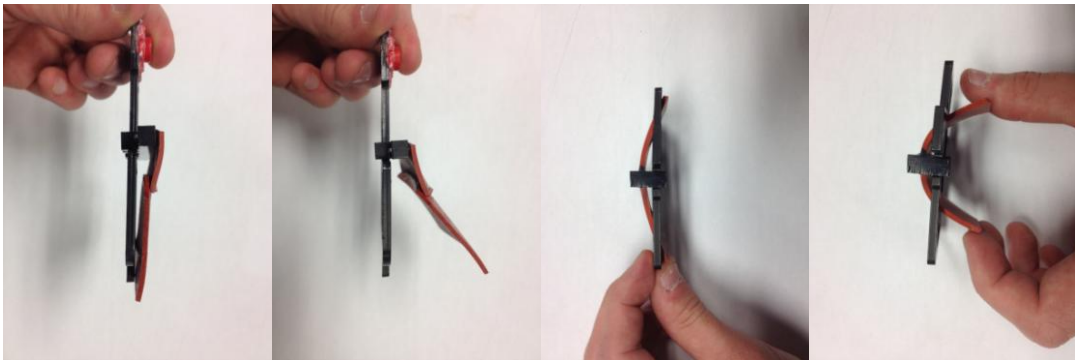


**Figure 36: Horizontal and Vertical Leg Configurations Demonstrating Forward Stroke and Back Stroke**

Non-rigid rubber sheets can often tear in use, which provides a problem when attached semi-permanently. In the spirit of both avoiding this and allowing for ease in experimental testing, the compliant flap was designed to be attached by means of a snap-on pillar in a modular system. Two leg designs were conceived: one employing a vertical pillar, one employing a horizontal pillar, referred to as vertical and

horizontal leg configurations. Experimental and simulation-based testing would then decide the worth of these possible configurations.

### 3.3 Experimental Leg Testing

The compliant flaps on the legs are the most novel component of the robot's design. As such, significant testing was required to weigh the various approaches to creating legs with compliant flaps. A major component of this testing was experimental in nature.

#### 3.3.1 Overview

The testing performed looked to isolate several factors. The first factor was the rubber used in the flaps themselves. To test this, eleven samples of silicone rubber were selected with thickness of either 1/32<sup>nd</sup>, 1/16<sup>th</sup>, 3/32<sup>nd</sup>, or 1/8<sup>th</sup> inches and hardness between 10A, 40A, or 60A durometer. Flaps of 3/32<sup>nd</sup> inch thickness and 10A durometer hardness were not included due to their unavailability from the same supplier as the other flap types. These samples were integrated into two different types of legs with their axis of compliance in either a horizontal or a vertical direction.

Leg positioning and configuration were also considered as major factors. Each flap and leg design was positioned in configurations specifically to test its efficacy on either the front of the robot or the back of the robot, and with the motor positioned either towards the outside of the robot or the inside.

Once data was collected from these, important information would be taken from the best flap designs' performance and used in a fluid simulation.

### 3.3.2 Setup

The robot was placed inside a tub of water with the two legs closest to the tub's wall removed; this would avoid issues of interference and allow for isolation of back propulsion and front propulsion. To measure force output, the robot was connected to a 5lb force sensor, which was, in turn, clamped to the side of the tub. This created a testing setup that had roughly one degree of freedom. The testing setup accounted for vertical bobbing motion in the sense that the force sensor was clamped while the robot was floating at its equilibrium point in the water. This was an effective deterrent for thinner flaps, but as flaps grew thicker and propulsion distance increased this was the cause of significant variation in measurement. Horizontal motion was not restrained in any explicit way; however, the symmetry of the design limited significant drifting in testing.

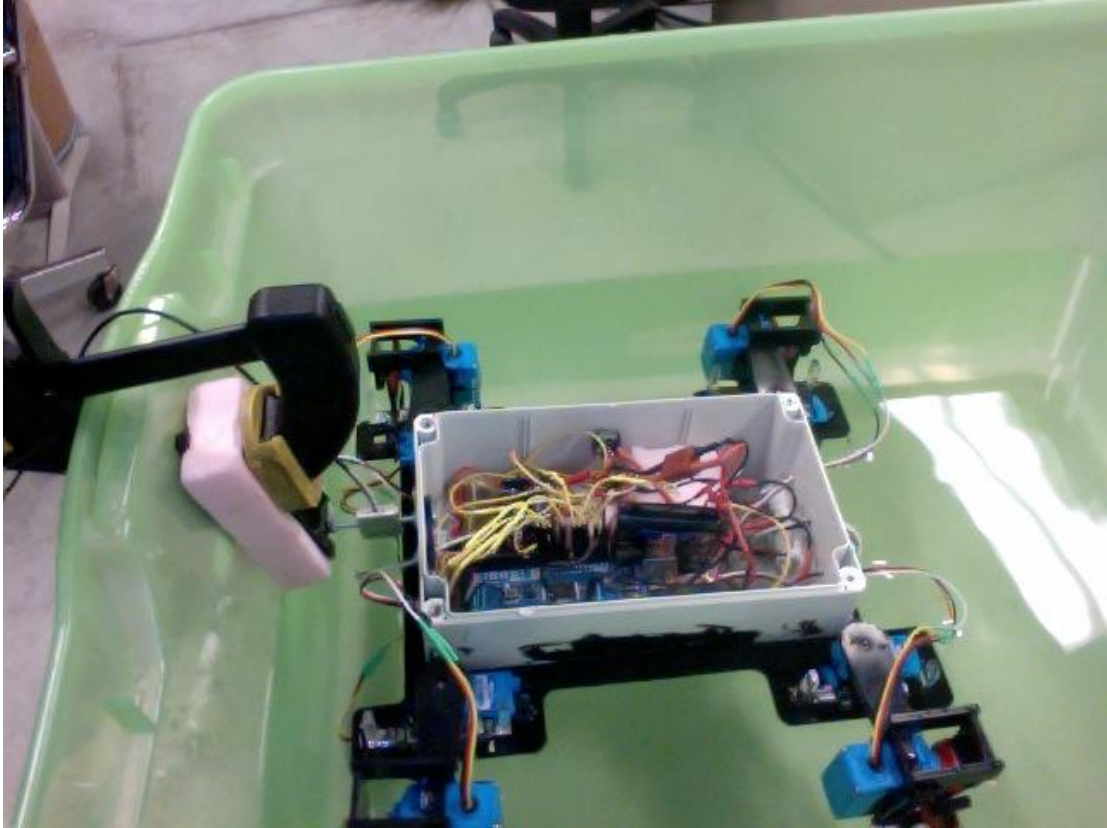


**Figure 37: Robot in test chamber**

The force sensor's output was input via a data acquisition (DAQ) card to a computer running LabVIEW. A LabVIEW virtual instrument was created to accept the raw input as a voltage for processing. This input had a source of 60 Hz noise on it, which was mitigated by an inline 5<sup>th</sup>-order 60 Hz Butterworth filter; following filtering, the filtered output was sent to a Microsoft Excel worksheet.

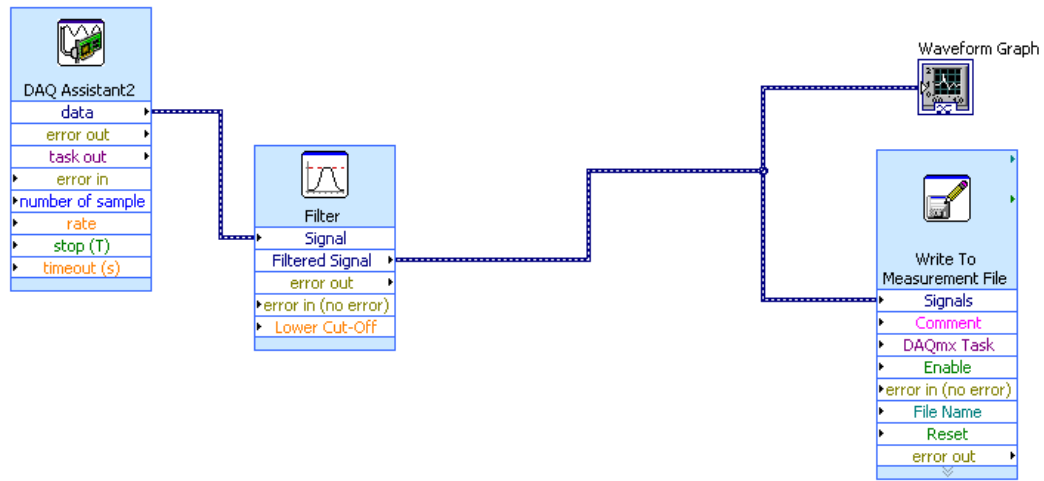


**Figure 38: LabVIEW block diagram**

Given that testing would involve significant amounts of flap switching, two types of leg subdesigns were created that would accommodate vertical and horizontal orientations with modularity in mind. The flaps of rubber were stapled to thin Delrin columns that were then fitted as necessary for testing onto the legs. Given that each subdesign was created to be potentially reversible, each could be used to represent front or back legs as the specific test required simply by reversing the column.



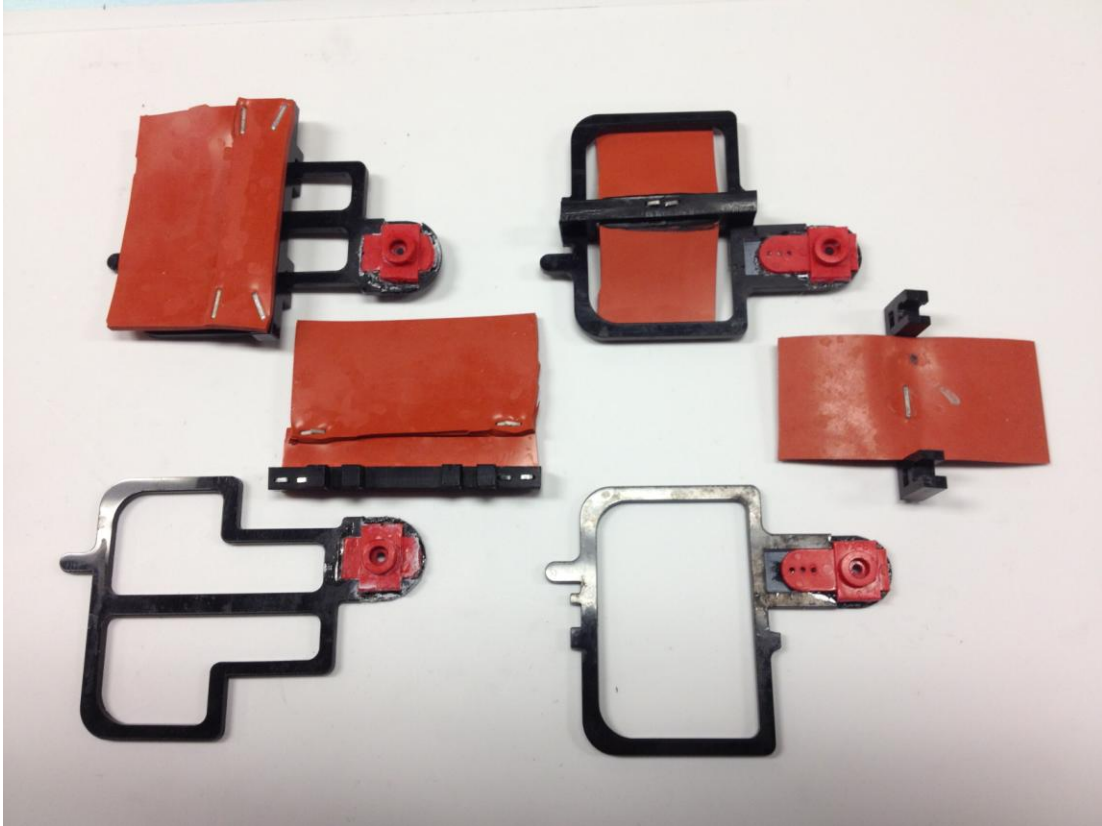


**Figure 39: Horizontal and vertical leg and flap assemblies**

The series of modular vertical and horizontal flaps, as well as the reversible nature of the flap placement, accounted for testing of flap rubber hardness, flap rubber thickness, and the set of legs in question. A fourth attribute was taken into consideration as well: specifically, the directionality of the motor spline, which thanks to the reversibility of the motor mount could easily be turned inward. While it was considered that inside-leg configurations could be potentially troublesome from the perspective of walking stability, the potential for useful results from collecting the data was deemed high, and as such each flap hardness, flap thickness, and leg pair was tested with both outside and inside configurations.

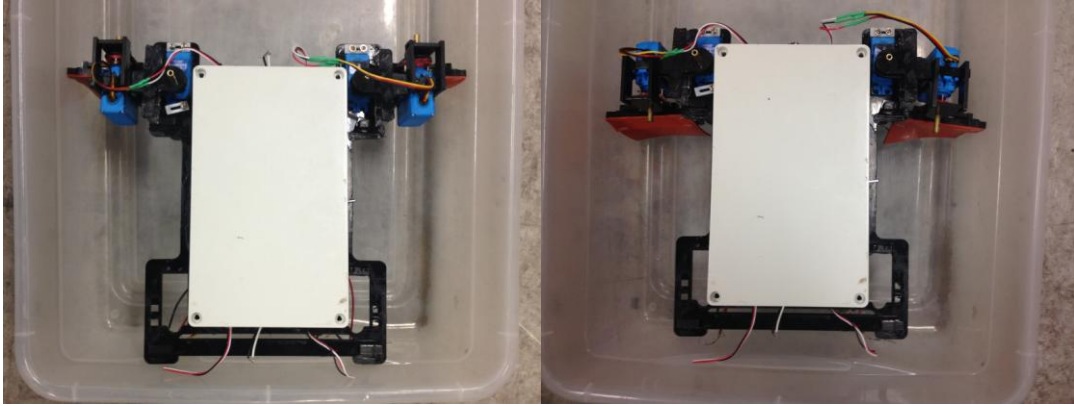


**Figure 40: Demonstration of outside (left) and inside (right) configurations**

Each set of legs and configurations was oscillated at approximately 2.34 Hz, rotating back and forth from -30 to 30 degrees. As mentioned previously, ten seconds of oscillation were recorded. The first second of each ten second recording was deleted to ensure initial unsteadiness would be minimized. Additionally, the force sensor was tested under various measured forces to determine the transfer function between output voltage and actual force to be used with each data set.

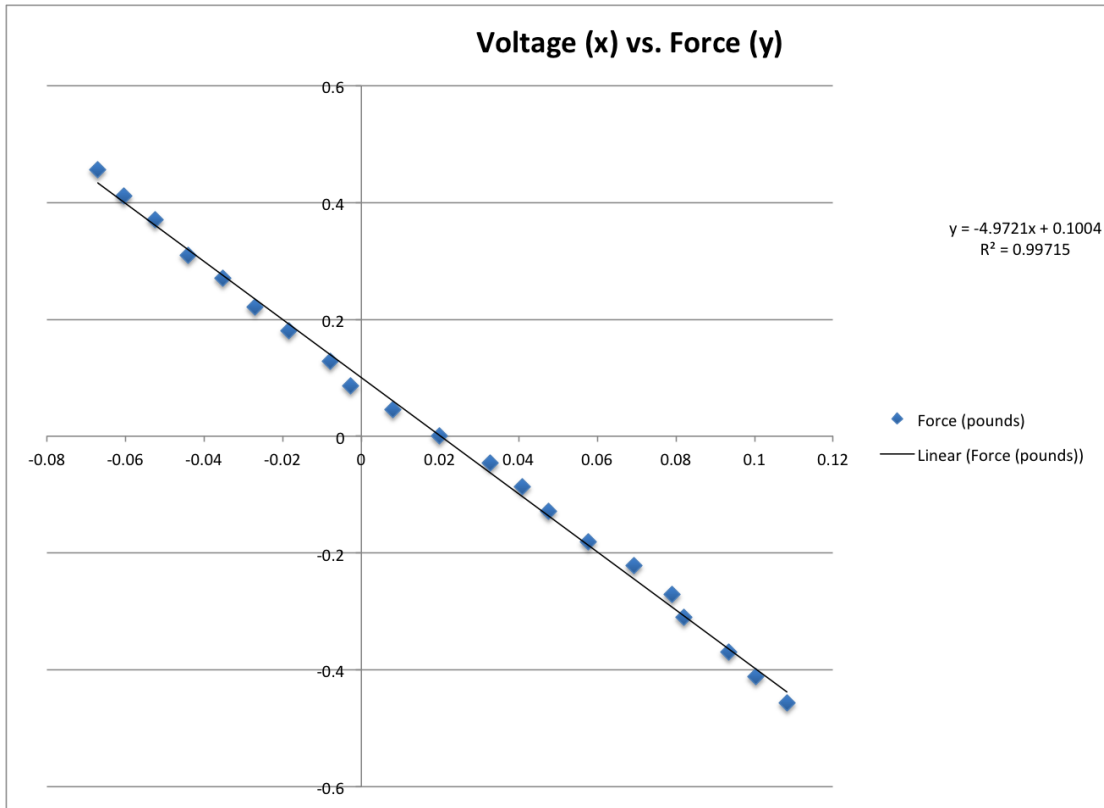


**Figure 41: Baseline data and the resulting transfer function**

The data was expressed in a form as below in Figure 42. Similar data from each combination was averaged to produce the results for the rest of this section.

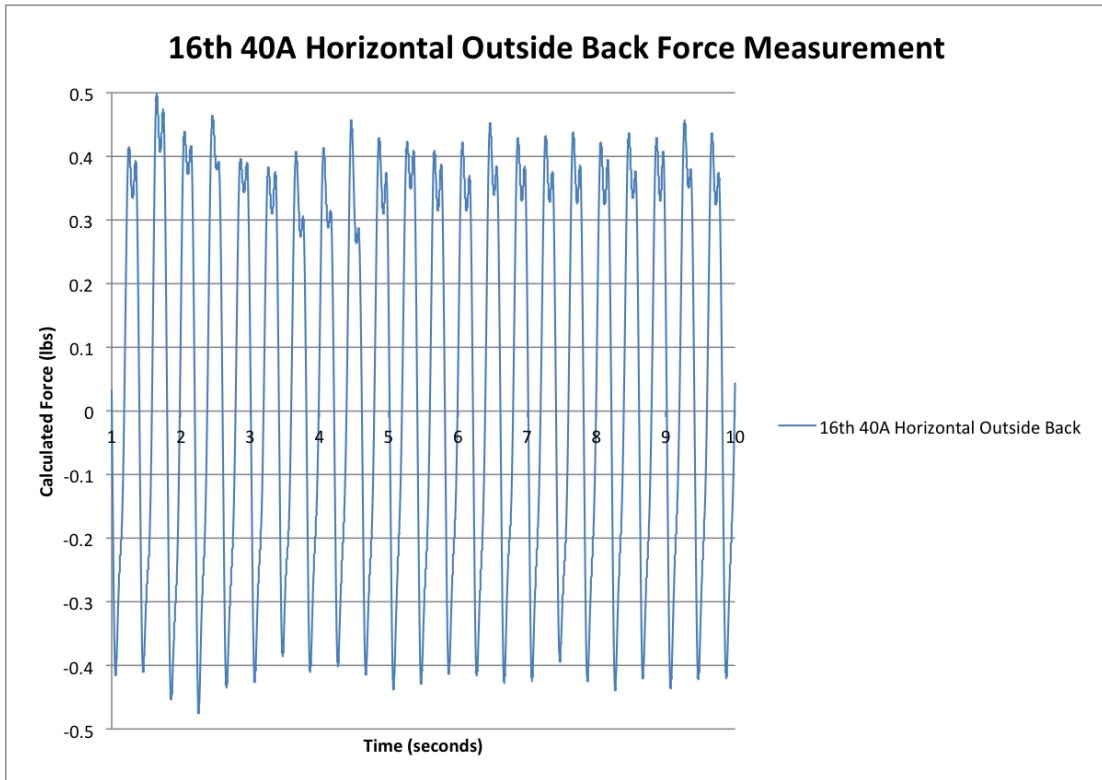


Figure 42: Sample Data from 16<sup>th</sup>/40A/Outside/Back

### 3.3.3 Horizontal and Vertical Comparison

The first comparison to be made is between propulsion from the horizontal and vertical flaps. The graphs below are displayed in order of thickness and hardness in the X-direction – thus, the first data point is at 10A hardness and 1/32<sup>nd</sup> inch thick, the second data point is at 40A hardness and 1/32<sup>nd</sup> inch thick, and so on. Each data point represents the average of 9,000 individual samples, displayed in pounds. The connecting lines between each data point are for visual comparison of trends and do not represent any form of interpolation.

The clearest comparison that can be made is the stratification of the vertical leg data compared to the horizontal leg data. Each vertical leg represents a clear tier of performance, while in comparison the horizontal leg data is more intermingled,

with only one data set noticeably superior. What is also noteworthy is the manner in which the vertical legs stratify. The two best are outside back and inside front, which differ from the two worst in that the propulsion direction aligns with the motor spline. Thus, the motor housing is on the opposite side of the direction of propulsion, which suggests that the housing significantly diffuses propulsion force, a fact which is consistent with the slightly less stratified peak and trough force averages.

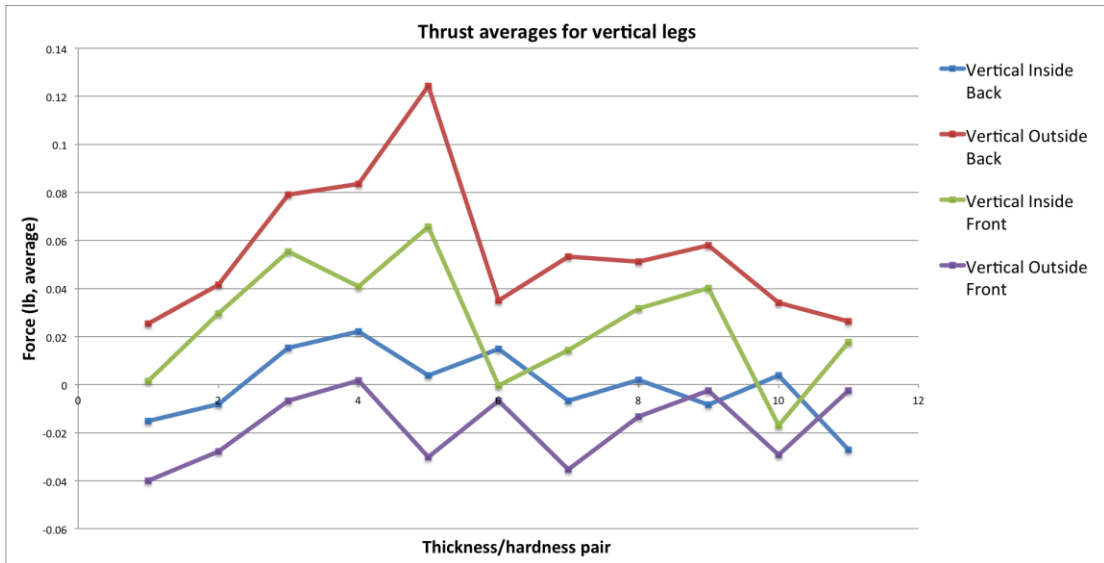


Figure 43: Thrust averages for vertical legs

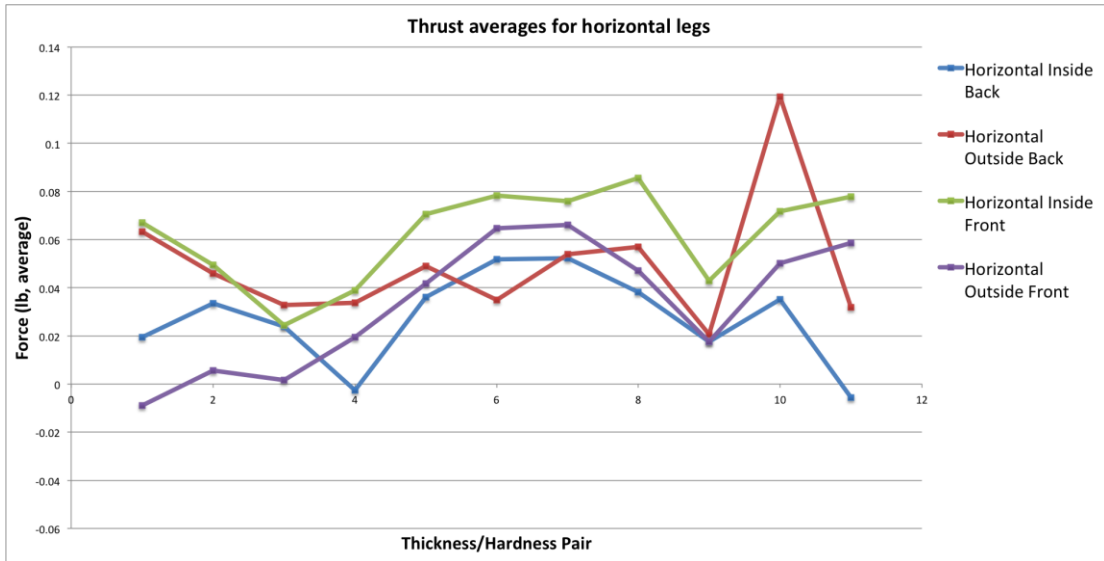
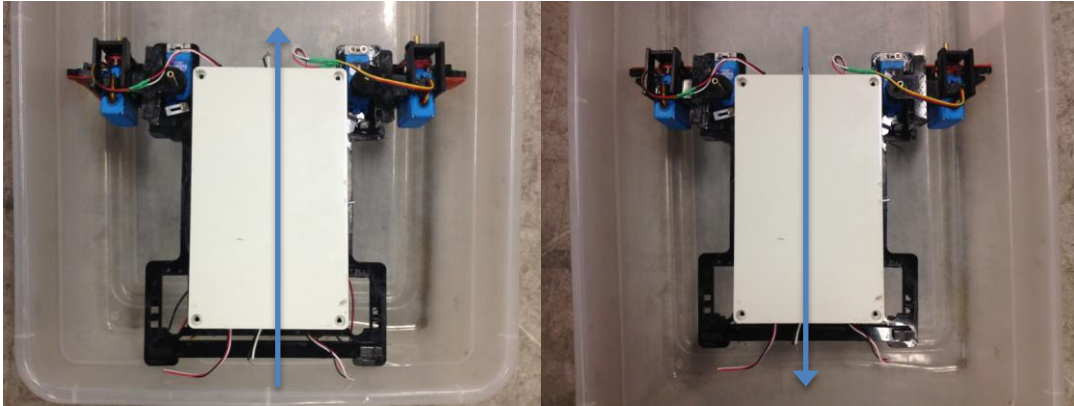


Figure 44: Thrust averages for horizontal legs

### 3.3.4 Front and Back Comparison

The idea to test front legs and back legs separately stemmed from the fact that turtles and platypuses are both bipedal swimmers – that is to say, propulsion is performed via two legs instead of four. This would test whether there was merit to using one set of legs instead of two for this design.

To test front legs compared to back legs, the robot was not rotated in place. Instead, the two actively tested legs had their compliant mechanisms reversed, and the transfer function was given a negative value to correspond to this reversal. Due to the linear nature of the force sensor response and the near symmetry of the robot’s geometry, this was considered a reasonable approximation. This is illustrated in Figure 45 below, in which the overlaid blue arrow represents the direction of recorded forward thrust.



**Figure 45: Outside front and outside back configurations relative to tub wall**

The general conclusion is that there is not a significant difference between the two data sets, outlier sets aside. As such, it is not specifically disadvantageous to employ a four-legged method of locomotion, due to the fact that neither leg location is particularly worse than the other. An interesting correlation can be seen in that the best two front legs are inside configuration, while the best two back legs are outside configuration. This will be discussed in more detail in the next section.

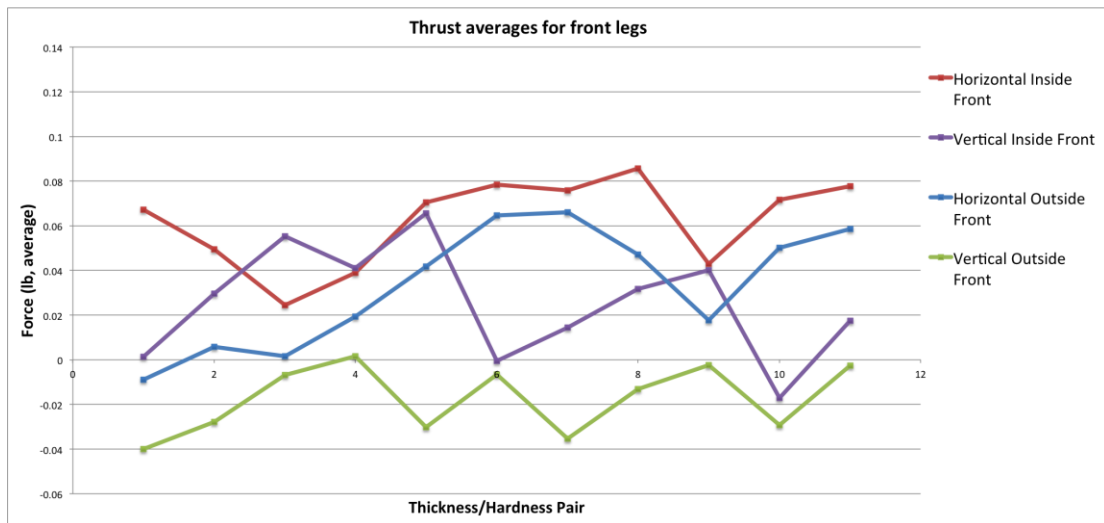


**Figure 46: Thrust averages for front legs**

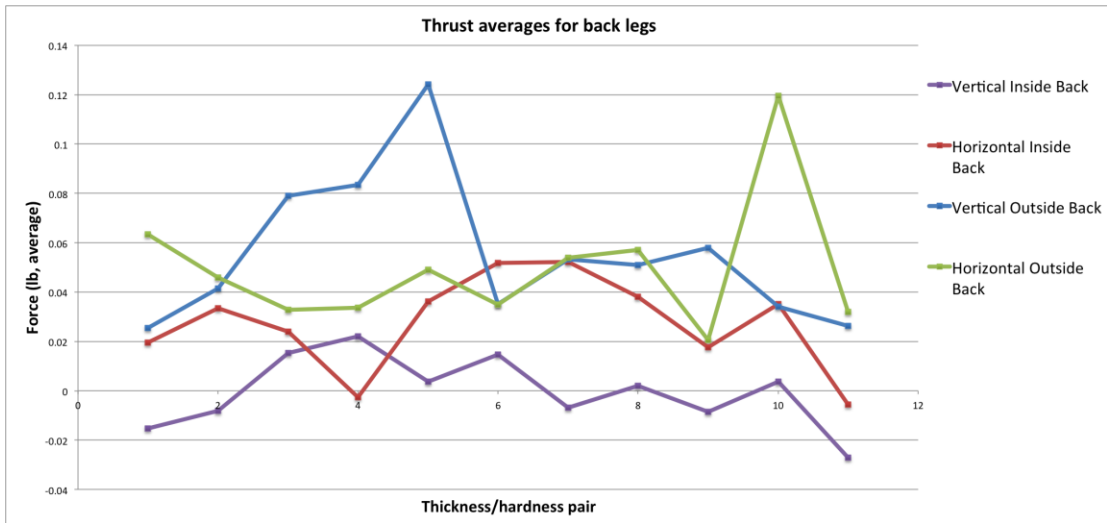


**Figure 47: Thrust averages for back legs**

### 3.3.5 Inside and Outside Configuration Comparison

Outside configurations are well known to be more stable for walking than inside or mixed configurations, due to a wider stance. However, there is little data on the difference between an inside and an outside configuration for swimming. The data is therefore examined for the purpose of determining whether inside configurations have any advantages in swimming due to side effects from the geometry.



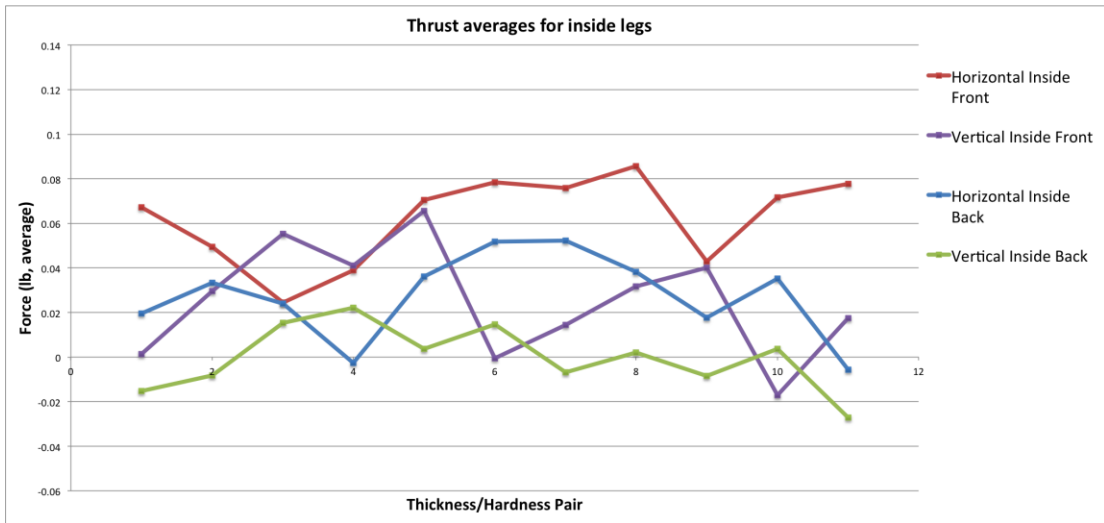


Figure 48: Thrust averages for inside legs

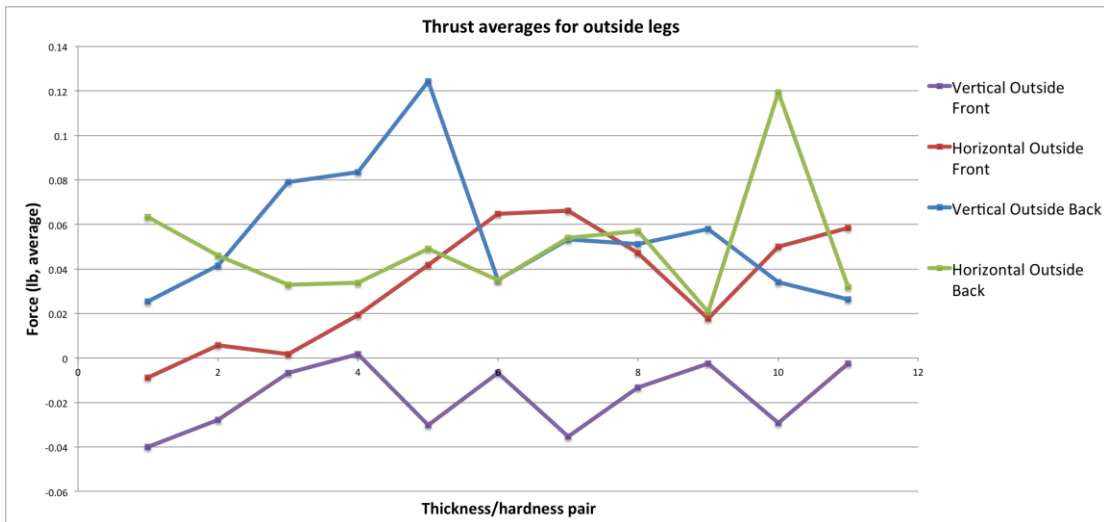


Figure 49: Thrust averages for outside legs

As mentioned before, the best front-legged configurations are inside configurations, while the best back-legged configurations are outside configurations. This is further reinforced by the findings from vertical and horizontal differences, which saw much the same conclusion in the stratification of the vertical legs and, to a lesser extent, the horizontal legs.

### 3.3.6 Peak-trough distance comparison

Of additional interest is the peak-trough distance. This distance is the difference between the average peak values – the maximum force recorded during a thrust and average trough values – the minimum force recorded. This measure gives an idea of the efficiency of the propulsion method, as a sufficiently high peak and low trough to maximize peak-trough distance signify both a heavy forward stroke and a heavy backward stroke, both of which require significantly more energy for the same net forward distance than a smaller forward and backward stroke.

The peaks and troughs were calculated from each data set by examining the periodic nature of the data. Due to each data set having the same periodicity, a typical period of 428 points was determined by dividing the total 9000 data points by the visually determined 21 displayed peaks. Taking a local maximum and minimum every 428 points created a set of 21 maximum and minimum values that were then averaged to create a mean peak and mean trough for each configuration.

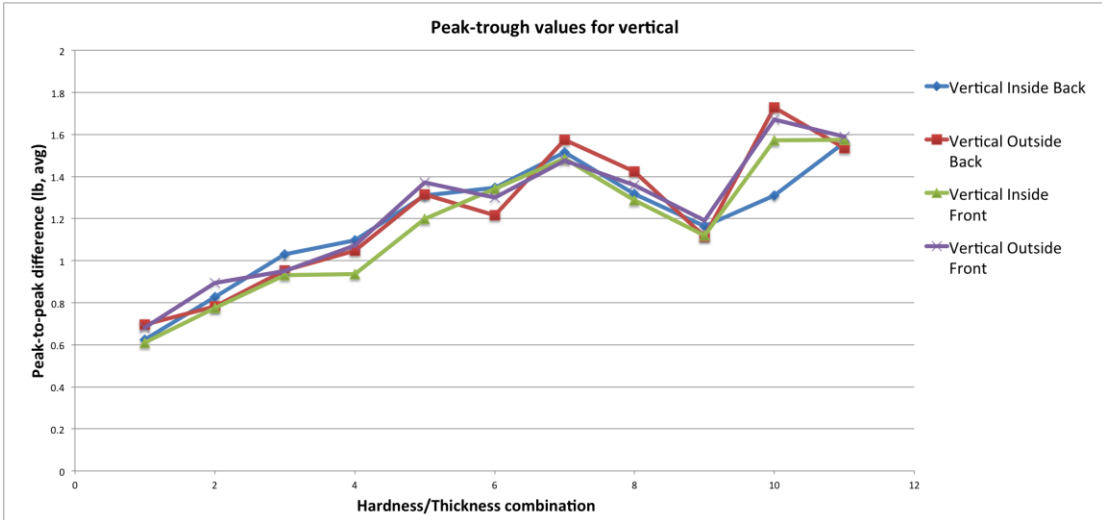


Figure 50: Peak-trough distances for vertical configurations

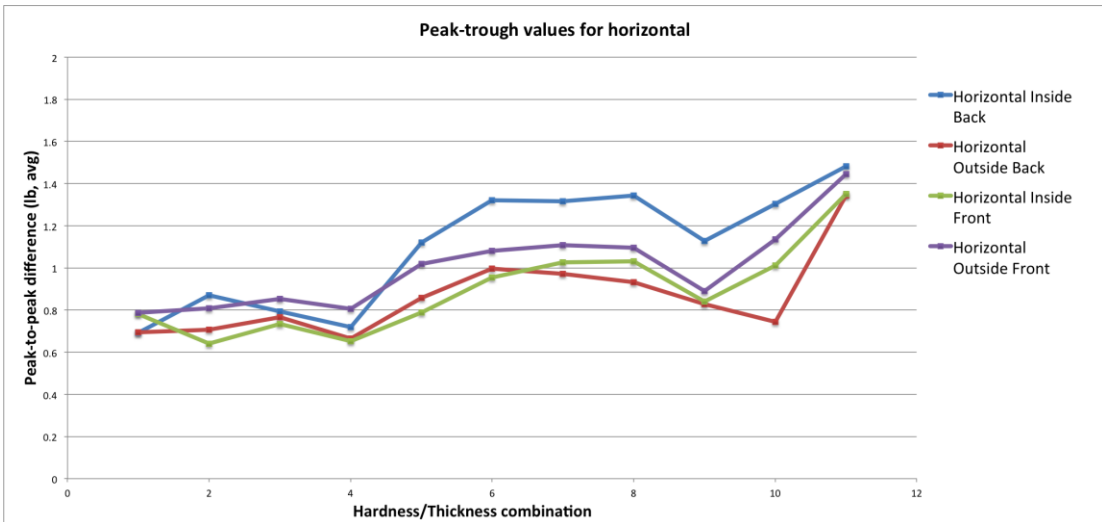


Figure 51: Peak-trough distances for horizontal configurations

Each of the horizontal and vertical sets are relatively uniform within each set, with Horizontal Inside Back being the one real outlier. The general trend is upward from the thinnest and softest to the thickest and hardest rubber, which was expected. This follows the observation during testing that as thicker and harder rubber pieces were tested, there was less compliance during oscillation. Thus, when rubber is

thicker and harder, it more resembles a rigid component than a flexible component. Likewise, the thinner and softer pieces were observed to comply considerably. In the most extreme cases, this had the effect of significantly reducing the total thrust, which is reflected in the lower average force as well.

Interestingly, there is a sharp drop at point 9, which corresponds to the drop between  $3/32^{\text{nd}}$  inch, 60A rubber and  $1/8^{\text{th}}$  inch, 10A rubber; similar, smaller dips can be seen at points 4 and 7, which correspond to  $1/16^{\text{th}}$  inch, 10A rubber and  $3/32^{\text{nd}}$  inch, 40A rubber both compared to preceding 60A rubber pieces. While thickness and hardness both increase peak-trough distance, the conclusion that can be drawn is that an increase in hardness generally creates a more precipitous change than an increase in thickness.

### 3.3.7 Conclusions

Ultimately, some interesting results came from this series of tests and comparisons. In general, vertical legs are more stratified and less efficient than horizontal, and inside-configuration legs perform better as front legs while outside-configuration legs perform better as back legs.

Three particular pairings seemed to stand out:  $1/16^{\text{th}}$  inch, 40A durometer for outside back and inside front vertical legs;  $1/16^{\text{th}}$  inch, 40A durometer for outside back and inside front horizontal legs; and  $3/32^{\text{nd}}$  inch, 40A durometer for outside back and outside front horizontal legs. Inside front, outside back configurations are consistent with the findings above; however, walking with such a configuration will require rebalancing of the center of gravity, most simply by shifting the position of the battery inside the robot back to compensate, if indeed it can walk using such a

configuration. Additionally, these kinds of configurations may not be as stable due to the smaller distance between feet, especially on slopes. As such, though it is less efficient for swimming, an outside back configuration is included for comparison's sake.

Each of the flaps from these superior configurations would be further examined using simulation tools. This allows for more control over parameters and detailed results for comparison.

### 3.4 Simulation

To explore the efficacy of the selected legs further, a set of fluid simulations were performed. Given the complexity of the mechanism involved, a simplified idea for simulation was conceived and executed, and its results analyzed.

#### 3.4.1 Overview

Due to the reactive compliance of the robot, it was determined initially that a truly dynamic simulation would be prohibitively difficult given the scale of data to be collected. Instead, a static setup would be employed in such a way as to mimic a dynamic environment. This setup was comprised of the combination of pre-bent flap models into the assembly of the robot's leg, and using a fluid simulation program, flow water with the representative velocity over the leg.

The goals of this simulation experiment were to confirm some of the conclusions drawn for leg comparisons from empirical testing. Specifically, the comparison of horizontal and vertical leg configurations and the comparison of the

more efficient inside front and outside back configurations with the less efficient inside back and outside front configurations were prioritized in the interest of discovering a specific mechanical reason for the conclusions drawn during experimental testing.

#### 3.4.2 Leg model preparation

Three particular configuration/rubber pairs were selected, as noted in the results section of the empirical testing above: 1/16<sup>th</sup> inch, 40A horizontal; 3/32<sup>nd</sup> inch, 40A horizontal; and 1/16<sup>th</sup> inch, 40A vertical. These three performed the best in empirical testing. During that same testing, each had its angle of bend noted: 45 degrees for the 1/16<sup>th</sup> inch 40A horizontal; 30 degrees for the 3/32<sup>nd</sup> inch 40A horizontal; and 30 degrees internally and 60 degrees externally for the 1/16<sup>th</sup> inch 40A vertical. The vertical differs for right and left due to the fact that each side is independent of one another.

In the interest of simplifying the problem, each horizontal leg flap was treated as a combination of two rigid plates, and each vertical flap was treated as a combination of four rigid plates, two to the right of the pillar and two to the left. The noted angle of bend was applied to each side and split in half to create a bend at the leg connection and at a central joint; the central joints were located at 0.5 inches from the pillar for the horizontal leg due to the flap hinging involved in the flap's creation, and 0.75 inches from the pillar on either side for the vertical leg due to the desire to simulate efficient loading. The leg flaps would be bent in both directions of flow, either to simulate the most severe stage of compliance or to consider the onset of compliant recovery from that extreme state.

The results of the comparison of horizontal and vertical empirical data stated that vertical experienced heavy variance while horizontal did not, and as such the first major goal of these simulations is to explore possible reasons for the difference. These three models were each split using another factor: anti-spline vs. pro-spline flap placement. This designation refers to the direction of thrust relative to the servomotor spline. Pro-spline thrust is directed away from the servomotor, and thus in the same direction as the spline points, while anti-spline thrust is directed towards the servomotor in the opposite direction of the spline's pointing direction. These designations were selected for comparative testing due to the results of the empirical tests, in which inside front and outside back configurations, which use the pro-spline setup, consistently produced more average thrust than outside front and inside back configurations, which use the anti-spline setup. The second goal, therefore, was to confirm these results in simulation and determine if that conclusion, if reached, was for a mechanically identifiable reason.

#### 3.4.2 Fluid simulation preparation

To describe the typical flow that any given leg will experience accurately, two major sources of water velocity must be considered: that from the movement of the leg due to thrust stroke or recovery stroke, and that from the movement of the whole body due to forward motion. These two will be combined to create a velocity field that will act upon the static leg to simulate the leg moving through still water. Thus, all velocity measurements here are from the reference frame of the moving leg.

The leg's velocity from pure oscillation was considered based upon its movement range. Based upon the empirical data, the measured frequency ( $f$ ) of oscillation was:

$$\frac{21 \text{ iterations}}{9 \text{ seconds}} = 2.34 \text{ Hz} = f$$

The angular travel was measured considering both a thrust and a recovery stroke from -30 to 30 degrees: thus, 120 degrees, to make 2.09 radians. This multiplied with the frequency gives the expected average angular velocity of the leg at any given time. Further multiplied by the radius ( $r$ ) of the leg at any given point, this gives us the average velocity of the water relative to the leg at any given point along the radius of the leg due to leg oscillation. Note that the oscillation velocity can either be positive in the case of thrust or negative in the case of recovery; these conventions are held as positive being a water velocity relative to the leg that is in the direction of movement, and negative being a water velocity that is pressed against the direction of movement.

$$V = fL_A r$$

$$|V_{oscillation}| = \left(2.34 \frac{1}{s}\right) * (2.09 \text{ rad}) * r = 4.89 * r \text{ in/s}$$

As such, velocity of oncoming water due to oscillation from the perspective of a leg is given as a linear gradient according to the above equation. This value is negative for recovery strokes and positive for thrust strokes.

This is considered in addition to the velocity from movement in water. This velocity was considered from testing of previous models to be a value equal to approximately one third of the dominant dimension per second: thus, given the



dominant body length of 8.5 inches, the water speed is assumed to be 2.83 in/s. This value is considered negative due to the convention of representing water opposing the direction of motion. Thus, the equations for each direction are defined as follows:

$$V_{thrust} = 4.89r - 2.83 \text{ in/s}$$

$$V_{recover} = -4.89r - 2.83 \text{ in/s}$$

A pictorial representation of this is below in Figure 52.

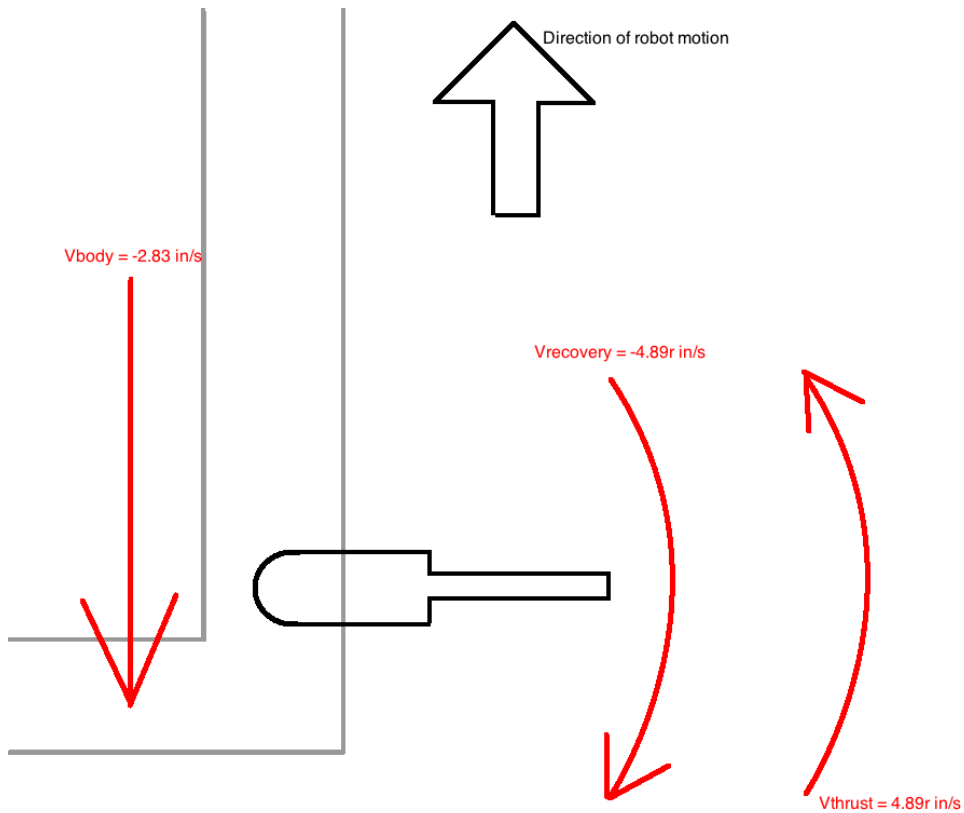


**Figure 52: Pictorial representation of input equation for simulation**

To simulate this, Solidworks 2012' flow simulation package was employed. Solidworks was chosen for this due to the ease of setup and speed of calculation compared to other programs with similar packages such as Fluent. The setup parameters for these simulations are below in Table 1.

<b>Parameter</b>	<b>Value</b>
Software specified	SolidWorks Education Edition 2012/SP 4.0 Flow Simulation 2012, SP 4.0, Build 2020
Liquid used	Water
Flow type	Laminar and turbulent
Default wall thermal condition	Adiabatic wall
Roughness	0 microinch
Pressure	14.6959473 lbf/in <sup>2</sup>
Temperature	68.09 degrees F
Turbulence intensity	2%
Turbulence length	.00393700787 in
Result resolution	3 (default)

**Table 1: Solidworks simulation operating parameters**

The leg assembly for each of the six setups, created in Pro Engineer, was imported to Solidworks; each setup was then resolved through 160 points on each model for both absolute velocity and X-directional velocity. The former was solved to potentially gain insight into the absolute speed of water on and around each leg, while the latter was solved to see more directly the total impact on thrust and drag.

### 3.5 Simulation Results

From the twenty-four simulations created, several important results arose from the comparisons of each. Absolute velocity is displayed as a spectrum from 0 (dark blue) to 25 (bright red) inches per second, while X-directional velocity is displayed as

a spectrum from approximately -4 to 18 inches per second using the same color range if unspecified.

### 3.5.1 Vertical and Horizontal Leg Configuration Performance

The empirical results defining vertical leg configurations as both inferior in net thrust and energy inefficient were presented without a clear answer as to why either point was true. The simulations present a more clear answer than that initially given.

Given the nature of how each leg swings to produce a thrusting force, the expected velocity is highest at a distance closer to the outside edge of each leg than the inside edge. Thrust force resulting from the drag created increases with the water velocity at any given point; thus, a greater force is created when the higher velocity flows are captured and reflected. Due to the nature of the vertical flap configuration, the rubber is bent in such a way as to initially allow those flows with the largest velocity to pass through unobstructed; this can especially be illustrated in the X-directional velocity diagram below in Figure 53 below. This can lead to less efficient thrust cycles in both force generated and energy employed.

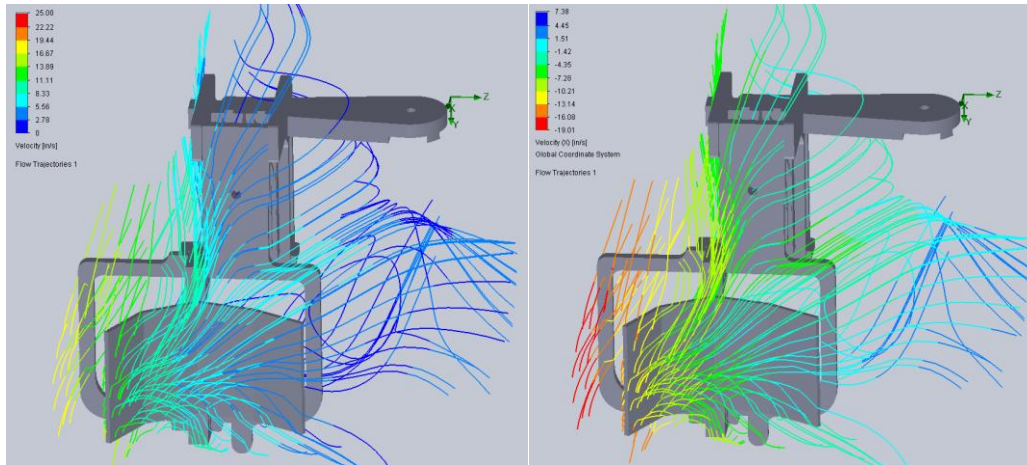


**Figure 53: Absolute and X-directional velocity for vertical leg configuration during thrust phase**

In contrast, high-velocity flows in the horizontal configuration are captured from the start of the thrust cycle due to the geometry of the situation. Additionally, the greater flowrate pushes the compliant flap against its frame so as to lay the flap flat as quickly as possible. This has the effect of maintaining a more efficient thrust cycle. The illustration of this can be seen in Figure 54 below.

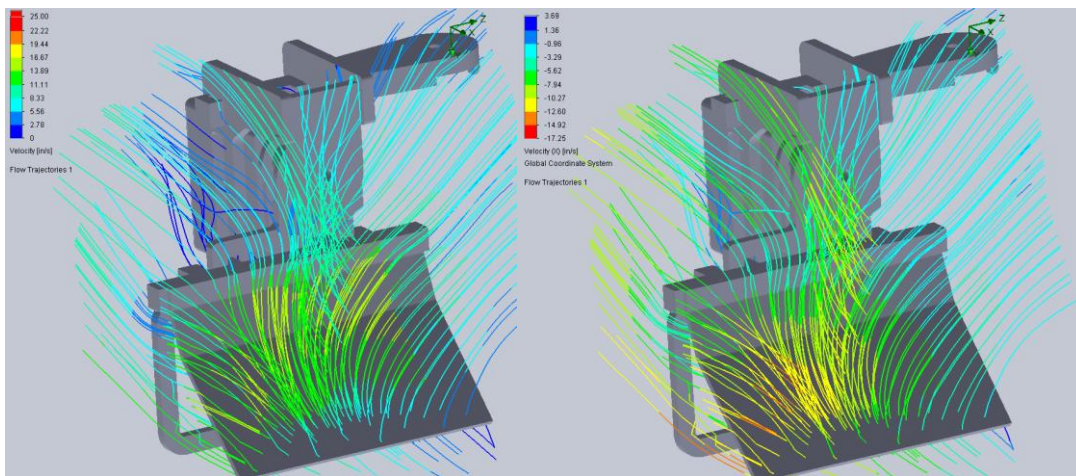


**Figure 54: Absolute and X-directional velocity for horizontal leg configuration during thrust phase**

Similar principles can be demonstrated when considering the recovery cycle. Greater presence of higher flowrates at the edge of the robot's leg promote faster recovery, which when complete reduces the effective surface area drastically, affording more efficiency in minimizing drag and minimizing energy loss. Examples of each can be seen below in Figures 55 and 56, and illustrate the problem very effectively, especially the X-directional velocity measurement.

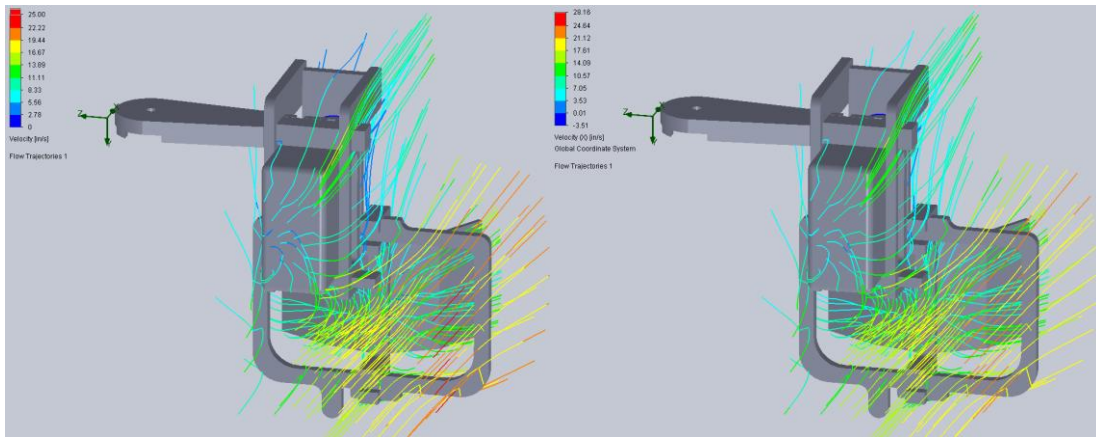


**Figure 55: Absolute and X-directional velocity for vertical leg configuration during recovery phase**

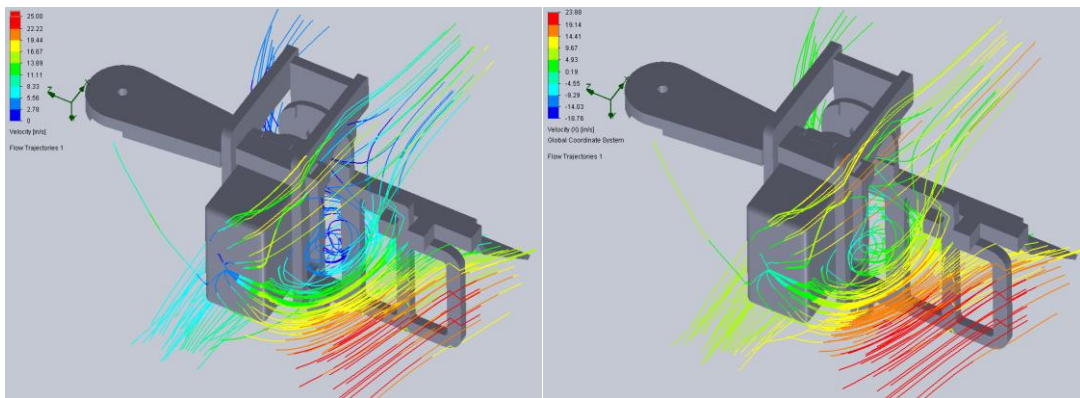


**Figure 56: Absolute and X-directional velocity for horizontal leg configuration during recovery phase**

### 3.5.2 Anti-spline and pro-spline leg configurations

In the process of considering inside and outside motor configurations during empirical testing, an alternate designation was created to group specific sets of results more accurately. It was discovered that inside front and outside back leg configurations produced a greater net thrust than outside front and inside back configurations, most noticeably within the heavily stratified vertical leg testing results. The commonality between each of these configuration pairs was the direction of the leg flap relative to the motor spline. The better of the two pairs had its flap set in such a way that the direction of the thrust produced matched the direction in which the servomotor spline pointed. In the worse of the two pairs, the opposite was the case. These two cases, named pro-spline and anti-spline for convenience, were tested for each leg configuration in both thrust and recovery phases.

The thrust comparison between anti-spline and pro-spline configurations presents a clear assumed line of reasoning for the disparity: the presence of the motor itself. The figures below suggest a considerable difference in effective X-directional water velocity due to the motor housing's diffusion of oncoming water with a forward velocity.

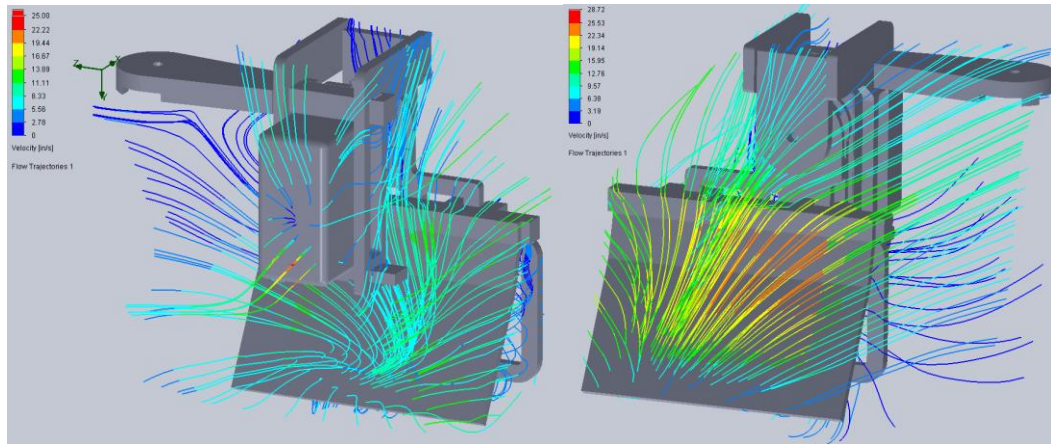


**Figure 57: Velocity profiles for anti-spline (left) and pro-spline (right) legs during thrust phase**

More telling is the X-directional velocity profile for each leg. The anti-spline figure below scales from -14 to 16, while the pro-spline figure scales from -4 to 18; this shows a concentration of approximately 7 in/s flow on the anti-spline, while the pro-spline has a concentrated density of approximately 12 in/s flow. This signifies a drastically reduced thrust.

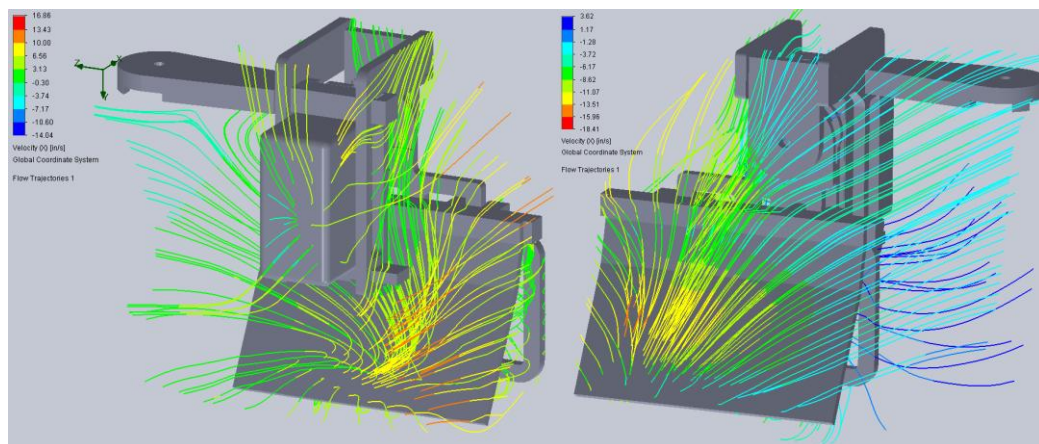


**Figure 58: X-directional velocity for anti-spline (left) and pro-spline (right) legs during thrust phase**

This trend is continued for recovery, but in a different sense. The lack of a motor housing to redirect flow creates a more distributed flowrate in the anti-spline configuration, which reduces the point force put upon the legs, causing them to

deform more slowly; in contrast, for the pro-spline configuration, the motor housing redirects the flow to a small area on the outside edge of the flap, putting a larger force upon the flap and causing it to deform more quickly. Note that in the X-directional velocity figures, the anti-spline configuration ranges from -6 to 30 in/s with a typical velocity of approximately 13 in/s across the flap, while the pro-spline configuration ranges from -18 to 24 in/s with a typical velocity ranging from 10 to 24 in/s from the middle to the outside edge of the flap.

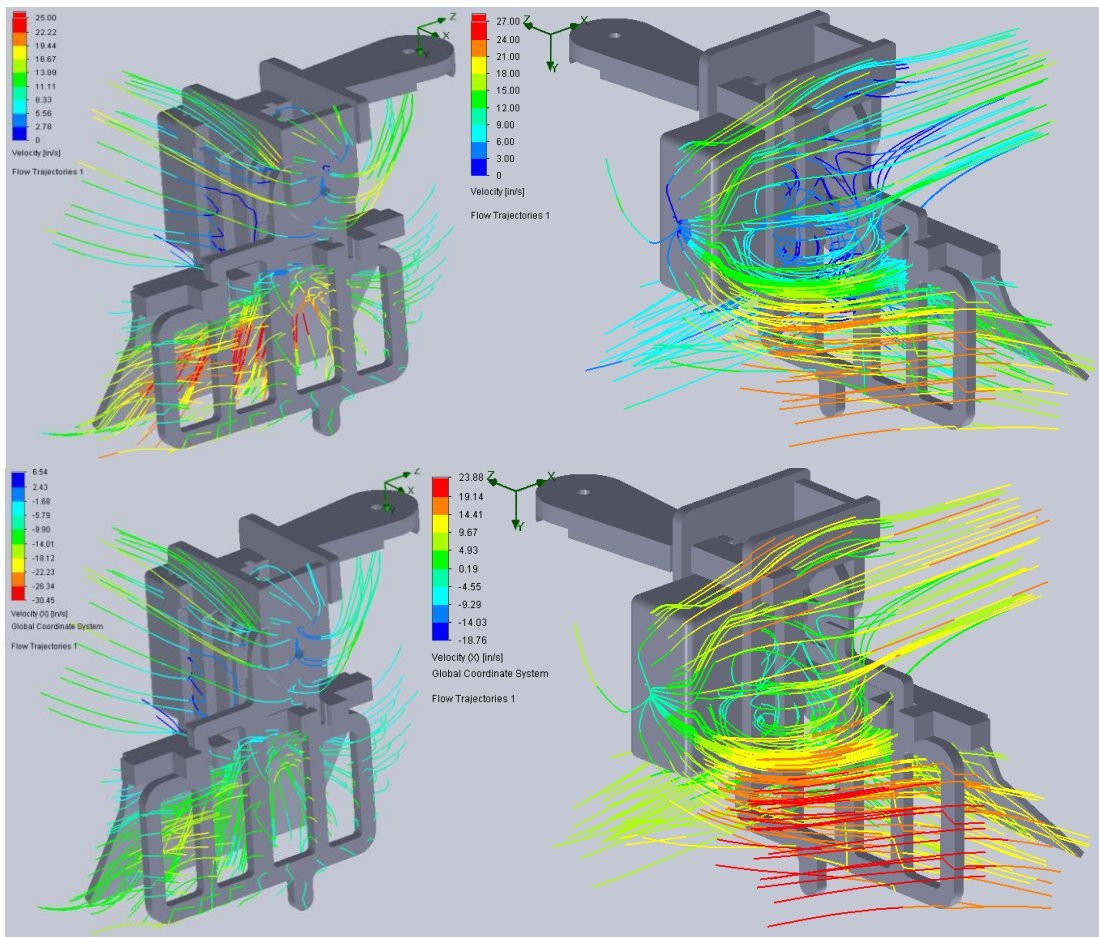


**Figure 59: Absolute and X-directional velocities for both spline configurations during recovery phase**

Similar conclusions can be reached with the vertical leg configuration; however, the effect is amplified by the aforementioned flaw in the vertical leg



configurations compared to horizontal configurations. This accounts for the heavily stratified nature of the vertical legs.

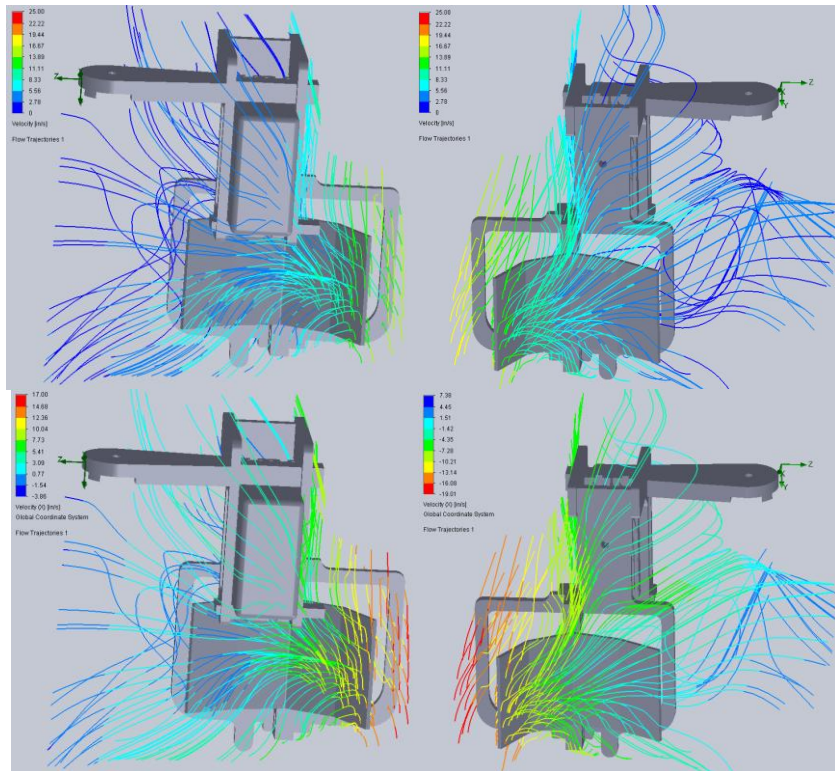


**Figure 60: Absolute and X-directional velocities for vertical configurations during thrust phase**

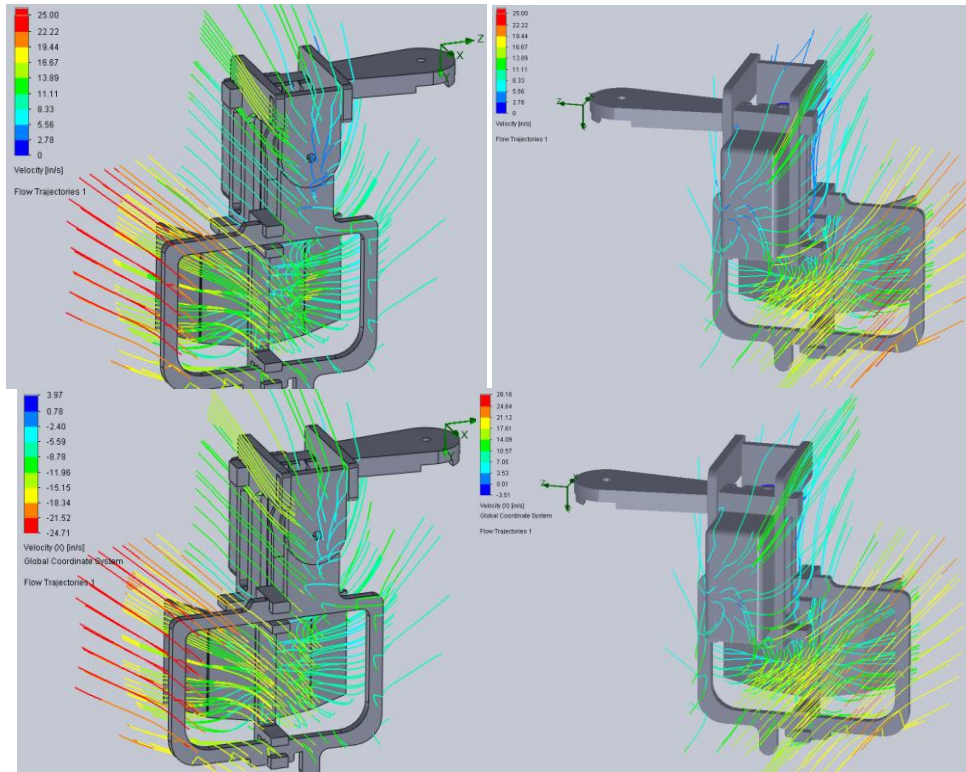


**Figure 61: Absolute and X-directional velocities for vertical configurations during recovery phase**

There are some definite conclusions that can be drawn by these experiments and simulations. The first important conclusion is the fact that there is, indeed, a marked difference between vertical and horizontal leg operation. The vertical leg as it has been presented is inefficient in design due to the nature of the way the legs create thrust. It cannot as quickly and easily assume the most efficient positions for thrust or recovery, and as such the average force created is lower. This disparity is due to the way in which force is distributed. Because the net force is centered more towards the edge than towards the middle of the leg, a leg-centered curve pattern is not advantageous.

The second important conclusion is that pro-spline configurations – thus, the inside front and outside back configurations – are inherently superior due to the

method interference of the leading servomotor. The servomotor housing does not block the incoming water for thrust, and diffuses the incoming water for recovery, both of which are advantageous. Thus, the most optimal configuration for swimming is to have the two sets of legs be pro-spline. Using an inside front/outside back configuration, this creates a stance that is unbalanced and leans forward. As expected, this can cause problems in walking, especially heading down slopes, as undue force is placed on the front legs to support the tilted center of gravity.

### 3.6 Summary of Design

Iteration through two major conceptual chassis and several configurations of each brought the design to its current form. The current design achieves all of its primary goals: it has the ability to walk, it has the ability to swim, and it is durable enough to withstand switching between different modes of operation. The internal microcontroller and electronics setup allow for the sensing and intelligence required for gait switching.

Considering the legs more in-depth, three leg configurations were selected from empirical testing, which was narrowed down to one when considerations of the necessary legs were made. Several conclusions were made when considering both the experimental and simulation testing: specifically, horizontal leg designs are more efficient and less susceptible to non-ideal configurations than vertical legs, and pro-spline configurations perform better than anti-spline configurations. This leads to the best leg swimming configuration being a horizontal configuration with its front legs in an inside configuration and its back legs in an outside configuration.

This setup is unfortunately biased towards leaning forward due to the nature of the servomotor placement, which greatly limits the acceptable force able to be placed on the front legs. Due to this balancing issue, an outside-outside leg setup is necessary to walk stably with the current design. As such, the leg selected employs 3/32<sup>nd</sup> inch thick, 40A rubber in the horizontal flap configuration, due to this being the most efficient outside-outside combination. However, this creates a tradeoff between swimming and walking which can be avoided in the future.

One way is to revise the leg design to position each lower leg centrally to the upper leg for the purpose of creating an equal weight distribution between front and back regardless of the configuration. This would necessitate having the servomotors hang off of the front or back of the legs, which could lead to continual moderate unbalancing; however, the effect would be considerably less than a typical forward configuration. A second way is to revise the leg design to place the motor out of the way out of the leg flow for the front legs. This may involve flipping the servomotors or extending the legs, either of which could lead to significant balancing issues or issues with the servomotor connections.

## Chapter 4: Design of Gaits

### 4.1 Overview

Any creature, and especially a legged creature, requires a set of movement patterns. While it is necessary that these be alterable to cope with changing situations, these relatively simple patterns comprise the primary modes of locomotion of an animal. “Gait” is the term used to refer to a locomotion pattern of this kind. It is defined in the Merriam-Webster dictionary as “a manner of walking or moving on foot,” “a sequence of foot movements,” or “a manner or rate of movement or progress” [33].

To define the possible types of motion of a robot with a complex locomotion type, it is necessary to define several gaits. Each of these gaits is required to serve a specific purpose. Additionally, sub-gaits may be required if gaits are sufficiently different that energy loss or significant frame stress would be incurred in switching.

### 4.2 Primary Gaits

#### 4.2.1 Semi-aquatic environments and required modes of locomotion

In a semi-aquatic environment, mixed terrain is very common. This variety of terrain will be considered as a combination of three explicit types of terrain; these will be referred to as terrestrial, shallow aquatic, and aquatic terrain.

Terrestrial terrain is simple in concept: this is terrain that is entirely composed of the ground and anything covering it. While this terrain can be wet, it is assumed that there is no standing water. The majority of it will be relatively firm. As such,

movement speed and efficiency are prioritized in gait composition; stability is less of a concern in this case.

Shallow aquatic terrain is halfway between terrestrial and aquatic. Specifically, this designation is used to refer to terrain that is covered in water but is still shallow enough to require terrestrial modes of movement such as walking. This presents different challenges than either terrestrial or fully aquatic terrain. Walking in such terrain requires movement over unsteady and slick ground, and in water that may hamper fast leg movement needed for dynamic stability; as such, any appropriate gait would prioritize maintaining stability over speed or efficiency.

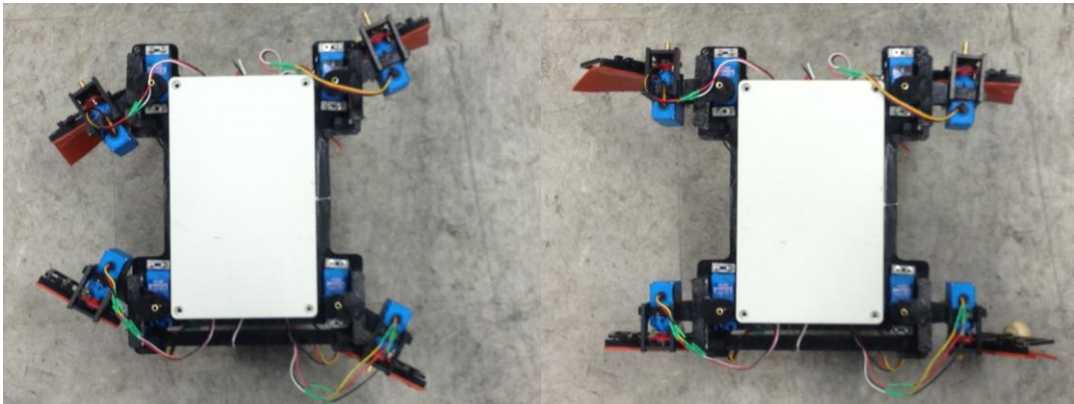


**Figure 62: Shallow aquatic terrain [34]**

Aquatic terrain is, simply enough, water deep enough to swim in. An appropriate swimming gait primarily needs to create more forward thrust than backward thrust while maintaining efficiency and avoiding uneven sideways loading.

#### 4.2.2 Terrestrial gait

The gait employed for pure terrestrial movement is a “trotting” gait. A trot is a two-beat gait in which diagonal pairs propel the robot forward, then lift up to recover while the other pair propels the robot. In this situation, it is split into four timesteps: two in which all four legs are on the ground, two in which two legs are in the air. This is a fast, efficient, and dynamically stable gait; however, it can have difficulty in situations where that dynamic stability is threatened. Figure 63 illustrates this gait with the top being the front of the robot, while Table 2 describes the various angles undergone and Figure 64 graphically plots those angles.



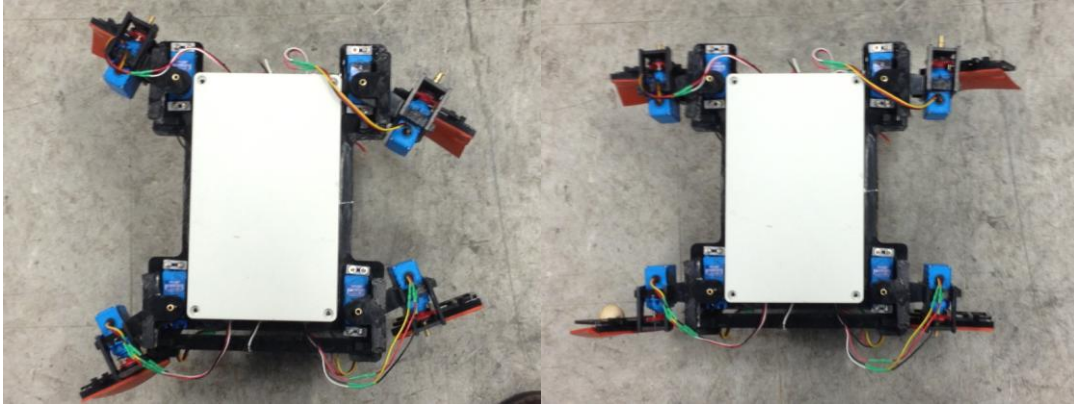


**Figure 63: Trotting gait**

Timestep (Time delay following)	Back right and front left lift	Back right and front left sweep	Back left and front right sweep	Back left and front right lift
1 (150ms)	0°	-30°	30°	0°
2 (150ms)	30°	0°	0°	0°
3 (150ms)	0°	30°	-30°	0°
4 (150ms)	0°	0°	0°	30°

**Table 2: Trotting servomotor position table**



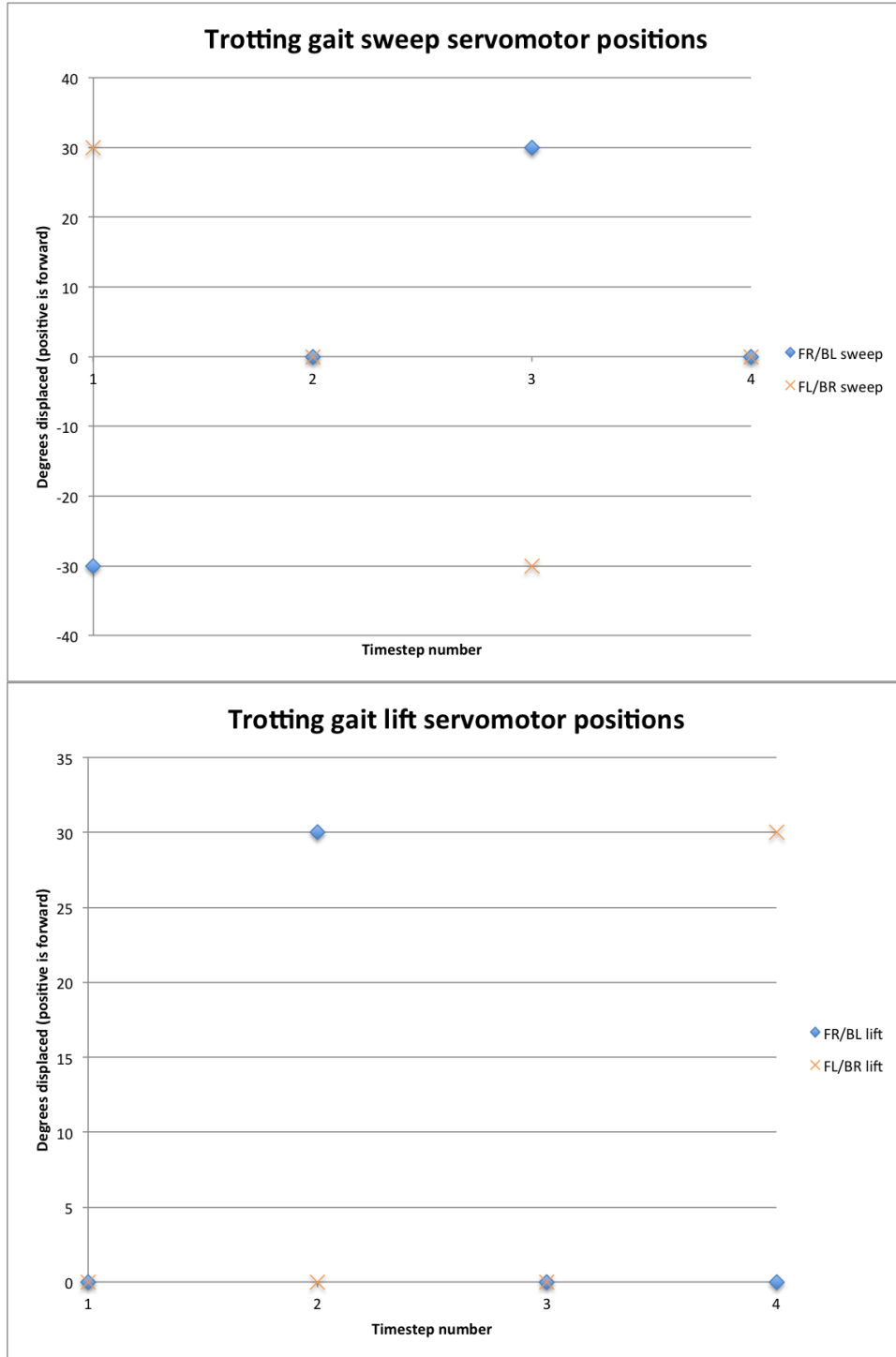
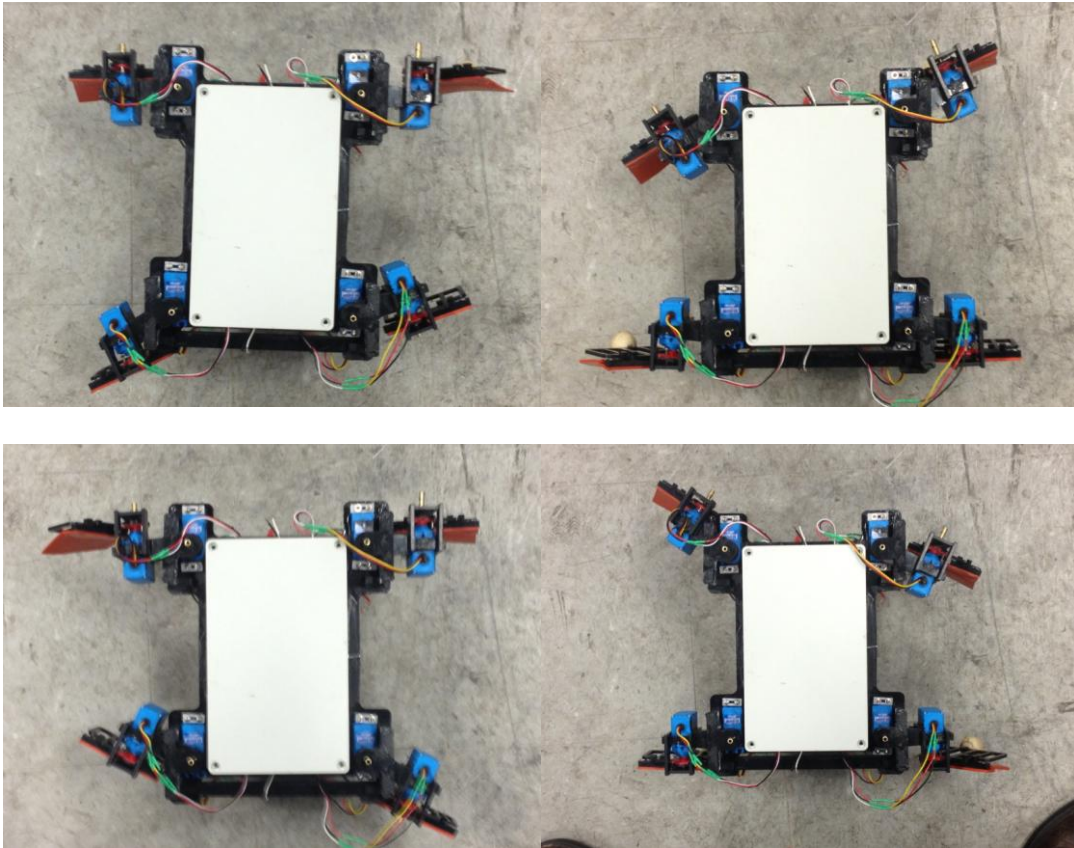


Figure 64: Trotting servomotor position graphs

#### 4.2.3 Shallow aquatic gait

The gait employed for shallow aquatic terrain is a stable walking gait. This is a four-beat gait in which there are always three feet on the ground at the end and beginning of any given timestep. While there is a momentary period of time in which there are only two feet on the ground, it is extremely short.

The movement pattern for any individual foot is similar to that employed in the trotting gait. The primary difference between walking and trotting, then, is that the back legs are each delayed by one timestep compared to the trotting gait. This doubles the effective number of beats while also splitting the recovery leg lifts such that there is one recovery during each timestep instead of switching between two recovery leg lifts and none. The staggered gait allows for more consistent static and dynamic stability; however, the propulsion is not as balanced as the trotting gait in the forward direction. The imbalance creates an inefficiency that slows the gait compared to trotting. Figure 65 illustrates this gait with the top being the front of the robot, while Table 3 describes the various angles undergone and Figure 66 graphically plots those angles.



**Figure 65: Walking Gait**

Timestep (Time delay following)	Back right lift	Back right sweep	Back left sweep	Back left lift	Front right lift	Front right sweep	Front left sweep	Front left lift
1 (150ms)	0°	30°	-30°	0°	30°	0°	0°	0°
2 (150ms)	0°	0°	0°	30°	0°	30°	-30°	0°
3 (150ms)	0°	-30°	30°	0°	0°	0°	0°	30°
4 (150ms)	30°	0°	0°	0°	0°	-30°	30°	0°

**Table 3: Walking servomotor position table**

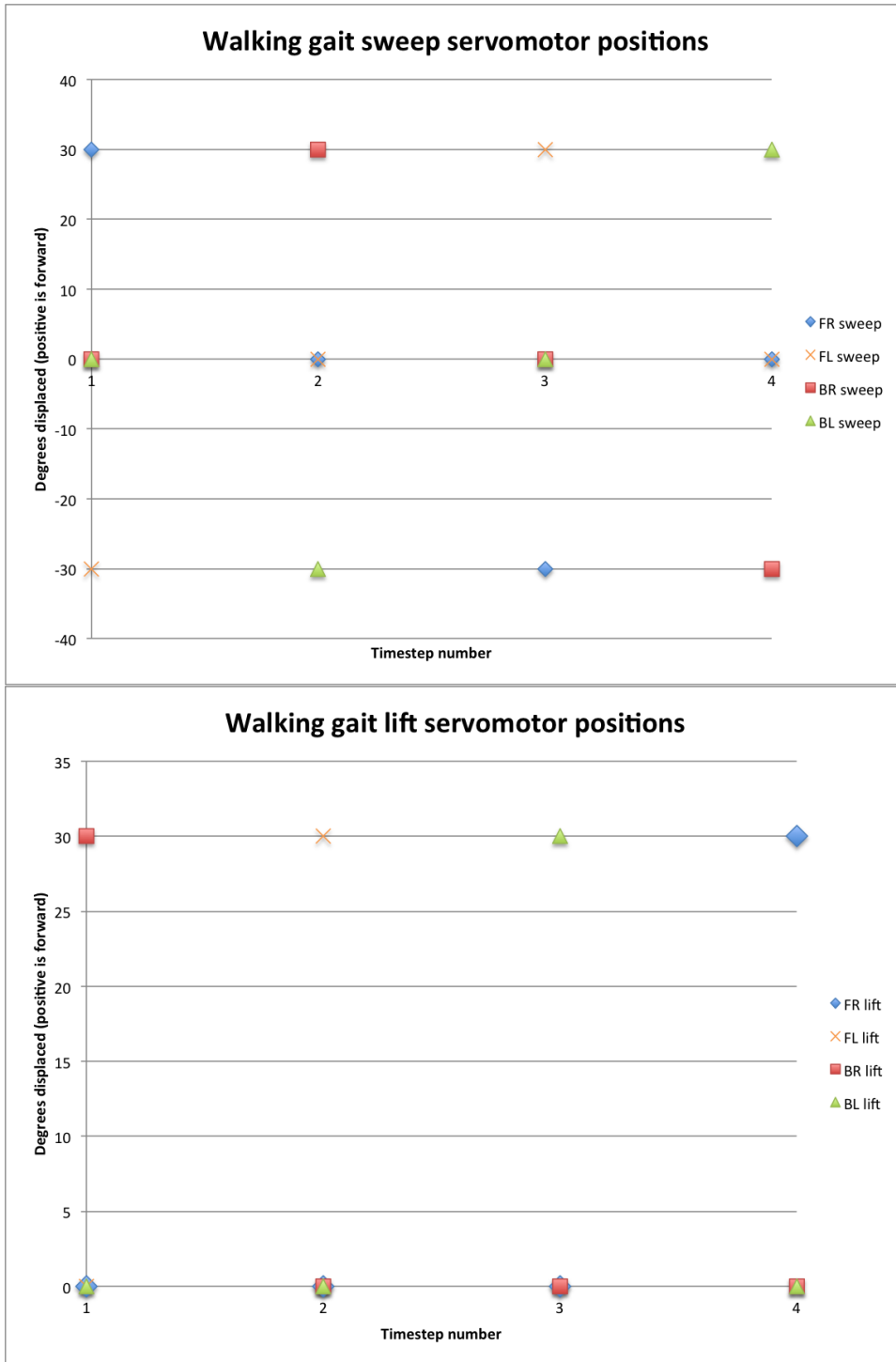


**Figure 66: Walking servomotor position graph**

#### 4.2.4 Aquatic Terrain

A simple swimming gait was developed to address aquatic terrain. In the context of this robot, this was conceptually very simple due to the compliant mechanisms. Since those mechanisms automatically regulate thrust and drag in such a way as to ensure a net forward thrust, the primary concern for swimming is maintaining constant thrust to promote acceleration and consistent forward motion. In this case, this is accomplished by using the front legs, then the back legs, for propulsion. Symmetrical leg movement promotes a reduction in losses due to lateral propulsion. A slightly longer time delay was employed to promote full range of motion with fewer timesteps than the other gaits. Figure 67 illustrates this gait with the top being the front of the robot, while Table 4 describes the various angles undergone and Figure 68 graphically plots those angles.

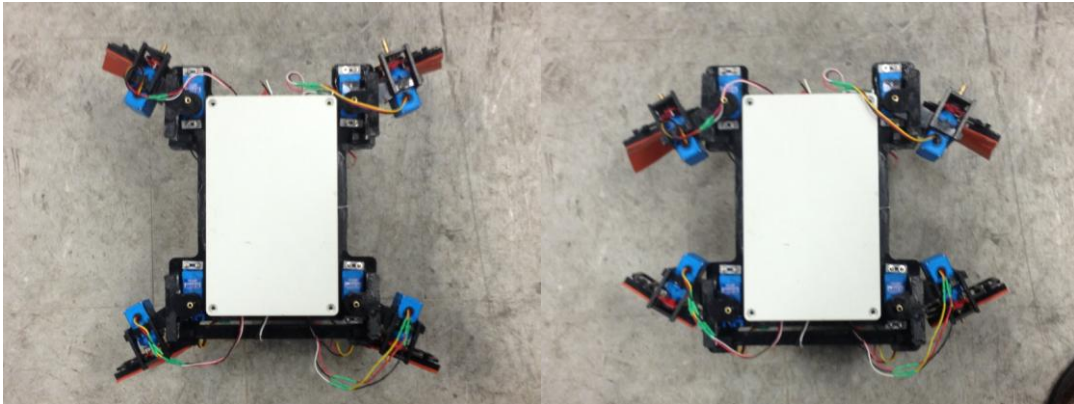


**Figure 67: Swimming Gait**

Timestep (Time delay following)	Lifts	Front sweeps	Back sweeps
1 (200ms)	0°	30°	-30°
2 (200ms)	0°	-30°	30°

Table 4: Swimming servomotor position graph



Figure 68: Swimming servomotor position graph

### 4.3 Secondary Gaits

The three primary gaits encompass most necessary motion in a semi-aquatic environment. However, these alone will not entirely suffice. To supplement these, secondary gaits are necessary.

#### 4.3.1 Secondary walking gaits

For more fluid traversal of terrain, it is necessary to define two sub-gaits for the walking gait. One of the most delicate transition areas is the waterline of a body of water. At many waterlines, the movement and presence of water create a mild slope over time. As such, a robot moving on that waterline into or out of the water would encounter more adverse conditions than normal: it would be expected to walk up or down a slope in terrain that can be expected to be slippery and unstable. This can be problematic and may potentially put undue stress on the robot as it leans forward or backward.



**Figure 69: An example of sloped terrain in water [35]**

To combat this, two variants of the walking gait have been created: one for moving up a watery slope, and one for moving down a watery slope. These variants bias horizontal plane motion ten degrees in the direction of the top of the slope: thus, the legs will swing forward further and back less when moving down the slope, and vice versa for up-slope movement. This action keeps the robot's center of gravity inside its vertical footprint, which reduces the chances of undue leg torque and toppling because of it. However, the primary movement pattern for each is the same as that of the walking gait; as such, they do not qualify as distinct primary gaits. Stability on a slope is demonstrated in Figure 70 below. Figure 71 below specifies the differences between up-slope, down-slope, and neutral walking.

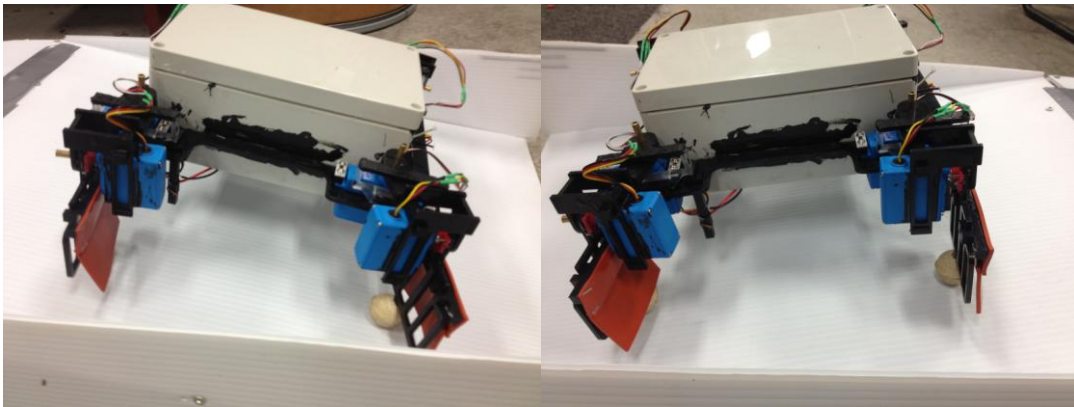


**Figure 70: Robot holding at biased zero position on upward and downward slope**



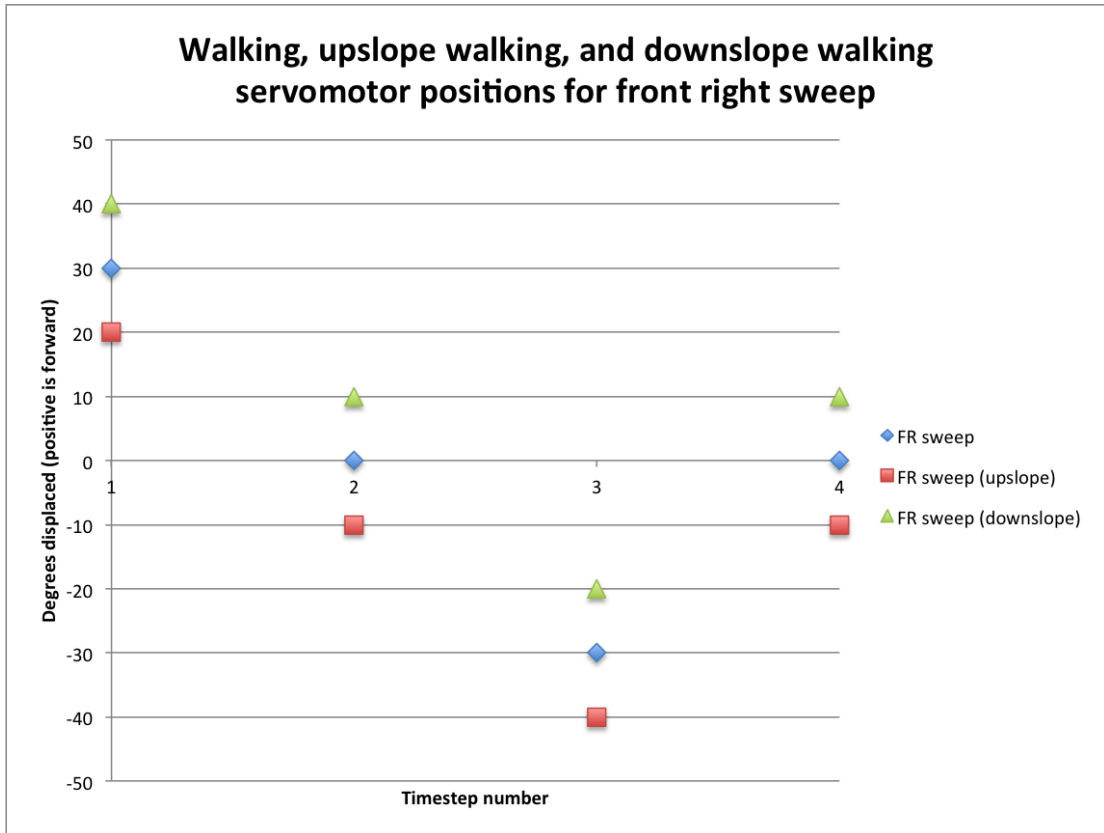


Figure 71: Walking gait servomotor position diagram comparing changes in sweep values

#### 4.3.2 Transition Gaits

One of the primary goals of this robot is to reduce energy loss from changing terrain modes and to facilitate mechanically seamless motion during gait switching. However, in some cases, the difference between the gait patterns is drastic enough to necessitate a small pattern to act as a buffer between the two gaits. These can be qualified into three categories: major transition, minor transition, and no transition.

Major transitions are those between two sets of gaits that have a wildly different set of assumed environmental and movement parameters. In this case, the swimming gait's operating parameters are vastly different than the parameters inherent in either the walking or trotting gaits: the assumption of floating and

symmetrical paddling as a means to maintain orientation is contrasted with ground movement and the use of asymmetrical steps to keep balance. An intermediary step is required here to both ensure that the destination state becomes sufficiently dominant before the gait associated with the destination state is implemented.

The transition associated with changing from swimming to walking or trotting assumes that the robot is partially floating as it switches gaits. As such, the transition is achieved by reaching forward with both forelegs toward the presumptive ground after zeroing. After doing so, the robot will pull both legs back, ensuring that it is solidly on the land. One leg at a time is used so that if the situation is such that the forelegs are both already on solid ground, there will be no unbalancing issues. This is illustrated graphically in Figure 72 below, while the specific leg positions are outlined in Table 5 and Figure 73.

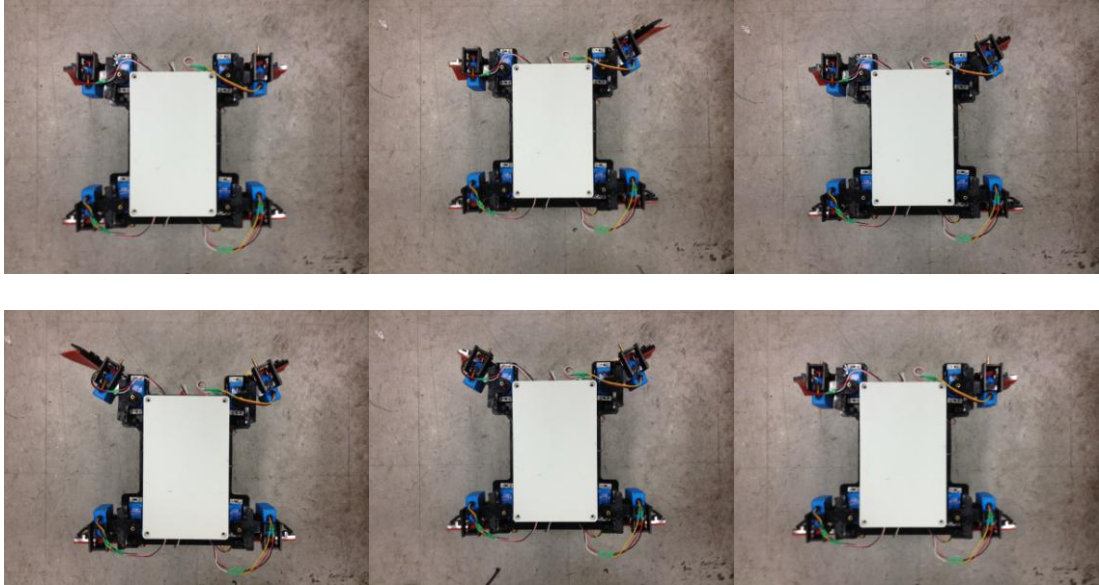


**Figure 72: Water to Land Transition**

Timestep (Time delay following)	Front right lift	Front right sweep	Front left sweep	Front left lift
1 (250ms)	0°	0°	0°	0°
2 (250ms)	30°	30°	0°	0°
3 (250ms)	0°	30°	0°	0°
4 (250ms)	0°	30°	30°	30°
5 (250ms)	0°	30°	30°	0°
6 (250ms)	0°	0°	0°	0°

**Table 5: Water to land transition servomotor position table**

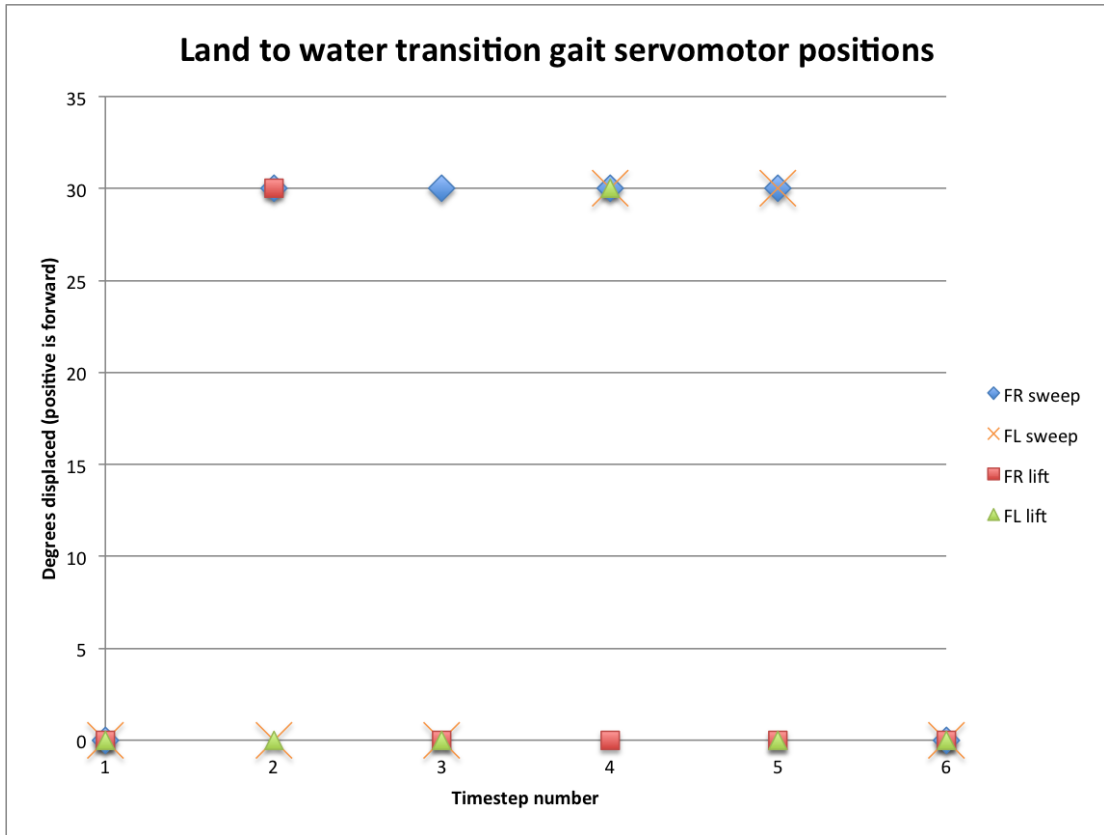


Figure 73: Water to land transition servomotor position diagram

Conversely, the transition between walking or trotting and swimming assumes that at least the front legs are either in open water or are close to it. As such, the strategy is to push off with all four legs at once, so as to potentially push the back legs away from the land. However, to recover from the full stroke immediately could potentially push the robot back onto land. Thus, recovery occurs in two steps, with small delays in between to mitigate continuous backwards thrust. This places the legs in the expected position so that it can begin the swimming gait. This is illustrated graphically in Figure 74 below, while the specific leg positions are outlined in Table 6 and Figure 75.

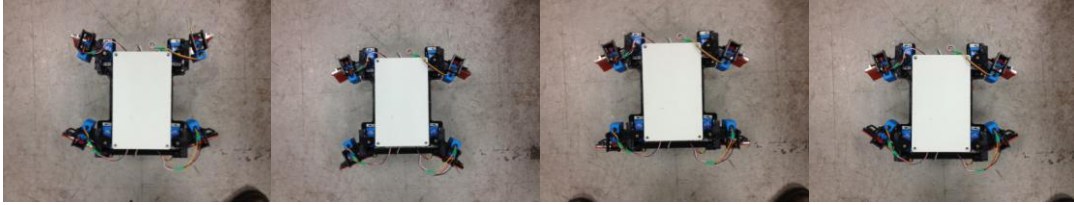


Figure 74: Land to Water Transition

Timestep	Front sweep	Back sweep
1 (600ms)	30°	30°
2 (350ms)	-30°	-30°
3 (350ms)	-30°	0°
4 (150ms)	-30°	30°

Table 6: Land to water transition servomotor position table

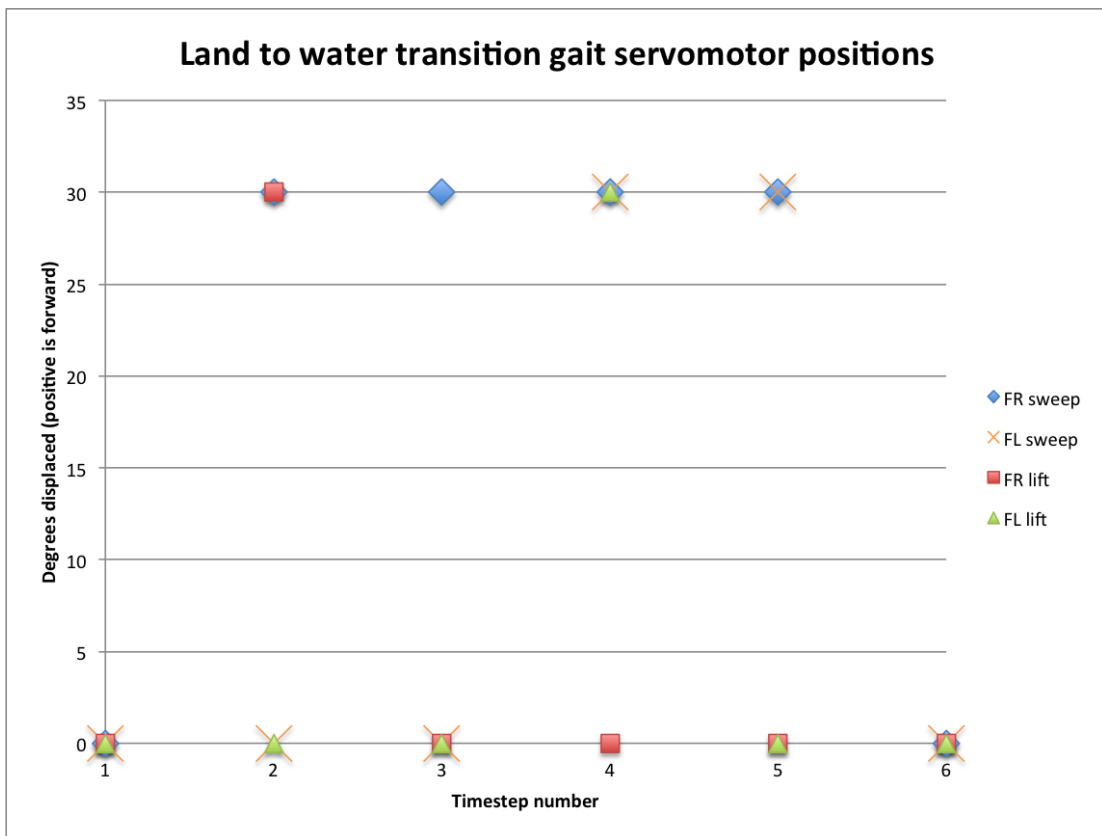
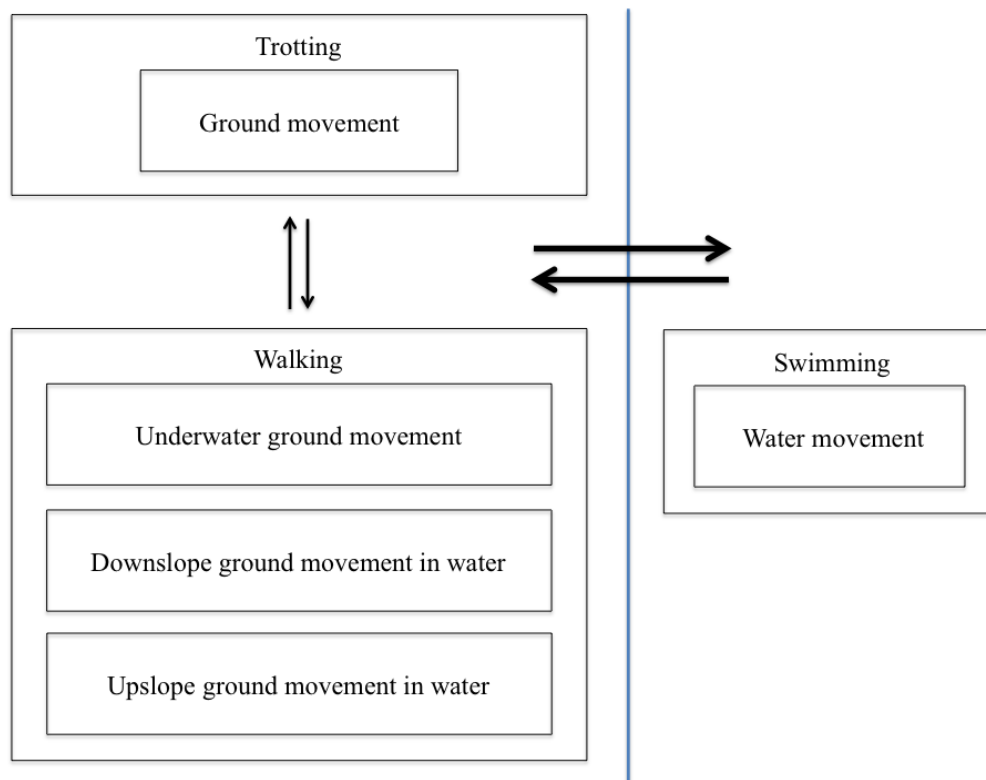


Figure 75: Land to water transition servomotor position table

Minor transitions are those in which the basic parameters of the terrain and movement type are similar, but differences in gait could potentially put undue stress on the robot if there were a direct switch. In this case, an explicit series of intermediate steps for each specific situation is not required. Instead, a simple zeroing action combined with slight pauses suffices to provide a barrier between the two. This is implemented between the trotting gait and the walking gaits. Similar to this is no transition, which eschews any sort of intermediary step. This lack of transition is noted to be between the upslope, downslope, and neutral slope gaits, which share the same primary gait pattern. The relationships between the three kinds of transitions can be seen in Figure 76 below.



**Figure 76: Diagram showing minor and major transitions between swimming, walking, and trotting**

#### 4.4 Gait Switching Algorithm

As previously stated, the robot is programmed entirely in Arduino's proprietary language, which is a functional programming language based upon C and C++. As such, the algorithm was written with the Arduino's capability for digital input and simple servomotor output in mind. These allow the four water sensors to be quickly interpreted as Boolean variables, and simple degree output to be given to servomotors, allowing the task of creating the algorithm to be more intuitive in nature.

##### 4.4.1 Primary loop

The primary routine that the robot checks every cycle is very simple in nature. Two state integers, CurrentState and DesiredState, are defined at the root of the code. DesiredState is determined by the desired state subroutine, which relies on sensor data to set DesiredState to one of five values. The program then compares this newly updated DesiredState to CurrentState. If they are the same, the robot will continue with whatever action the shared state corresponds to. If they are different, a transition subroutine is called in which the appropriate transition is decided based upon the combination of states.

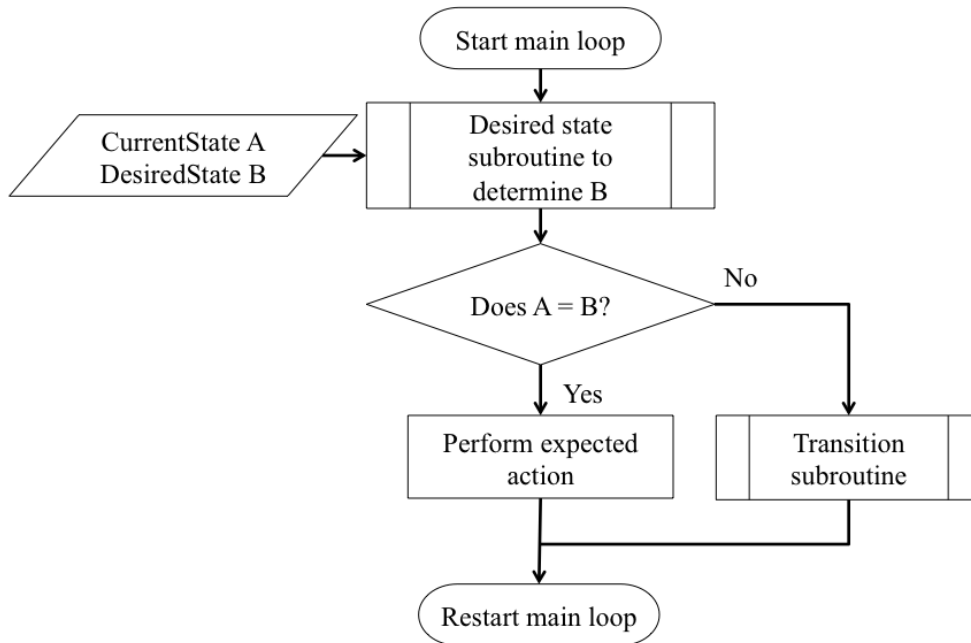


Figure 77: Flowchart for main loop

#### 4.4.2 Desired state subroutine

This subroutine is where the expected behavior based upon sensor feedback is checked. First, each of the four water sensors is read as a Boolean variable: FT, BT, FB, BB correspond to Front Top, Back Top, Front Bottom, and Back Bottom respectively. A high voltage reading would be due to a connection between the two sensor terminals, which signifies the presence of water and sets the variable to true; otherwise each variable defaults to false.



Next, several conditions are checked to ascertain the appropriate state, in order of most specific to least specific. First, if all four sensors are engaged, the robot is considered to be fully in water or close enough to it that swimming is recommended. If both top sensors are dry and both bottom sensors are triggered, the robot is in relatively level watery terrain, and as such the neutrally sloped walk gait is recommended. Each bottom sensor is then checked in turn, producing a result that leads to upslope or downslope walking as appropriate. Finally, if no sensors are triggered, the robot will begin to trot. This is outlined graphically in Figure 75 below.

The labeled numbers were chosen specifically for the purpose of explicitly separating a major transition, a minor transition, and no transition. In this case, the swimming value (50) is designed to be greater than any other two states added together. The walking values (20, 21, 22) are very close to each other, which allows a difference to select small state difference as no transition, whereas the trotting state (10) is far enough away from each to be considered a minor transition instead of no transition. In a system with more states, these conventions of small difference, minor difference, and major difference could be further applied. These will be examined further when considering the transition algorithm.

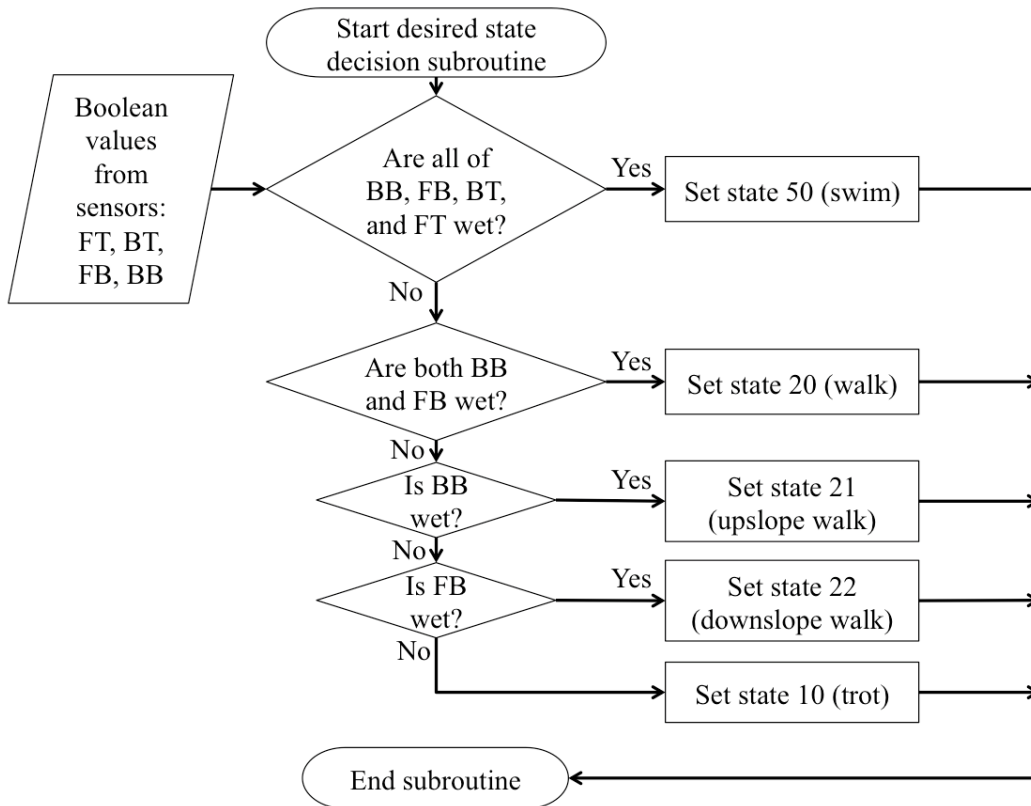


Figure 78: Flowchart for desired state decision subroutine

#### 4.4.3 Transition subroutine

This subroutine is called when the desired state and current state are in conflict. Several different combinations of A and B are checked to determine the expected result. This can end with one of two major transitions, one minor transition, or no transition, as detailed in Section 4.3.

First, the two states' values are added, and compared to 50. Because no two states that suggest a transition between walking or trotting gaits combine to a number greater than 50, this checks to see if a major transition between swimming and land motion is required. The state that has swimming is then checked by a value

comparison, since swimming is given the numerically highest state value, and the appropriate transition is suggested.

If neither state includes swimming, the absolute value of the two states subtracted is then checked against 9. This is because the difference between the trotting state and any of the walking gaits' states is 10 or more, and the difference between each of the walking gaits is less than 9. As such, the combination that triggers this condition requires a minor transition of zeroing with a slight delay. If neither of these conditions is true, then no transition is required. In all cases, the current state is set to whatever the previous desired state was. This is outlined graphically in Figure 79 below.

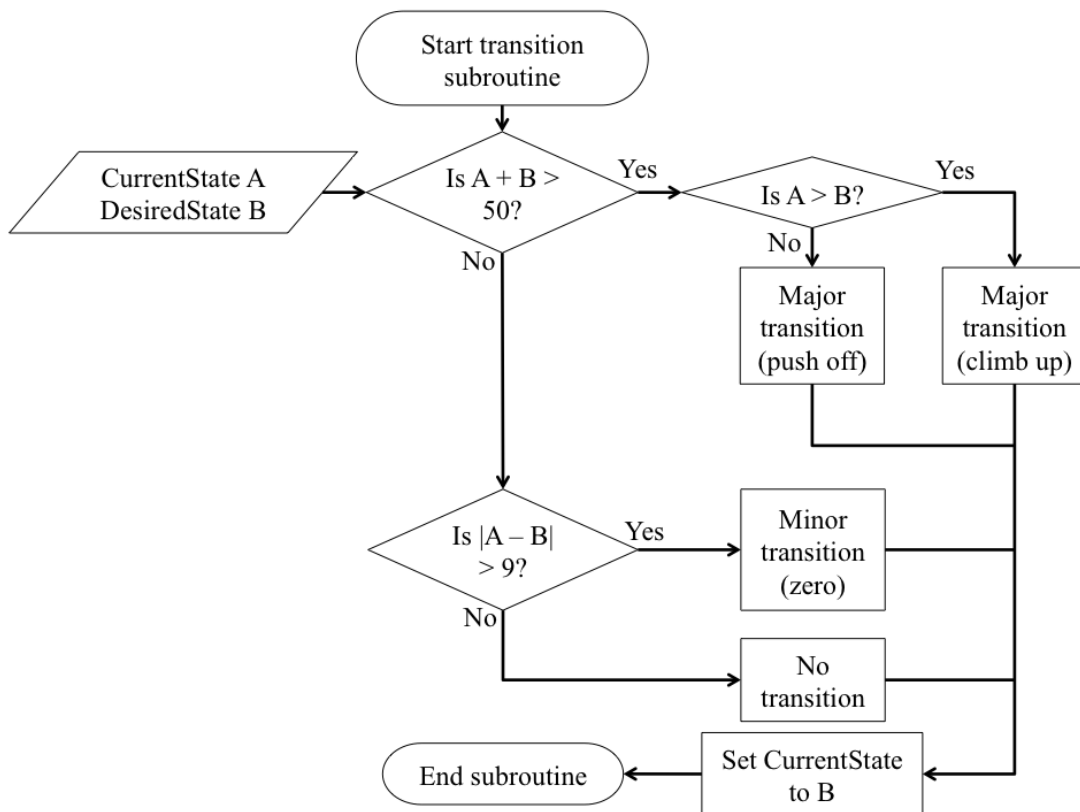


Figure 79: Flowchart for transition subroutine

#### 4.5 Experimental Testing

To test this gait theory, two field experiments were performed. One would test walk/trot gait transitions, while the other would test swim/walk transitions.

##### 4.5.1 Experimental setup

The theory to be tested when considering walking and trotting was the transition between the two, especially on a sloped waterline. Thus, a test chamber was created from a thin plastic box, half-filled with water, and a thin sheet of corrugated polypropylene bent in its middle; the slickness of the polypropylene would provide an unsteady surface, especially when wet, which would test the viability of the gaits and their stability. The robot would trot into the test chamber by means of the flat top, then transition down into the water and begin to walk down the slope and then walk on the neutral box bottom. The same test would be repeated for walk-to-trot. A picture of this test chamber setup is below in Figure 80.

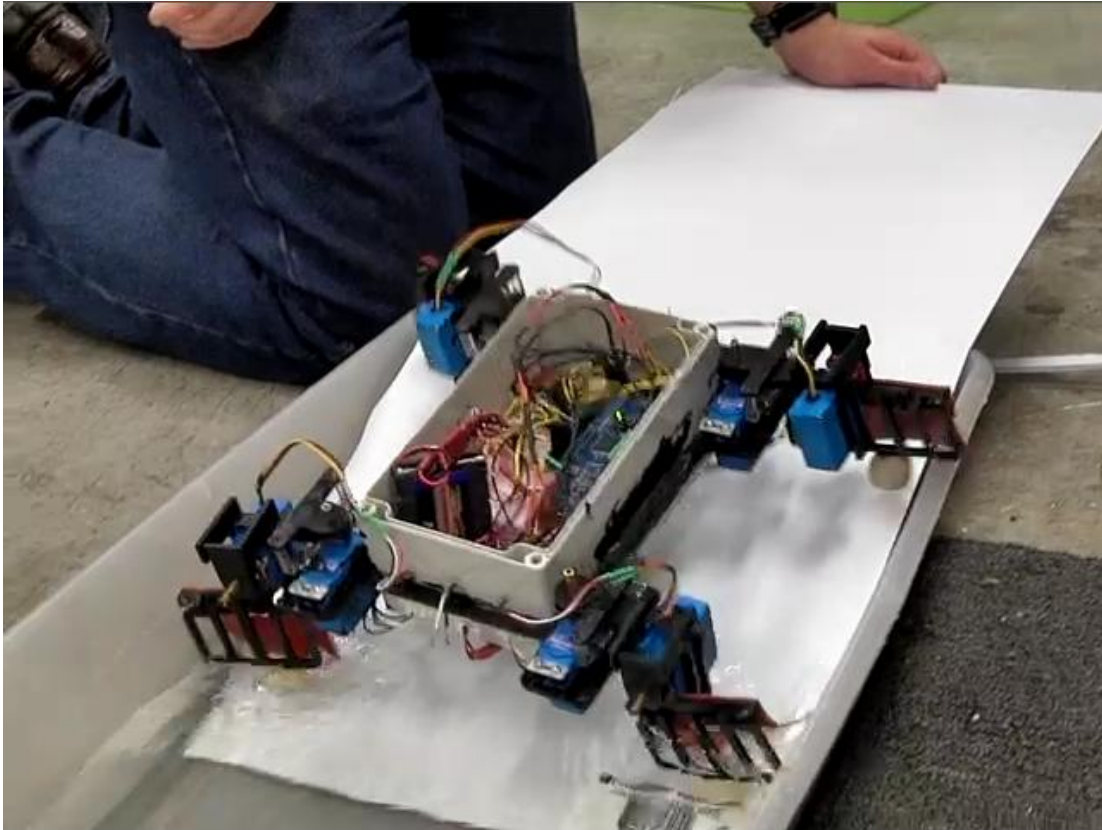


**Figure 80: Experimental setup for walk/trot transitions**

This solution would not be sufficient for swim/walk transition testing, as deep water was required; however, a similar idea would need to be used to properly test the walk-to-swim transition. Thus, a platform was constructed that would rest upon a plastic box. With proper weighting, the platform would rest on the box with ease. This platform was 12 inches tall, while the body of water picked was 15 inches tall; this difference ensured the lower water sensors would be tripped and that there would be a clean transition into the water. Similar to the walk/trot transition test, the robot would be placed on the flat part of the platform to transition from walking to swimming, and then vice versa to test swimming to walking. A picture of this platform setup is below in Figure 81.



**Figure 81: Experimental setup for swim/walk transitions.**

#### 4.5.2 Experimental testing

Each test was performed, and certain findings became fairly apparent. These results did not massively impair the operation of the robot, but provided important feedback as to potential flaws.

The walk/trot test was the first major test of the robot on a slick surface, as described in the setup. While the trotting gait had major problems staying on the polypropylene platform and moving forward, the walking gaits had significantly less problems, although slipping was still visible. The nature of the slipping suggests that the robot is not able to easily pull itself straight from a situation where a leg is raised. This suggests that land that is slick but not fully wet would still require a major degree of stability, which the trotting gait lacks.

On the slope, a major flaw became more apparent. The robot operated well when the water was raised to the top of the slope. The delay in the minor transition allowed for it to catch itself before diving fully in, and enter the water in a more

measured way. In a situation where the slope itself is primarily not underwater, the robot will not trigger its stable gaits, and especially not those meant for walking on slopes. Thus, it will employ its trotting gait until such a time that the robot is underwater. This can lead to a situation where the robot becomes unbalanced and falls down the slope, especially while walking downhill. This does not change the demonstrated principle as outlined in this thesis, but instead provides an avenue for future improvement.

The swim/walk test was more successful, though not without its issues. The primary problem with the test was the natural buoyancy of the platforms combined with the current within the body of water, which caused the test platform to begin floating. To combat this, the platform was physically held in place while the test occurred. A secondary problem was that the testing occurred on an especially windy day. This was considered, along with the current, to be a representative environment, and as such testing results would be gauged based upon this.

In testing, the robot walked stably using the walking gait, as expected, and continued into the water. However, as the algorithm was set to switch to swimming only when all four sensors were engaged, due to the wind causing the water surface to be uneven, the robot continued its walking gait upon initial disembarkment from the platform. After a few seconds, however, the robot's sensors were finally submerged. In spite of the backwards drift it had gained due to the wind and current, it built up enough thrust to maintain a forward velocity. A temporary change was made to the algorithm that altered the swimming gait to trigger with one top sensor instead of two; however, this was not a perfect solution, as it could create situations where the robot

swam prematurely or would not switch to walking due to a steep or irregular slope situation.

#### 4.6 Results and Conclusions

The net result of the gait testing was positive. Each gait worked in its respective environment, be it walking, slope walking, trotting, or swimming. However, there was some distinct friction in certain transitions. Trotting, walking, and slope walking transitioned acceptably when given the expected situation, but deviations caused trouble: partially wet, but not water-filled, walking environments presented a challenge for the less stable trotting gait, while the slope walking transition was shown not to trigger in a relatively common slope condition. These problems are both related to the nature of the sensors employed; sensors to gauge the presence of water do not work as well when the water in question is only a thin layer. Additionally, as was found with slick polypropylene, a surface may not even have a true layer of water so much as a trace amount that makes an already slippery surface even more so. Neither of these impacts the specific goals of the robot; however, they are significant concerns for non-ideal circumstances.

One solution to this would be to couple water sensing with a secondary source of movement state sensing, such as an IMU or gyroscope, for consideration of changing states; this is quite possible given the existence of IMU shields for Arduino microcontrollers [40]. Given that the robot moves in place when slipping during its trotting gait, for example, such a sensor might be able to acknowledge the separation between the desired gait, current gait, and current motion, and switch gaits in an



effort to correct this. Given the stringent power and weight requirements that are already being stretched to their limits, this is not feasible to add to the current model; however, in a future model, it is a distinct possibility, especially as more advanced microcontrollers that can process more data in real time are added to the market.

The swim testing presented its own share of problems: namely, the question of triggering the swimming gait in choppy water. The initial solution was to change the switching requirement to one of the two top sensors from both top sensors. However, as noted, this was an imperfect solution, as it increases the chances of falsely triggering swimming or not triggering walking. Additionally, there was significant interference from both water current and wind in operation. While these sources of interference are expected and their impact is largely outside the scope of this thesis, the general issue is worth addressing for the consideration of future application.

One solution to triggering issues in swimming would be to add more sophisticated water depth sensing than the current system of two binary sensors per water level. This would allow a similar situation to be thwarted by considering relative water depths for sensing and triggering the state when one is saturated and the other is not unsaturated. The replacement would also address the trot-walk and walk-sloped walk transitions, replacing four simple sensors with two moderately complex sensors. The issue of drift due to current and wind could, similarly to the walking issues, be solved by a motion state sensor. These two additions would bring the sensor package to three relatively complex sensors. Unfortunately, the simplicity of the current algorithm would be necessarily lost with such a solution, along with the fast response time afforded by that simplicity; a modern microcontroller can likely

not handle the kind of constant checking that all three of those kinds of sensors would require. In addition, the same power and weight requirements as mentioned above still hamper this implementation in the current robot.

## Chapter 5: Conclusions

The goals of this thesis were to develop and build a quadrupedal legged robot that can handle four kinds of terrestrial and aquatic locomotion, and to develop sub-gaits that transition smoothly between gait modes. As demonstrated, the robot accomplished these tasks.

### 5.1 Intellectual Contributions

Contributions from this project come from both the construction of the robot and the gait synthesis thereafter. Specific contributions included the following:

- An efficient design for a quadruped robot which has demonstrated the ability to walk on flat dry and wet terrains and sloped wet terrains as well as swim was created. This robot is unique in that its method of locomotion is not based upon rotation, but upon limited-range servomotors, similar to the joints of animals. With eight degrees of freedom, both walking and swimming locomotion have been achieved.
- The use of compliance in conjunction with rigid limbs to achieve both walking and swimming was established.
- Three primary gaits for a single quadrupedal design with eight degrees of freedom were demonstrated, along with two secondary gaits and two major transition gaits.
- Transitions between each gait, taking into account the nuances of each gait's mode of travel, were developed.

### 5.2 Anticipated Benefits

Each contribution comes with significant benefits for the overall field of robotics.

- The construction of the robot, most specifically the waterproof nature of the robot and the use of compliant mechanisms in propulsion, serves as a prominent example for any further aquatic or amphibious robots.
- The three primary, two secondary, and two transition gaits can be used as a basis for further gait research. Each of these is inherently parametric, and as such any of them could be adapted for more sensitivity to their operating environment.
- The analytical method used for transition can be applied to more gaits than those developed here for the sake of achieving the same smooth transition. The transition algorithm demonstrated can be applied to more kinds of robots and modes of locomotion than those explored in this thesis, especially in cases in which parametric design was performed.
- The methods of considering robot-fluid interaction, including the simulation model employed to examine the compliant mechanisms' operation, can be applied to similar problems in amphibious robotics.

### 5.3 Future Work

This robot has shown capability for robust walking, swimming, and gait transition. However, there is significant room for improvement. Many limitations

imposed by the scope of the project may be surpassed and explored in subsequent projects.

### 5.3.1 Structural improvement

While the robot's structure performed its task adequately, the final product can be improved significantly. This is especially pronounced with regard to the central box that contains the electronics, as it is not especially built with aerodynamics in mind. Besides that concern, however, the issue of overall construction is still present. Consistent reduction of weight and designing away from adhesive use in construction would be beneficial both from the robustness and maintenance point of view.

### 5.3.2 Energy considerations

The Hitec HS-646WP servomotors employed in the current version of the robot excel in weight, torque, and ability to remain waterproof. However, they are very power-intensive, due to being digital servomotors, which leads to drastically reduced running time. There are two primary avenues of mitigation possible for this problem. One is selection of suitable analog servomotors as those become more available, possibly employing conversion techniques to waterproof them. The second avenue is continued improvement of the physical design and gait so as to reduce the amount of current pulled by the servomotors in each step or stroke.

In addition, there is a lack of information on energy expenditure relative to robot kinematic configuration, especially as pertains to swimming and other aquatic

motion. As such, it would be extremely advantageous to aquatic robotics to more fully examine and document this.

### 5.3.3 Introduction of sophisticated sensing and controls

The robot employs very simple sensors and controls to accomplish its goals, using a single direct input to a simple program that produces one of several outputs. More capable sensing would allow for more inputs and input ranges, which can allow for better environment state discrimination within the program. Conversely, functional output with higher sensitivity to changes in short timeframes would allow for more sophisticated reactions to stimuli.

### 5.3.4 Broadening of terrains and conditions for operation

While a major strength of legged robots is that they can easily handle highly varied terrain, this particular robot was not built to tackle extremely varied terrain or a large variety of water conditions. As such, some areas worthy of exploration are increased robustness on terrain with features such as variable ground height and mud, compensation for water current and surface conditions, and water-land interfaces such as breaking waves or sudden change from land to water. These could be realized by purely physical means such as shock-absorbent legs for walking and more sophisticated swimming compliance, electronic means such as more reactive programming, or a combination of the two.

### 5.3.5 Submerged swimming

The current robot employed is designed to float on the surface as it swims; the configuration as it currently exists would not operate fully submerged. A design that can handle being submerged and modulate its underwater depth would expand the possibilities of such a platform significantly in application. In addition, promising possibilities such as land-to-water diving and switching between submerged and floating swimming should be explored in future work.

## Scholarly References

- [1] B. Labrom, “Platypus”, [online] 2012,  
<http://troghead.blogspot.com/2012/04/platypus.html> (Accessed: August 2012)
- [2] J. Hillman, “Florida Nature: Alligator mississippiensis – American Alligator,” [online] 2002,  
[http://www.floridanature.org/species.asp?species=Alligator\\_mississippiensis](http://www.floridanature.org/species.asp?species=Alligator_mississippiensis)  
(Accessed: August 2012)
- [3] K. Harper, M. Berkmeier, and S. Grace, “Decreasing the Energy Costs of Swimming Robots through Passive Elastic Elements,” *Int. Conf. Robotics and Automation*, Albuquerque, NM, 1997, pp. 1839-1844
- [4] D. Lachat, A. Crespi, and A.J. Ijspeert, “Boxybot: a swimming and crawling fish robot controlled by a central pattern generator,” *Proc. of the First IEEE /RAS-EMBS Int. Conf. Biomedical Robotics and Biomechanics*, 2006
- [5] M. Triantafyllou and G. Triantafyllou, “An Efficient Swimming Machine”, *Sci. Amer.*, vol. 3, no. 242, pp. 64-67, 1980.
- [6] “Fukushima Lab”, [online], [http://www-robot.mes.titech.ac.jp/robot/snake/acm-r5/acm-r5\\_e.html](http://www-robot.mes.titech.ac.jp/robot/snake/acm-r5/acm-r5_e.html) (Accessed: August 2012)
- [7] A. Crespi, A. Badertscher, A. Guignard, and A.J. Ijspeert, “AmphiBot I: an Amphibious Snake-like Robot,” *Robotics and Autonomous Systems*, vol. 4, no. 50, pp. 163-175, 2005
- [8] A. Crespi, A. Badertscher, A. Guignard, and A.J. Ijspeert, “Swimming and Crawling with an Amphibious Snake Robot,” *Proceedings of the 2005 International Conference on Robotics and Automation*, pp. 3024-3028, 2005
- [9] A.J. Ijspeert and A. Crespi, “Online Trajectory Generation in an Amphibious Snake Robot Using a Lamprey-like Central Pattern Generator Model”, *International Conference on Robotics and Automation*, 2007
- [10] J.H. Long Jr., J. Schumacher, and N. Livingston, “Four Flippers or Two? Tetrapodal Swimming with an Aquatic Robot,” *Bioinspiration and Biomimetics*, vol. 1, no. 1, pp. 20-29, 2006
- [11] U. Saranli, M. Buehler, and D.E. Koditschek, “RHex: A Simple and Highly Mobile Hexapod Robot,” *Int. J. Robotics Research*, vol. 20, no. 7, pp. 616-631, 2001
- [12] E.Z. Moore, D. Campbell, F. Grimminger, and M. Buehler, “Reliable Stair Climbing in the Simple Hexapod ‘RHex’,” *Proc. 2002 IEEE Int. Conf. Robotics and Automation*, Washington, D.C., pp. 2222-2227, 2002
- [13] Summary of the Rhex robot platform, n.d., from <http://www.rhex.web.tr/>
- [14] S.H. Park, D.S. Kim, and Y.J. Lee, “Discontinuous Spinning Gait of a Quadruped Walking Robot with Waist-Joint”, *Intelligent Robots and Systems*, pp. 2744-2749, 2005
- [15] I.M. Koo, T.D. Trong, T.H. Kang, G.L. Vo, Y.K. Song, C.M. Lee, and H.R.



- Choi, "Control of a Quadruped Walking Robot Based on Biologically Inspired Approach," *Proceedings of the 2007 IEEE/RSJ International Conference on Intelligent Robots and Systems*, Institute of Electronics and Electrical Engineers/Robotics Society of Japan, pp. 2969-2974, 2007
- [16] Y. Tang, C. Liu, A. Zhang, J. Yu, "Optimal Distribution of Propulsion for an Amphibious Robot Based on Wheel-Propeller-Leg Mixed Thrusters," *Proceedings from International Conference for Control, Automation, Robotics and Vision*, pp. 822-826, 2010
- [17] C. Prahacs, A. Saunders, M.K. Smith, D. McMordie, M. Buehler, "Towards Legged Amphibious Mobile Robotics," *Journal of Engineering Design and Innovation*, vol. 1P, 2005
- [18] E. Ackerman, "Video Friday: Warm Robot Hand, Rugged RHex, and ROBO-ONE", [online] 2012, <http://spectrum.ieee.org/automaton/robotics/diy/video-friday-warm-robot-hand-rugged-rhex-and-roboone> (Accessed: August 2012)
- [19] J. Sattar, P. Giguere, G. Dudek, C. Prahacs, "A Visual Servoing System for an Aquatic Swimming Robot," *Proceedings from Intelligent Robots and Systems*, pp. 1483-1488, 2005
- [20] "IRIS AQUA 2004 Photos", [online], [http://quintessence.cim.mcgill.ca:8080/AQUA/photos/index\\_html](http://quintessence.cim.mcgill.ca:8080/AQUA/photos/index_html) (Accessed: August 2012)
- [21] Screenshot from "Gait Switch", [online], <http://www.youtube.com/watch?v=pXXikLMXhtY> (Accessed: August 2012)
- [22] M. Eich, F. Grimminger, F. Kirchner, "A Versatile Stair-Climbing Robot for Search and Rescue Applications," *Proceedings from International Workshop on Safety, Security, and Rescue Robotics*, , pp. 35-40, 2008
- [23] "ASGUARD II", online, <http://robotik.dfki-bremen.de/en/research/robotsystems/asguard-ii.html> (Accessed: August 2012)
- [24] A.J. Ijspeert, A. Crespi, D. Ryczko, and J.M. Cabelguen, "From Swimming to Walking with a Salamander Robot Driven by a Spinal Cord Model," *Science*, From Swimming to Walking with a Salamander Robot Driven by a Spinal Cord Model, vol. 315, no. 5817, pp. 1416-1420, 2007
- [25] "Acetal sheet – Delrin® (Thermoplastic Polymer): TAP Plastics", [online], [http://www.tapplastics.com/product/plastics/cut\\_to\\_size\\_plastic/acetal\\_sheet\\_delrin/525/](http://www.tapplastics.com/product/plastics/cut_to_size_plastic/acetal_sheet_delrin/525/) (Accessed: November 2012)
- [26] "Futaba standard analog servos", [online], <http://www.futabarc.com/servos/analog.html> (Accessed: November 2012)
- [27] "Coatings and adhesives, Rubber and Plastic Coatings | Plasti Dip International", [online], <http://www.plastidip.com/> (Accessed: November 2012)
- [28] "HS-646WP – Hitec RCD", [online], <http://www.hitecrd.com/products/servos/analog/waterproof-servos/hs-646wp.html> (Accessed: November 2012)
- [29] "VLS 3.60 | Universal Laser Systems", [online],

- <http://www.ulsinc.com/products/vls360/> (Accessed: November 2012)
- [30] “Hammond Mfg. – Watertight ABS Plastic Enclosures (1554 series), [online], <http://www.hammondmfg.com/1554FLA.htm> (Accessed: December 2011)
- [31] “Arduino - ArduinoBoardMega2560”, [online], <http://arduino.cc/en/Main/ArduinoBoardMega2560> (Accessed: December 2011)
- [32] “Tenergy NiMH 2000mAh Side by Side RX Batter Packs w/Hitec Connector”, [online], <http://www.tenergy.com/11106?sc=59&category=38217> (Accessed: December 2011)
- [33] “Gait – Definition and more from the free Merriam-Webster Dictionary”, [online], <http://www.merriam-webster.com/dictionary/gait> (Accessed: April 2013)
- [34] “Everglades Wildlife Images – Everglades National Park”, [online], <http://www.nps.gov/ever/parknews/evergladeswildlifeimages.htm> (Accessed: April 2013)
- [35] “Topic Mini-Research & Literature Site by Ashton Roller”, [online], <http://ww2.valdosta.edu/~abroller/topic.html> (Accessed: April 2013)
- [36] F.E. Fish, “Biomechanics and Energetics in Aquatic and Semiaquatic Mammals: Platypus to Whale”, *Physiological and Biochemical Zoology*, vol. 73, pp.683-698, 2000
- [37] S. Haughton, “On the Muscular Anatomy of the Alligator”, *Proceedings of the Royal Irish Academy*, vol. 9, 1864
- [38] J. Davenport, “A comparison of the swimming of marine and freshwater turtles”, *Proc. Royal Society of London*, vol. 220, no. 1221, 1984
- [39] A.B. Howell, “The Swimming Mechanism of the Platypus”, *J. Mammalogy*, vol. 18, no. 2, 1937
- [40] “6 DOF IMU shield”, [online], [http://www.dfrobot.com/index.php?route=product/product&product\\_id=788#.UXgGbaKKqpc](http://www.dfrobot.com/index.php?route=product/product&product_id=788#.UXgGbaKKqpc) (Accessed April 2013)
- [41] K. Williams, *Amphibionics*. New York, NY: McGraw-Hill, 2003.
- [42] “Design, Simulation, Fabrication, and Testing of a Bio-Inspired Amphibious Robot with Multiple Modes of Mobility” *J. Robotics Mechatronics*, vol. 24, no. 2, pp. 629-639, 2012
- [43] R.D. Quinn, “Improved Mobility Through Abstracted Biological Principles”, *Intelligent Robots and Systems*, vol. 3, pp. 2652-2657, 2002
- [44] P. Werk, R.D. Quinn, R. Vaidyanathan, “Design of an Autonomous Amphibious Robot for Surf Zone Operation: Part I Mechanical Design for Multi-Mode Mobility”, *Proc. Adv. Intelligent Mechatronics*, pp. 1459-1464, 2005
- [45] R. Harkins, “Design of an Autonomous Amphibious Robot for Surf Zone Operation: Part II Hardware, Control Implementation, and Simulation”, *Proc. Adv. Intelligent Mechatronics*, pp. 1465-1470, 2005
- [46] A.S. Boxerbaum, “Introducing DAGSI Whlegs: The latest generation of Whlegs

- robots, featuring a passive-compliant body joint”, *Int. Robotics and Automation*, pp. 1783-1784, 2008
- [47] J.L. Tangorra.; S.N. Davidson; I.W. Hunter; P.G.A. Madden; G.V. Lauder; D. Haibo.; M. Bozkurtas; Rajat, Mittal, "The Development of a Biologically Inspired Propulsor for Unmanned Underwater Vehicles," *Oceanic Engineering, IEEE Journal of* , vol.32, no.3, pp.533-550, July 2007
- [48] S. Imai, H. Mizoguchi, E. Inagakii, "Proposition of new control method of Eel-like swimming robot for swimming in narrow water ways," *10th Int. Conf. Control, Automation, Robotics and Vision*, pp.681, 684, 17-20 Dec. 2008
- [49] Dan Xia, Junkao Liu, Weishan Chen, Luhui Han, "Hydrodynamic analysis of fishlike robot swimming in the straight forward way," *Int. Conf. Mechatronics and Automation*, pp.3342-3347, 9-12 Aug. 2009
- [50] Yuan Fu-cai; Sun Hai-liang; Hu Shi-jian; Wang Li-zhu, "Design of cleaning robot for swimming pools," *Int. Conf. Management Science and Industrial Engineering*, pp.1175-1178, 8-11 Jan. 2011
- [51] J. Davenport and W. Clough, "Swimming and diving in young loggerhead sea turtles", *Copeia*, vol. 1986, no. 1, 1986
- [52] G. Miller, "SnakeRobots.com", [online] 1999-2005, <http://www.snakerobots.com> (Accessed May 2013)